Role of gut microbiota glycosyl hydrolases in rotavirus and norovirus infection

Doctoral thesis

Doctorate Programme of Biomedicine and Biotechnology

Valencia, October 2023

VNIVERSITAT DE VALÈNCIA

Nazaret Peña Gil

Supervisors:

Dr. Jesús Rodríguez Díaz

Dr. Roberto Gozalbo Rovira

VNIVERSITAT DE VALÈNCIA Facultat de Medicina i Odontologia
Departament de Microbiologia i Ecologia

Jesús Rodríguez Díaz, Doctor en Biología y Profesor Titular de Microbiología de la Facultat de Medicina i Odontologia de la Universitat de València, y

Roberto Gozalbo Rovira, Doctor en Bioquímica y Biología Molecular y Contratado Postdoctoral de la Facultat de Medicina i Odontologia de la Universitat de València,

INFORMAN

Que el presente trabajo de investigación titulado **"Papel de las glicosil-hidrolasas de la microbiota intestinal en las infecciones por rotavirus y norovirus"** ha sido realizado bajo nuestra dirección por Dª **Nazaret Peña Gil**, graduada en Biotecnología, para optar al título de Doctora.

En Valencia, 11 de octubre de 2023

JESUS| RODRIGUEZ| DIAZ
Firmado digitalmente por JESUS|RODRIGUEZ|DIAZ
Fecha: 2023.11.24 11:28:19 +01'00'

Dr. Jesús Rodríguez Díaz

ROBERTO VICENTE| GOZALBO|ROVIRA
2023.11.24 10:40:00 +01'00'

Dr. Roberto Gozalbo Rovira

Departament de Microbiologia
Facultat de Medicina i Odontología
Av. Blasco Ibàñez, 17
VALÈNCIA, SPAIN

Telèfon +34 96 386 46 58

Fax + 34 96 386 49 60

The thesis has been developed in the Microbiology and Ecology Department of the Medicine Faculty of the University of Valencia thanks to the predoctoral fellowship of the Generalitat Valenciana ACIF/2020/085. This work was also supported by grant PID2020-115403RB-C22 from the Spanish Ministry of Science and Innovation.

Agradecimientos

Ya han pasado tres años desde que empecé la tesis y casi cinco desde que llegué al laboratorio. Cuántos sentimientos y emociones se me vienen a la cabeza. Cuánto he aprendido y disfrutado en mi departamento de micro. Me voy con el corazón lleno de vivencias, de recuerdos y de personas bonitas. Aunque como en todo, siempre hay días buenos y no tan buenos, la gente con la que me he cruzado ha hecho que todo valga la pena y siempre os estaré agradecida.

Gracias a mis directores, Jesús y Rober. Gracias de verdad, por estar siempre ahí, por enseñarme tanto, guiarme en cada paso del camino, por transmitirme todos vuestros conocimientos y experiencias y buscar lo mejor para mí. No podría pedir mejores directores.

Gracias a Jesús, por enseñarme en mis inicios en el laboratorio, por saber dar la vuelta a resultados que pensamos que son un desastre y en verdad abren el camino a cosas mucho más grandes, por tus chistes malos, por haber confiado en mí, por abrirnos las puertas de tu casa y por alegrarte de mis logros como si fueran tuyos.

Gracias a Rober, por tener tanta paciencia conmigo y con todos los que te hacemos mil preguntas al cabo del día, por cantar Rafael y amenizarnos los días, por enseñarnos todos los trucos que sabes de laboratorio, por saber arreglar cualquier cosa y estar dispuesto a desmontar lo que sea. No sé cómo el resto de laboratorios funcionan sin un Rober, no te cambiamos por nada del mundo.

Gracias a Javier Buesa, por tu sabiduría y tu buen hacer. Eres un gran referente científico y académico.

Gracias a Noemi y Cristina, mis hermanas de tesis. Vaya aventuras hemos vivido en estos años. Gracias por estar ahí en los días malos, por hacerme sentir mejor cuando los *Western* no eran más que un borrón negro e intentábamos ver bandas donde no había nada, o cuando me equivocaba de mil formas. Gracias por el congreso de Málaga, todavía me acuerdo de lo bien lo pasamos cantando Mónica Naranjo en el sofá, de las charlas, las risas y los bailes que tanto nos unieron. Cuánto hemos aprendido y nos hemos esforzado en este camino. Qué orgullosa estoy de mis doctoras Navarro y Santiso.

Gracias a Noemi, por tener el corazón que tienes, ser tan generosa y simpática con todo el mundo, por buscar la parte buena a todo y saber qué decir en cada momento. Hemos compartido

momentos buenos y malos, canciones, cotilleos, tardes eternas de trabajo, dramas, clases, viajes… cuántas aventuras, y no podría elegir mejor compañera.

Gracias a Cristina, por animar todos y cada uno de los días de trabajo, por tu locura y espontaneidad, por dar siempre los mejores consejos y por ser tan valiente. Cuánto te he echado de menos estos últimos meses entre estancias, verano y fin de contratos, no ha sido lo mismo sin ti, la gente no se animaba tanto a ir al bar.

Gracias a Rober Jr. y Sergi (Zipi y Zape). Vaya par os habéis juntado. Gracias por alegrar el día con vuestras bromas y chistes, por estar siempre con una sonrisa y dispuestos a ayudar. Os deseo lo mejor en esta etapa. Seguro que vais a aprender muchas cosas nuevas y sobre todo sé que sacaréis la mejor receta de sándwich del mundo.

Gracias a Elvira, por ayudarnos en todo lo posible y compartir siempre todo lo que tienes. Gracias a Carmen, la pieza clave del departamento, sin ti nada sería posible. Gracias a las dos, mis compañeras puntuales de las 8, por alegrar los almuerzos con vuestras historias y simpatía.

Gracias a Carmen Argudo, por ser imparable, fuerte, generosa y buena gente. Gracias por abrirnos tu casa desde el principio, te has ganado un hueco en todos nosotros. Seguro que la ciencia te abre un camino pronto.

Gracias a Irene, por los buenos ratos y por lo buena que eres. Mis inicios en el laboratorio fueron contigo, entre nervios y dudas y, aunque no nos vemos tanto como nos gustaría, tu foto sigue en tu sitio, no nos olvidamos de ti. Gracias a Eva Moya, por los ratos que compartimos en el laboratorio entre células y *Western blots*, donde me di cuenta de lo buena persona que eres. Solo os deseo cosas bonitas, mis compis del IATA.

Gracias a mis brasileñas Sibele y Juliana, por contagiar vuestra alegría allá donde vais. Qué suerte haberos conocido. Gracias a Eva Mateo, por tener una sonrisa cada vez que paso por el despacho. Gracias a todos los compañeros con los que he compartido laboratorio y buenos ratos en todo este tiempo, Pedro, Ester, Víctor, Sara, Dani, Silvia, Laia, Alejandro, Marta y un largo etc. He aprendido mucho de cada uno de vosotros, os deseo lo mejor.

Thanks to my Belgium people. To Joana, for giving me the amazing experience of sharing 3 months with you and treating me like one of the team. To Nanci, for sharing all your knowledge, being so generous and helping me so much. The stay wouldn’t have been the same without you, I

still remember all the hours we shared at the P2. To Jana, for always being willing to help, for being so funny and such a good person. To Anaïs, for smiling and transmitting such good vibes every day. To Emma, for your kindness and friendliness. To the rest of the Rega people, I have really good memories of all of you.

Gracias a mi familia, mis padres y mi hermana, por estar siempre ahí, querer lo mejor para mí, por vuestra entrega y aconsejarme día a día. Por preocuparos por mis experimentos y preguntarme tantas veces cómo van mis células y si ya las he dado de comer, aunque todo esto de la ciencia a veces os suene a chino. Nada de esto habría sido posible sin vuestra guía desde pequeña. Gracias por vuestras visitas a Lovaina, recorrer juntos Bélgica fue muy especial. Gracias por todo, ahora y siempre.

Gracias a Rubén, por ayudarme y escucharme cada día desde hace tantos años, por tu paciencia, comprensión, cariño y alegría. Gracias por hacerme reír cuando lo veo todo negro, por los viajes y experiencias que hemos vivido, y las que nos esperan. Por escucharme con interés e ilusión hablar de las qPCRs, enteroides, electroforesis y extracciones de RNA aunque no sepas lo que son. Gracias por estar siempre ahí sea la hora que sea por muchos kilómetros que nos separen. Gracias por todo.

Gracias a mi ayudante de escritura de tesis, a mi Blanqui. Aunque tu ayuda se base en ronronear y dormir mientras yo me devanaba los sesos por escribir algo que tuviera sentido, solo mirarte me transmite la paz que necesito, me has ayudado más de lo que puedas pensar. Te quiero infinito.

Gracias a la familia que se elige y a la que no, qué suerte he tenido con todos vosotros.

GRACIAS

Contents

I. Acronyms and abbreviations

2’ FL	2’-fucosyllactose
2xYT	2x yeast extract tryptone medium
3FL	3-fucosyllactose
6FN	6-fucosyl-N-acetylglucosamine
AARS	Anti-adherence rinsing solution
AGE	Acute gastroenteritis
BG A	Blood group A trisaccharide
BG B	Blood group B trisaccharide
COG	Cluster of orthologous genes
DEPC	Diethyl pyrocarbonate treated water
DFJ	1-deoxyfuconojyrimicin HCl
DLP	Double-layered particle
DMEM	Dulbecco's modified Eagle's minimum essential medium
dpi	Days post infection
EC50	Half maximal effective concentration
FBS	Fetal bovine serum
FUT2	α1-2 fucosyltransferase
FUT3	α1-3/4 fucosyltransferase
GCE	Genome copy equivalent
GH	Glycosyl hydrolase
GSK-3	Glycogen synthase kinase-3
HBGA	Histo-blood group antigen
HIE	Human intestinal enteroid
hpi	Hours post infection
HPRT-1	Hypoxanthine phosphoribosyltransferase 1
kDa	KiloDaltons
LB	Luria-Bertani
Le^a	$Lewis^a$ antigen
Le^b	$Lewis^b$ antigen

Le^x	$Lewis^x$ antigen
Le^y	$Lewis^y$ antigen
LNB	Lacto-N-biose
MEM	Mínimum essential medium
MMTV	Mouse mammary tumour virus
MOI	Multiplicity of infection
Neu5Ac	N-acetylneuraminic acid
NoV	Norovirus
NTPase	Nucleoside-triphosphatase
ODM	Organoid differentiation media
OGM	Organoid growth media
ORF	Open reading frame
P	Protruding
P/S	Penicillin and spreptomycin
PBS	Phosphate buffer saline
PBS-T	Phosphate buffer saline 1X containing 0.05% Tween 20
*p*NP-fuc	4-nitrophenyl-α-L-fucopyranoside
*p*NP-gal	p-nitrophenyl β-D-galactopyranoside
RdRp	RNA-dependent RNA polymerase
Rock	Coiled-coil containing protein kinase
RV	Rotavirus
RVV	Rotavirus vaccine
S	Shell
SRA	Sequence read archive
TLP	Triple-layered particle
UPGMA	Unweighted pair group method with arithmetic mean
VLP	Virus-like particles
VPg	Viral protein genome-linked

II. List of figures

III. List of tables

IV. Resumen extendido

Introducción

Los virus entéricos rotavirus (RV) y norovirus (NoV) causan gastroenteritis aguda, una enfermedad que se manifiesta con diarrea, vómitos, malestar general, fiebre, deshidratación e incluso la muerte del paciente en los casos más graves. En el año 2016 RV ocasionó la muerte de 128.500 niños menores de 5 años y NoV la de 218.800 personas de todos los grupos de edades, siendo la mayoría de los casos registrados en países de bajos ingresos. A pesar de la reducción significativa de las muertes en las últimas dos décadas gracias a la introducción de la vacuna contra RV (RVV), la prevalencia de esta enfermedad continúa siendo preocupante.

Aunque se han detectado distintos compuestos con capacidad antiviral frente a RV y NoV, como la nitazoxanida, actualmente no se dispone de ningún tratamiento frente a estos virus, por lo que estas infecciones son tratadas principalmente evitando la deshidratación del paciente.

RV es un virus de ARN de doble cadena que pertenece a la familia *Sedoreoviridae*. Su genoma está fragmentado en 11 segmentos, donde cada uno codifica una proteína, excepto el segmento 11 que codifica dos. El virión está compuesto por una triple capa (TLP), donde la capa interna se compone de la proteína VP2, la intermedia por la proteína VP6 y la más externa está compuesta por las glicoproteínas VP7 y VP4. En función de las características antigénicas de la proteína VP6, RV se clasifica en 10 grupos (A-J), siendo el grupo A el responsable de las infecciones humanas. Este grupo se divide a su vez en genotipos G, en función de la glicoproteína VP7 y en genotipos P, en función de la proteína sensible a proteasas VP4. La cepa más comúnmente notificada en todo el mundo es la G1P[8], seguida de G2P[4], G3P[8], G4P[8], G9P[8] y G12P[8]. La proteína VP4 se proteoliza en su paso por el sistema digestivo en las subunidades VP5* y VP8*, siendo esta última responsable de la interacción con el receptor celular. Actualmente, un total de 116 países han incluido RVVs en su programa de vacunación, lo que ha reducido su incidencia, pero un gran número de niños siguen muriendo cada año debido a este virus.

Por otro lado, NoV, que se ha convertido en la principal causa de AGE después de la introducción de la RVV, es un virus ARN monocatenario, poliadenilado y de polaridad positiva que pertenece a la familia *Caliciviridae*. Su cápside está formada por las proteínas VP1 y VP2. VP1 se subdivide en los dominios S (porción interna de la cápside) y P (porción protuberante), dividiéndose

este último a su vez en los subdominios P1 y P2. El subdominio P2 se localiza en la parte más externa de VP1, por lo que es el responsable de la interacción con el receptor en la célula diana. En función de la secuencia de la proteína VP1, NoV se clasifica en 10 genogrupos (GI-GX), de los cuales GI, GII, GIV, GVIII y GIX infectan humanos. El genotipo GII.4 Sydney 2012 es la cepa más prevalente de NoV, y a diferencia de RV, no existe una vacuna disponible. Actualmente la vacuna HIL-214 se encuentra en la fase clínica 2b, donde se han encontrado resultados prometedores.

Los antígenos de grupos histosanguíneos (HBGAs) actúan como receptores tanto para RV como para NoV. Son carbohidratos complejos presentes en las superficies células sanguíneas, mucosas del tracto respiratorio, genitourinario y gastrointestinal, así como oligosacáridos libres en saliva, sangra y leche materna. La síntesis de HBGAs es catalizada por varias enzimas, incluyendo α1-2 fucosiltransferasa (FUT2), α1-3 o α1-4 fucosiltransferasa (FUT3) y dos glucosiltransferasas (enzimas A y B), a partir de los precursores lacto-N-biosa (LNB) y N-acetil-lactosamina. *FUT2* determina el estado secretor, mientras que *FUT3* determina el estado Lewis. La ausencia de una enzima funcional FUT2 lleva a individuos secretor negativos, mientras que la ausencia de FUT3 lleva a individuos Lewis negativos, lo que implica la falta de HBGA específicos. Tanto RVs como NoVs reconocen a los HBGAs de manera dependiente de genotipo, lo que significa que la presencia o ausencia de ciertos antígenos afecta la capacidad viral de infectar las células huésped. Se ha reportado que el estado secretor es una de las causas de susceptibilidad a los RVs P[8] y P[4], así como a los NoVs GII.4.

Por otra parte, la microbiota intestinal contiene una amplia variedad de enzimas glicosil-hidrolasas (GH) que permiten la utilización de glicanos del huésped como fuente de nutrientes. Estas enzimas incluyen fucosidasas y sialidasas para eliminar fucosas y ácido siálico de las cadenas de glicanos, así como exo- y endo-β-N-acetilglucosaminidasas, β-galactosidasas, α-N-acetilglucosaminidasas, endo-β1,4-galactosidasas y α-N-acetilgalactosaminidasas.

Diversos estudios han demostrado el papel de la microbiota intestinal en la modulación de las infecciones virales. Por una parte, inhiben la infección de virus entéricos al unirse a sus receptores bloqueando la adhesión viral; unión a los virus promoviendo su eliminación en las heces; estimulando el sistema inmune; la secreción de moco; así como cambios en la glicosilación. Por otra parte, también se ha demostrado que las bacterias intestinales pueden desempeñar un papel en la promoción de infecciones de virus entéricos al estabilizar viriones, promover su adhesión a células huésped y alterando la respuesta inmune antiviral.

Los principales modelos celulares empleados en el estudio de RV son las células MA104, Caco-2 y HT29, junto con el modelo de enteroides humanos (HIEs). A excepción de la primera, el resto expresan HBGAs en su superficie. NoV, por su parte, no replica en las líneas inmortalizadas, pero sí en HIEs. En cuanto a modelos *in vivo*, ratones y cerdos gnobióticos son usados en el estudio de RV y NoVs, además de pez cebra para este último.

Las principales cepas de RV empleadas para la realización de experimentación básica son aquellas adaptadas a su cultivo en el laboratorio, concretamente las cepas Wa y SA11, que han sido adaptadas en la línea celular MA104. En cuanto a NoV, al no poder replicar en cultivos celulares convencionales, se emplean partículas P y partículas pseudovirales (VLPs). Las primeras provienen de la expresión del dominio P, que resulta en dímeros. Doce de esos dímeros forman las partículas P, que mantienen la capacidad de unión a HBGAs. Las VLPs, por su parte, consisten en proteínas VP1 ensambladas, sin ARN viral, por lo que no son infecciosas. También se usa comúnmente el NoV murino.

Puesto que tanto RV como NoV infectan células del tracto gastrointestinal, el empleo de cepas adaptadas a cultivo de RV, cepas de NoV murino, y líneas celulares que no expresan HBGAs podría ocasionar sesgos y/o resultados difícilmente extrapolables a humano.

Hipótesis y objetivos

Una vez establecido que RV y NoV reconocen HBGAs del tracto gastrointestinal, que la microbiota posee GHs para obtener nutrientes a partir de los glicanos, que la microbiota favorece la replicación de RV y NoV y teniendo en consideración las interacciones que tienen lugar entre el huésped, la microbiota y los patógenos, la principal hipótesis planteada en el presente trabajo converge en el papel de las enzimas GHs de la microbiota intestinal, concretamente de las fucosidasas, en la replicación de RV y NoV.

Por tanto, el principal objetivo de la tesis fue estudiar el efecto de las fucosidasas codificadas por la microbiota intestinal en las infecciones de RV y NoV. Para ello, los objetivos específicos que se establecieron fueron:

- El estudio del metagenoma de heces infantiles y la búsqueda de fucosidasas no caracterizadas mediante análisis bioinformático.

- La clonación, purificación y caracterización de fucosidasas seleccionadas.
- El mantenimiento de líneas celulares con diferentes perfiles de HBGA.
- La detección de aislados clínicos de RV y NoV capaces de replicarse en células dCaco-2 y HIEs.
- El estudio de la replicación de aislados clínicos de RV y de la cepa de RV adaptada a cultivos celulares Wa en líneas celulares con diferentes perfiles de HBGA.
- El estudio del efecto de las fucosidasas en la replicación de RV y NoV en cultivos celulares, HIEs y ratones.
- El estudio del efecto de un inhibidor de fucosidasas en la replicación de RV y NoV en cultivos celulares, HIEs y ratones.

Material y métodos

-Estudio del metagenoma y caraterización de fucosidasas

En primer lugar, se llevó a cabo la extracción de ADN de una muestra fecal que contenía heces de 4 niños lactantes de entre 1 y 3 años, para posteriormente construir una librería que fue secuenciada con el equipo MiSeq Sequencer. Tras realizar las comprobaciones de calidad, corte de adaptadores y filtrado oportunas, se llevó a cabo el ensamble metagenómico usando metaSPAdes. A continuación, se emplearon según el siguiente orden el programa RAST-MGRAST, la base de datos Cluster of Orthologous Genes, el servidor dbCAN2 y los programas SignalP y CLUSTAL Omega para obtener finalmente las secuencias de fucosidasas putativas que no habían sido previamente caracterizadas.

Se clonaron un total de diez fucosidasas en el vector pQE80 L etiquetadas con 6x histidina en posición amino terminal. Un clon de cada fucosidasa fue expresado en *E. coli* BL21, junto con dos fucosidasas previamente caracterizadas, AfcA y AfcB (proveídas por el Dr. Katayama, Japón). Las bacterias se crecieron hasta alcanzar una OD_{600} de 0,5, tras lo que se indujeron con 0,1 mM IPTG a 18 ºC durante 16 h. Posteriormente, las bacterias se recogieron por centrifugación durante 10 min a 7.000 g a 4 ºC y se resuspendieron en tampón de lisis (0,015 g de lisozima, 3 U de DNasa y PMSF 0.8 mM). Los extractos celulares se purificaron mediante cromatografía de afinidad con columnas de 5 mL HisTrap empleando el equipo Äkta Prime FPLC. Las proteínas obtenidas se resuspendieron en PBS 1X con 15% de glicerol.

A continuación, se llevó a cabo la caracterización de las fucosidasas aisladas del metagenoma, junto con AfcA y AfcB mediante ensayos Western blot y Dionex. Tras comprobar la especificidad de los distintos anticuerpos primarios en la técnica de Western blot, se incubaron diferentes glicoconjugados con las fucosidasas obtenidas durante 16 h a 37 ºC. Posteriormente, las muestras se separaron en geles de poliacrilamida y se transfirieron a membranas de nitrocelulosa. Tras bloquear e incubar con los respectivos anticuerpos primarios específicos producidos en ratón frente a los diferentes glicanos y el anticuerpo secundario común anti-ratón, se revelaron las membranas. La desaparición de la banda correspondiente al determinado glicoconjugado evidencia que la fucosidasa empleada es capaz de hidrolizar la fucosa que contiene dicho glicoconjugado. Alternativamente, se utilizó el equipo Dionex, que permitió ver el efecto directo sobre los propios oligosacáridos; para ello se incubaron los oligosacáridos con las respectivas fucosidasas y posteriormente se analizaron las muestras en el equipo HPLC Dionex. La presencia de fucosa como parte del producto de digestión evidenció que la fucosidasa empleada era capaz de hidrolizar el enlace entre la fucosa y el resto del oligosacárido.

-Preparación de filtrados virales de heces humanas

Se resuspendieron 0,5 g de heces humanas positivas para RV o NoV en el tampón TNC 1X o PBS respectivamente. Tras disgregar los sólidos presentes mediante la acción de una pipeta y la posterior incubación a temperatura ambiente, las muestras se sonicaron y se centrifugaron. Finalmente se filtró el sobrenadante secuencialmente mediante filtros con el tamaño de poro cada vez menor, tras lo que las muestras se alicuotaron y almacenaron a - 80 ºC hasta su utilización.

-Mantenimiento de líneas celulares

Las líneas celulares Caco-2 y MA104 se mantuvieron en medio mínimo esencial (MEM) suplementado con 10 % suero bovino fetal, penicilina, estreptomicina, glutamina y aminoácidos no esenciales. Las líneas celulares HT29 y HT29 M6 se cultivaron en medio mínimo esencial modificado por Dulbecco (DMEM) suplementado con 10 % suero bovino fetal, penicilina, estreptomicina y bicarbonato sódico. Ambas se crecieron en frascos T75, una vez que los frascos alcanzaron un 80-

90% de confluencia, las células se pasaron a placas de 96 pocillos. Para los experimentos con las células Caco-2, se requirió de un periodo de diferenciación celular complementario de 14 días.

-Mantenimiento de enteroides intestinales humanos

Los HIEs se mantuvieron en matrigel con el medio de crecimiento de organoides (OGM). Para las infecciones en 3D, estos se diferenciaron con medio de diferenciación (ODM) durante 5 días. En el caso de las infecciones 2D, tras un periodo de crecimiento de 7 días, se disociaron y se sembraron en placas de 96 pocillos. Una vez alcanzaron la confluencia, se sometieron a un proceso de diferenciación durante 5 días.

-Infecciones de líneas celulares y enteroides intestinales humanos con RV

Una vez las placas alcanzaron la confluencia, se llevó a cabo el cribado de los filtrados de RV para detectar aquellos con capacidad de infección sobre células Caco-2 diferenciadas (dCaco-2). Para ello, los virus se activaron durante 1 h a 37 ºC con 10 µg/mL tripsina IX. El inóculo se añadió a los pocillos correspondientes durante 1 h (2 h en el caso de HIEs en crecimiento 3D) tras la cual se eliminó y se añadió medio MEM completo sin suero suplementado con 1 µg/mL tripsina IX. Una de las placas se guardó congelada a – 80ºC, mientras que la otra se incubó a 37 ºC el tiempo estipulado.

A continuación, tanto las líneas celulares previamente nombradas como los HIEs se infectaron con los aislados clínicos seleccionados, junto con la cepa adaptada a cultivo Wa, empleando el medio MEM suplementado sin suero.

-Infección de enteroides intestinales humanos con norovirus

Se ensayó la capacidad de los diferentes aislados clínicos de NoV para infectar HIEs. Para ello, se diluyeron los NoV en medio ODM y se añadieron a cultivos 2D o 3D de HIEs durante 1 h o 2 h, respectivamente. Tras ello, se eliminó el inóculo y se añadió medio ODM completo. Finalmente, las células correspondientes al periodo de infección de 1 o 2 h se resuspendieron en tampón de lisis y se congelaron a – 80ºC. El resto de células se incubaron a 37 ºC el tiempo determinado y posteriormente se congelaron de igual forma.

-Efecto de fucosidasas e inhibidor de fucosidasas en la replicación de rotavirus en células Caco-2 diferenciadas y de norovirus en enteroides intestinales humanos

A continuación, se estudió el efecto de las fucosidasas de la microbiota intestinal en la replicación de aislados clínicos de RV, así como de la cepa Wa y aislados clínicos de NoV. Para ello, se utilizaron células dCaco-2 en el caso de RV y células HIEs en el caso de NoV, ambas se trataron con las fucosidasas seleccionadas durante 2 h a 37 ºC. Posteriormente, se lavaron las células y se realizó la infección según el protocolo previamente descrito.

En el caso del estudio del inhibidor de fucosidasas, se incubaron tanto los RV como los NoVs durante 1 h con el iminosacárido 1-deoxyfuconojyrimicin (DFJ), en el caso de RV, la incubación se realizó durante el proceso de activación por tripsina. Una vez transcurrido el proceso de incubación, la infección prosiguió acorde al procedimiento descrito con anterioridad.

-Extracción de ARN y qPCR

El proceso infectivo se monitorizó mediante PCR cuantitativa a tiempo real (qPCR), para ello, una vez realizados los diferentes experimentos, se realizó la extracción de ARN de los diferentes cultivos y las qPCR pertinentes. Los datos se analizaron mediante el método $2^{-\Delta\Delta Ct}$ para comprobar expresión diferencial.

-Infección del modelo animal murino con rotavirus y norovirus

Se utilizaron diferentes grupos de ratones de la cepa C57BL/6, que fueron infectados con el RV adaptado a cultivo Wa y con un aislado clínico de NoV perteneciente al genotipo GII.4 2012 Sydney. Inicialmente se deplecionó la microbiota propia con un cóctel de antibióticos (1 g/L ampicilina, 1 g/L metronidazol, 1 g/L neomicina y 0.5 g/L vancomicina) en el agua de bebida. Tras tres semanas del tratamiento con antibióticos, se inició el proceso experimental. Se realizaron un total de 3 experimentos diferentes, cada uno de ellos condicionado a un determinado virus, un grupo fue infectado con RV y otro con NoV:

Grupo 1: se administró a dos grupos de ratones 50 µg/ratón de fucosidasa AfcA, suministrada en liposomas, una vez al día durante 2 días, al tercer día, se infectaron con 10^{10} equivalentes genómicos de RV o NoV.

Grupo 2: se infectaron dos grupos de ratones con 10^{10} equivalentes genómicos de RV o NoV junto con 20 mM del inhibidor de fucosidasa DFJ.

Grupo 3: Se infectaron dos grupos de ratones con 10^{10} equivalentes genómicos de RV o NoV como controles.

Para todos los grupos, se recogieron heces hasta el séptimo día post infección. A partir de dichas muestras, se realizó la extracción de RNA y se cuantificaron los respectivos títulos virales mediante qPCR, para ello se utilizó una recta de regresión de equivalentes de genoma generada con cantidades conocidas de DNA plasmídico con la secuencia diana de los cebadores empleados en la propia qPCR.

Resultados y discusión

-Identificación y caracterización de glicosil-hidrolasas del metagenoma bacteriano

Se identificaron un total de 60.354 secuencias proteicas con función conocida, estas incluyeron diferentes proteínas con actividad GH, de las cuales 36 tenían actividad fucosidasa y 22 de ellas presentaron secuencia codificante completa. Tras descartar proteínas previamente caracterizadas o con alto porcentaje de similitud, se seleccionaron un total de 10 fucosidasas, Fuc18, Fuc19A, Fuc35A, Fuc1584, Fuc193, Fuc39, Fuc2358, Fuc5372, Fuc30 y Fuc35B.

Se expresaron y purificaron las diferentes fucosidasas, junto con AfcA y AfcB. Los resultados de la caracterización enzimática mediante ensayo Western blot reveló que únicamente AfcA presentaba actividad fucosidasa α1-2. Respecto a la actividad fucosidasa α1-3/4, AfcB mostró actividad completa, mientras que las fucosidasas Fuc18, Fuc19A y Fuc39 era una actividad parcial. Las fucosidasas Fuc39, Fuc35A, Fuc1584, Fuc193, Fuc2358, Fuc5372 y Fuc30 presentaron una actividad mínima o nula.

Alternativamente, se utilizó el equipo Dionex para comprobar la actividad sobre los oligosacáridos y se pudo comprobar que Fuc18, Fuc39 y Fuc35B presentaban actividad α1-3/4

completa, mientras que Fuc19A y Fuc1584 presentaban actividad parcial. También se detectó que Fuc35A, Fuc2358 y Fuc5372 tenían actividad α1-2 parcial.

Estas diferencias encontradas en Western blot y mediante Dionex fue atribuida a una mejor accesibilidad de las fucosas en los oligosacáridos empleados en el ensayo Dionex, que podrían no ser accesibles en las neoglicoproteínas empleadas en Western blot por impedimentos estéricos. Por tanto, se emplearon las fucosidasas AfcA y AfcB tanto en los ensayos con las células dCaco-2 y HIEs como en los ensayos con ratones, ya que estos presentan oligosacáridos mucho más complejos y únicamente las fucosidasas con capacidad de cortar fucosas presentes en los glicoconjugados resultarían efectivas.

-Cribado de rotavirus y norovirus

4 de los 41 aislados clínicos de RV obtenidos presentaron capacidad de replicación en células dCaco-2, concretamente los RV RV7, RV18, RV39 y RV41. La baja tasa de muestras positivas observada podría deberse a la presencia de contaminantes en las heces que inhibieran la replicación viral, así como la coinfección con otros virus o bacterias. Aunque se restringió la presencia de bacterias en las muestras virales mediante la filtración de las propias muestras, el periodo de almacenamiento de las heces desde su recolección hasta la preparación de las mismas podría haber afectado a la viabilidad de los RVs, ya que algunas de las muestras fecales fueron almacenadas durante un período de tiempo elevado. Finalmente, los virus RV7 y RV39 fueron los elegidos para su utilización en experimentos posteriores debido a su robustez en la replicación puesta de manifiesto tras la realización de varios experimentos independientes.

Posteriormente, se concluyó que el tiempo de infección adecuado para los RV seleccionados era de 72 h en células dCaco-2 y de 48 h en HIEs.

En cuanto a NoV, únicamente dos de los cinco analizados replicaron en cultivos 3D de HIEs, los NoV NoV43 y NoV44, de los cuales se seleccionó el NoV43 para realizar los experimentos debido a su mayor robustez en los diferentes experimentos de replicación.

-Infección con rotavirus en líneas celulares con diferente composición de HBGAs

Una vez identificados aquellos RV con capacidad de replicación (RV7, RV39 y Wa), se investigó el papel en la infección de los diferentes HBGAs presentes en la superficie celular. Se utilizaron las líneas celulares dCaco-2, HT29, HT29 M6, junto con cultivos 2D y 3D de HIEs como líneas celulares productoras de HBGAs. Alternativamente, las líneas MA104 y Caco-2 sin diferenciar (uCaco-2) fueron seleccionadas como líneas sin la presencia de HBGAs en su superficie. Los resultados indicaron que RV7 y RV39 replicaron de manera más eficiente en las células dCaco-2 y HIEs que en las células uCaco-2 y MA104, es decir, en células que expresan HBGAs en su superficie. Lo mismo ocurrió para el RV7 en las células HT29 y HT29 M6. Por su parte, Wa resultó en una mayor replicación en la línea celular MA104. Estos hallazgos indican que los aislados clínicos, es decir, aquellos RVs humanos que circulan de forma habitual entre la población, infectan de manera más eficiente las líneas celulares con presencia de HBGAs en su superficie y que, por tanto, se asemejan más al ambiente intestinal. Al contrario, la cepa Wa, RV adaptado al cultivo en laboratorio, replica mejor en las células MA104 y de manera deficiente en las otras líneas celulares ensayadas, llegando al extremo de no poder adherirse a las células HT29, HT29 M6 y cultivos 3D de HIEs.

-Efecto de las fucosidasas en la replicación de rotavirus y norovirus

Una vez se caracterizada la replicación de los RVs en las distintas líneas celulares, se estudió el efecto de las fucosidasas en la replicación de RV7, RV39 y Wa en las células dCaco-2. Respecto al RV7, el tratamiento con AfcB causó una mayor adhesión, aunque no se obtuvieron resultados significativos. A su vez, el tratamiento con fucosidasas ocasionó un aumento en la replicación, obteniendo resultados comparables con ambos virus no adaptados (RV7 y RV39). El rendimiento viral se duplicó cuando las células se trataron con las fucosidasas AfcA o AfcB de manera independiente. Sin embargo, el tratamiento simultáneo con ambas enzimas supuso el mayor rendimiento viral, incrementando 5,8 veces el título viral en el caso de RV7 y 2,8 en el caso de RV39. En cuanto a la replicación, esta fue similar cuando las células no recibieron tratamiento o fueron tratadas con AfcB, mientras que el tratamiento con AfcA o con ambas enzimas resultó en una mayor replicación. En cuanto al virus Wa adaptado a cultivos celulares, se obtuvo una mayor adhesión tras tratar las células con AfcA y con AfcB simultáneamente y un mayor rendimiento viral al emplear AfcB.

Interesantemente, resultados previos del laboratorio mostraron que la fucosa α1-4 presente en los antígenos Lewis del precursor tipo 1 (fucosa-α1-4-N-acetil-glucosamina) dificulta la unión del antígeno de H tipo 1 y sus precursores al bolsillo de unión de la proteína VP8* del genotipo P[8]. Dado que la unión de la proteína VP8* de la cepa Wa es más débil, la eliminación de la fucosa parece beneficiar la unión viral, así como incrementar el título viral después de 72 h. Además, en los virus del género *Influenza,* responsables de la gripe, está comúnmente descrito y aceptado que las actividades hemaglutinina y neuraminidasa deben estar equilibradas para garantizar una replicación idónea. Dado que, a diferencia de los virus de la influenza, los RVs no poseen su propia fucosidasa, estos podrían estar aprovechando la actividad fucosidasa proporcionada por los miembros de la microbiota. Teniendo esto en cuenta, nuestros resultados parecen indicar que para una actividad lectina (capacidad de las partículas virales para unirse a los carbohidratos) más débil (cepa Wa), la fucosidasa AfcA superaría la actividad óptima necesaria para una replicación adecuada, mientras que en el caso de lectinas de mayor afinidad presentes en los RV7 y RV39, la adición de la actividad α1-2 fucosidasa equilibraría el proceso de unión/liberación viral promoviendo la replicación óptima del virus in vitro.

La replicación de NoVs en cultivos 3D de HIEs también se vio afectada por el tratamiento con fucosidasas. En este caso, se observó una disminución de la de la adhesión, del rendimiento viral y de la replicación. Estos datos en conjunto estarían evidenciando que el tratamiento con las fucosidasas resulta perjudicial para el equilibrio de unión/liberación de NoVs humanos *in vitro*.

Por último, se estudió el papel de las fucosidasas *in vivo* en el modelo de ratón. Se observó un aumento en la eliminación de RV en ratones tratados con AfcA, con diferencias estadísticamente significativas durante los días 1 y 2 en comparación con los ratones del grupo control. Además, el periodo de excreción viral se prolongó dos días, ya que se pudo detectar ARN viral en los días 5 y 6 en comparación con el grupo de control que sólo excretó virus durante 4 días. El experimento realizado con NoV también mostró un aumento significativo en la excreción viral durante los días 1 y 4. Es importante destacar que, en el modelo de infección murino, la microbiota autóctona fue eliminada con antibióticos y, por tanto, la actividad fucosidasa fue aportada por los enzimas recombinantes. Hay que tener en cuenta que las diferencias encontradas *in vitro* e *in vivo* con la cepa Wa y los NoV procedentes del filtrado de heces podrían explicarse por anomalías en el equilibrio entre la actividad lectina y la actividad fucosidasa.

-Efecto del inhibidor de fucosidasas

Una vez confirmada la capacidad de las fucosidasas a mejorar o disminuir la replicación de RV y NoV en función del equilibrio lectina/fucosidasa en los diferentes modelos celulares estudiados, se procedió a analizar el efecto del inhibidor de fucosidasas DFJ. Inicialmente se hipotetizó que en los propios filtrados virales existía cierta cantidad de fucosidasas bacterianas, ya que, por ejemplo, AfcA y AfcB son enzimas extracelulares que pueden ser co-purificados con los propios virus después del proceso de filtración; a su vez se han encontrado muchas otras fucosidasas extracelulares en el microbioma de las heces. Los experimentos realizados *in vitro* mostraron que la infección de células dCaco-2 con RVs tratados con DFJ resultó en una disminución en la replicación viral. Mediante análisis por qPCR, se observó que la inhibición máxima se obtuvo con una concentración de DFJ 800 nM, sin embargo, se obtuvieron diferentes niveles de inhibición en función del virus utilizado. La cepa Wa también fue inhibida a pesar de su adaptación a cultivos celulares carentes de HBGAs en su superficie, lo que implicaría que la fucosidasa celular FucA1 humana, presente en los endosomas de las células huésped, también podría desempeñar un papel en las infecciones por RV *in vitro*.

El efecto del inhibidor de fucosidasas en la replicación de los filtrados de NoVs se estudió en cultivos de HIEs, disminuyendo significativamente la replicación del NoV43 cuando se utilizaba DFJ a una concentración de 2 µM.

Finalmente, se pasó a estudiar el efecto del inhibidor de fucosidasas en el modelo de infección murino. Estos fueron infectados con los virus Wa o con el filtrado de heces de NoV GII.4 Sydney 2012 junto con 20 mM de DFJ. El efecto del inhibidor se reprodujo en ambos virus, ocasionando una ligera reducción en la eliminación viral que no fue significativa durante los primeros tres días de la infección en compararon con los grupos de control. A su vez, los ratones mostraron una reducción significativa en la eliminación viral en el día 4 en ambos virus; en RV, hubo una disminución de 2,87 veces en la eliminación viral a los 4 días, mientras que en el caso de NoV humano sólo se detectó ARN viral durante 3 días en el grupo tratado.

Según la información disponible, esta es la primera vez que este iminosacárido inhibidor de fucosidasas ha sido utilizado *in vivo*, por lo que la biodisponibilidad del compuesto es desconocida, lo que podría interferir en los resultados. Los iminosacáridos se han investigado como antivirales para la gripe, el virus de la inmunodeficiencia humana, la hepatitis C y el virus del dengue, entre otros, lo que facilita el camino para la investigación de inhibidores de fucosidasas como inhibidores de RV y

NoV. En el caso de la gripe, uno de los tratamientos comercialmente disponibles consiste en un inhibidor de la neuraminidasa, es decir, un inhibidor de la actividad sialidasa. El oseltamivir, conocido comercialmente como Tamiflu, es la opción más utilizada y se administra dos veces al día durante cinco días. Múltiples estudios han demostrado la eficacia del inhibidor en la reducción de complicaciones relacionadas con la gripe y su mortalidad sin efectos secundarios graves, especialmente cuando se administra dentro de los 2 días posteriores a la aparición de síntomas. Estos datos indican que la administración ocasional de un inhibidor de GH para el tratamiento viral no implicaría riesgos para la salud. Consecuentemente, dados los cientos de miles de casos y muertes que RV y NoV causan anualmente en todo el mundo (principalmente en países de bajos ingresos) la introducción de un antiviral que reduzca esas cifras tendría un gran impacto en la salud humana.

Conclusiones

En el presente trabajo nos centramos en el efecto de las modificaciones de HBGAs en la infección por RV y NoV, es decir, sus receptores y/o co-receptores. Específicamente, en el papel de las fucosidasas. Para ello, se emplearon fucosidasas con actividades α1-2 y α1-3/4 en células dCaco-2, HIEs y en un modelo murino de infección por RV y NoV. Se detectó un aumento en la replicación de aislados clínicos de RV, la cepa de RV adaptada a cultivo celular Wa y aislados clínicos de NoV en los diferentes modelos cuando había un equilibrio entre lectina y fucosidasa. Más tarde, se evaluó un inhibidor de la fucosidasa. Nuestros resultados confirmaron que la actividad de la fucosidasa es relevante para la biología de ambos virus. El hecho de que la mayoría de los virus respiratorios con actividad de hemaglutinina lleven consigo sus propias glicosidasas para equilibrar el proceso de unión/desprendimiento, mientras que tanto RV como NoV no llevan esta actividad glicosidasa, podría explicarse por un papel de las fucosidasas de la microbiota intestinal, así como de la fucosidasa humana endosomal FucA1. Los resultados presentados aquí muestran por primera vez un nuevo objetivo terapéutico para dos virus que necesitan fucosa para su proceso de infección.

Las conclusiones más relevantes extraídas de esta tesis son las siguientes:

1. La microbiota intestinal expresa una amplia variedad de enzimas hidrolíticas, según lo determinado por el estudio del metagenoma. Entre otras, se detectó la presencia de β-galactosidasas, β-N-acetilhexosaminidasas, α-sialidasas y α-L-fucosidasas que podrían ser

utilizadas por los miembros de la microbiota para alimentarse de los glicanos del huésped presentes en la superficie del tracto gastrointestinal.

2. Las α-L-fucosidasas AfcA y AfcB demostraron una actividad fucosidasa α1-2 y α1-3/4 completa, respectivamente, en neoglicoproteínas, lo que condujo a su selección para experimentos posteriores.
3. El cribado de RV en dCaco-2 reveló un bajo porcentaje de muestras positivas capaces de replicar, lo que puede ser atribuido a la coinfección con otros virus o bacterias, presencia de inhibidores de replicación viral o a largos períodos de almacenamiento.
4. El tiempo de infección adecuado para RV en dCaco-2 es de 72 h y en HIEs es de 48 h.
5. Los aislados clínicos RV7 y RV39 replicaron de manera más eficiente en tipos celulares con expresión de HBGA, principalmente en dCaco-2 y HIEs en 3D. Por su parte, la cepa Wa adaptada a cultivo celular mostró una mayor replicación en MA104, que carece de expresión de HBGAs, reforzando así su preferencia por líneas celulares sin HBGAs.
6. La infección de aislados clínicos de RV en células dCaco-2 tratadas con la fucosidasa α1-3/4 resultó en un aumento en la adhesión viral. El tratamiento celular con la fucosidasa α1-2 mejoró la replicación viral. El tratamiento con ambas fucosidasas resultó en un efecto sinérgico donde se obtuvo el rendimiento viral máximo.
7. La infección de Wa en dCaco-2 mostró resultados significativos después del tratamiento con la fucosidasa α1-3/4 AfcB, lo que provocó un aumento en la adhesión y replicación viral, y, por lo tanto, un mayor rendimiento.
8. El papel de las fucosidasas en la infección del aislado clínico de NoV en HIEs en 3D mostró una disminución en la adhesión y replicación viral después del tratamiento con la fucosidasa AfcB.
9. La incubación de RVs con DFJ resultó en una disminución de la replicación viral en dCaco-2 tanto para el RV clínico RV7 como para el adaptado al cultivo celular Wa.
10. DFJ disminuye la replicación de NoV, como se observó tras la infección de NoV tratados con DFJ en HIEs en 3D.
11. El modelo murino con microbiota deplecionada es un modelo adecuado para el estudio de la replicación de RV y NoV *in vivo*. Los ratones infectados con RV y NoV excretaron virus durante 4 días.
12. El tratamiento con la fucosidasa AfcA en ratones que posteriormente fueron infectados con RV mostró una mayor eliminación viral los días 1 y 2 tras la infección, así como un

período de eliminación más largo que en los ratones de control. En los ratones tratados con AfcA, se detectó ARN viral hasta el día 6, mientras que solo hasta el día 4 en el grupo de control.

13. El tratamiento con la fucosidasa AfcA provocó una mayor excreción viral en ratones infectados con NoV, con diferencias significativas detectadas en los días 1 y 4 tras la infección.
14. El inhibidor de fucosidasas en ratones infectados con RV y NoV causó una disminución significativa en la excreción viral el día 4 post infección para ambos virus, donde incluso NoV no fue NoV.
15. Las propiedades antivirales de DFJ demostradas con RV y NoV en los diferentes modelos celulares y animales lo convierten en candidato para su investigación como un antiviral contra virus que infectan a través de fucosas.

V. Abstract

Rotavirus (RV) and norovirus (NoV) are enteric viruses that cause acute gastroenteritis (AGE). The symptoms associated with this disease are diarrhoea, vomiting, malaise, fever, dehydration and in the most severe cases, mortality. In 2016, RV caused the death of 128,500 children under 5 and NoV of 218,800 people of all age groups, with the majority of the cases occurring in low-income countries. Despite a substantial decrease in deaths in the last 20 years after RV vaccine (RVV) introduction, the prevalence of this disease remains a concern.

RV is a double-stranded RNA virus that belongs to the *Sedoreoviridae* family. Its virion is a triple-layered particle (TLP), being the most external layer composed of the glycoprotein VP7 and the protease-sensitive protein VP4, which define the G and P genotypes respectively. The most reported strain worldwide is G1P[8], followed by G2P[4], G3P[8], G4P[8], G9P[8] and G12P[8]. VP4 is cleaved post-translationally into the subunits VP5* and VP8*, being the second one responsible for cellular receptor interaction.

As for NoV, the leading cause of viral AGE after RVV introduction, it is a single-stranded RNA virus, polyadenylated and with positive polarity, which belongs to the family *Caliciviridae*. Its capsid is composed of VP1 and VP2 proteins, with the P2 subdomain of the VP1 at the outermost part. The genotype GII.4 Sydney 2012 is the most prevalent strain. Contrary to RV, no vaccine is available.

Histo-blood group antigens (HBGAs) act as RV and NoV receptors or co-receptors. These are complex carbohydrates found on the mucosal surfaces of the gastrointestinal tract, among others. This means that both RV and NoV have lectin activity. The synthesis of HBGAs at the digestive tract is catalysed by an α1-2 fucosyltransferase (FUT2), an α1-3 or α1-4 fucosyltransferase (FUT3) and two glycosyltransferases (A and B enzymes). FUT2 determines the secretor status while FUT3 the Lewis status. These enzymes catalyse the production of Lewis antigens (lewis^{a}, lewis^{b}, lewis^{x} and lewis^{y} antigens), H type-1 and type-2 antigens, A type-1 and type-2 antigens and B type-1 and type-2 antigens. The absence of functional FUT2 leads to secretor negative individuals while the absence of FUT3 to Lewis negative individuals, and thus, the absence of specific HBGAs. RVs and NoVs recognize HBGAs in a genotype-dependent manner, thereby the presence or absence of specific antigens affects the viral ability to infect its host cells. Secretor status is reported to be a cause of P[8] and P[4] RVs and GII.4 NoVs susceptibility.

Gut microbiota present a wide range of glycosyl hydrolases (GHs) that allow them to use the host glycans as a nutrient source. They possess fucosidases and sialidases to remove fucoses and sialic acid from the end of the glycan chains, as well as exo- and endo-β-N-acetylglucosaminidases, β-galactosidases, α-N-acetylglucosaminidases, endo-β1,4-galactosidases, and α-N-acetylgalactosaminidases. Many studies have stated the role of bacteria in the promotion of RV and NoV infections. Among other mechanisms, they might modulate viral replication by modifying the HBGAs.

The present work has been focused on the investigation of the role of the GHs of the gut microbiota on RV and NoV infections. It was hypothesized that bacterial fucosidases may modulate RV and NoV attachment and replication. To test this hypothesis, it was performed a metagenome study from infant faeces. A total of 10 bacterial fucosidases were selected and characterized. Finally, two fucosidases from the microbiota member *Bifidobacterium bifidum* JCM 1254, previously characterized, were chosen to perform further experiments, being AfcA, with α1-2 fucosidase activity and AfcB, with α1-3/4 fucosidase activity.

Later, two clinical RV isolates (RV7 and RV39) and the cell culture-adapted RV strain Wa were used to infect various cell lines with different HBGAs composition. Differentiated Caco-2 (dCaco-2), HT29, HT29 M6 and human intestinal enteroids (HIEs) were employed as cell lines bearing HBGAs, while MA104 and undifferentiated Caco-2 (uCaco-2) served as cell types without HBGAs. It was detected that clinical isolates replicated more efficiently on those cell lines displaying HBGAs on their surface, while Wa on MA104, cell type which lacks HBGAs on which Wa had been adapted. Once it was determined that HBGAs are relevant for human circulating RV infection, the role of fucosidases was studied. AfcA and AfcB fucosidases were used to treat dCaco-2 prior to RV infection. Results showed higher attachment, viral yield and replication for RV7 and RV39. A less but notable increase in viral yield was also detected for Wa. As for NoV, infections were performed on 3D HIEs. However, decreases in viral attachment, yield and replication were observed after fucosidase treatment. Fucosidases were also tested on mice. Those were infected with Wa and GII.4 NoV after treatment with AfcA, where it was detected significant increases of the viral shedding for the two viruses, even a more prolonged shedding in the case of RV.

Since both RV and NoV seemed to benefit from the fucosidase treatment, the effect of a fucosidase inhibitor, the 1-deoxyfuconojyrimicin, was also investigated. Once it was confirmed the specificity of the compound, viral stocks were incubated with different concentrations of the

inhibitor. Many assays were performed *in vitro* an *in vivo* including the infection of clinical RV isolates and Wa in dCaco-2 cells, NoV infection of 3D HIEs, and RV Wa and NoV infection of mice. All the experiments gave the same result: viral treatment with the fucosidase inhibitor caused a decrease in viral replication.

We can conclude that the HBGAs binding activity (lectin) /fucosidase balance is relevant for both enteric viruses, RV and NoV. In the *in vitro* models the addition of bacterial fucosidases resulted in an increased RV replication and this effect was found *in vivo* in RV and NoV infections in mice. Furthermore, the fucosidase inhibitor 1-deoxyfuconojyrimicin HCl showed an antiviral effect in both viruses *in vitro* and *in vivo* pointing to a new antiviral target and opening new avenues for the development of new antiviral treatments.

1. INTRODUCTION

1. Introduction

1.1. Enteric viruses and their relevance in human health. Rotavirus and norovirus classification and structure

Despite the reduction in the diarrhoeal related-deaths in the last 20 years (from 2.6M in year 2000 to 1.5M in year 2019), diarrhoeal diseases remain one of the most important causes of death in children under 5 in developing countries. According to World Health Organization (WHO), diarrhoeal diseases were one of the top 10 causes of death worldwide and the top 5 in low-income countries in 2019 [1].

Gastrointestinal viruses such as rotaviruses (RVs) and noroviruses (NoVs) cause acute gastroenteritis (AGE). A variety of symptoms are associated with this disease, including diarrhoea, vomiting, malaise, fever and dehydration among others, which in the most extreme cases may result in death. Enteric viruses are transmitted by the faecal-oral route, by direct contact with infected patients or by contact or consumption of food or contaminated water. Treatment includes rehydrating with oral fluids and taking probiotics since no antiviral medication is available [2,3].

RV is a double-stranded RNA virus that belongs to the family *Sedoreoviridae* [4], whose genome is fragmented into 11 segments. Each segment codes for one protein, except for segment 11, which codes for two. Six of the proteins are structural (VP1, VP2, VP3, VP4, VP6 and VP7) and the other six non-structural (NSP1-NSP6). RV infectious virion is an icosahedral particle with a triple-layered capsid, where the internal layer is composed of VP2 molecules. It encloses the viral genome, and the VP1 and VP3 proteins, located in the inner surface of the VP2 layer. They form the transcription complex, being VP1 the viral RNA dependent RNA polymerase (RdRp), and VP3 the capping enzyme. The core is surrounded by the middle layer capsid VP6, forming the double-layered particle (DLP). The outer layer is composed of VP7 and VP4 proteins, thus generating the triple-layered particle (TLP) (Fig. 1). These two outer capsid proteins elicit neutralizing antibodies. Furthermore, trimers of VP4 extends from VP7 as spikes, and it is composed of the subunits VP5* and VP8*, the second one responsible for cellular receptor interaction during the infection process [5]. VP4 and VP7 forms trimers, the second one being stabilized by Ca^{2+}. Removal of Ca^{2+} *in vitro* causes the dissociation of VP7 and VP4 outer membrane [6–9].

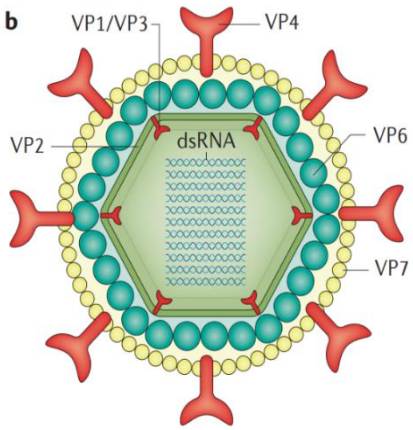

Figure 1. *Structure of RV.*

RV structure consists of an inner layer of VP2, a middle capsid layer of VP6 and an outer one of VP7 and spikes of VP4. The core is constituted by VP2, the transcription complex formed by VP1 and VP3, and the viral genome. VP6 protein defines RV groups. The external capsid layer protein VP4 is proteolytically cleaved in VP5* and VP8* subunits. VP4 and VP7 elicit immune response [10]. This is a schematic representation and it's not in proportion.

Based on the sequence and antigenic differences of VP6, RVs are classified into 10 groups (A-J), where group A is responsible for most human infections. This group is further classified into P and G genotypes. P genotypes are based on sequence differences of the protease-sensitive protein VP4, where 58 genotypes are found, while G genotypes depend on the sequence differences of the glycoprotein VP7, where 42 genotypes have been described [11]. Since VP4 and VP7 are coded by different segments, a great variety of combinations can be found. Globally, the most reported strains are G1P[8], G2P[4], G3P[8], G4P[8], G9P[8] and G12P[8], with G1P[8] being the most prevalent worldwide.

Most human RV infections occur in infants and children. Currently, there are oral, live attenuated RV vaccines (RVVs) from human and/or animal strains that replicate in the human intestine, eliciting an immune response. Rotateq obtained the WHO prequalification in 2008, Rotarix in 2009 and Rotavac and Rotasiil in 2018. Rotateq and Rotasiil are pentavalent, being the first one composed of the human-bovine reassortants G1, G2, G3, G4, and P[8], and the second one of G1, G2, G3, G4 and G9. Rotarix and Rotavac are monovalent, being Rotarix composed of G1P[8] and Rotavac of G9P[11]. Up to now, 116 countries have included them in their universal vaccination program: 76 countries use Rotarix, 16 countries Rotateq, 8 use Rotarix and Rotateq, 3 use Rotavac, 3 use Rotasiil and 1 uses Rotavac and Rotasil [12,13].

Despite that 48% of the global population is unvaccinated and 32% do not have access to the vaccine [14], thanks to RVVs introduction the number of child deaths associated with RV has

decreased from 518,000 (range, 465,000–591,000) in 2000 to 215,000 (range, 197,000–233,000) in 2013 [15], 146,000 (118,000–183,000) in 2015 [16] and 128,500 (104,500-155,600) in 2016 [17]. The trend keeps decreasing but an alarming number of children keep dying every year because of RV infections.

After the introduction of RVVs, NoVs have been replacing RV outbreaks. Regarding NoVs, they belong to the *Caliciviridae* family, and have a polyadenylated single-stranded RNA of positive polarity, which is covalently bound to a non-structural protein NS5 at the 5' end and polyadenylated at the 3' end. Its genomic RNA codes for three open reading frames (ORFs), where ORF1 codes for a large polyprotein that is proteolytically cleaved into six mature non-structural proteins (NS1/2 to NS7). These proteins are p48 (NS1/2), nucleoside-triphosphatase (NTPase, NS3), p22 (NS4), VPg (viral protein genome-linked, NS5), protease (NS6) and the RdRp (NS7). The ORF2 codes for the major capsid protein VP1 and ORF3 for the minor structural protein VP2 (Fig. 2). There is also a subgenomic RNA which codes for ORF2 and ORF3 and it is also covalently linked to the VPg protein at the 5' end and polyadenylated at the 3' end. 90 dimers of VP1 compose the viral capsid, which is further subdivided into the shell (S) and protruding (P) domains. The S domain alone, which is highly conserved, can assemble the capsid shell. The P domain, on the other hand, is more variable and consists of two subdomains, P1 and P2. The P1 domain connects S and P2 that is VP1 outermost structure, thus acting as a target for neutralizing antibodies and key to host receptor interactions. VP2 interacts with the S domain of the VP1 and stabilizes the formation of the capsid [18].

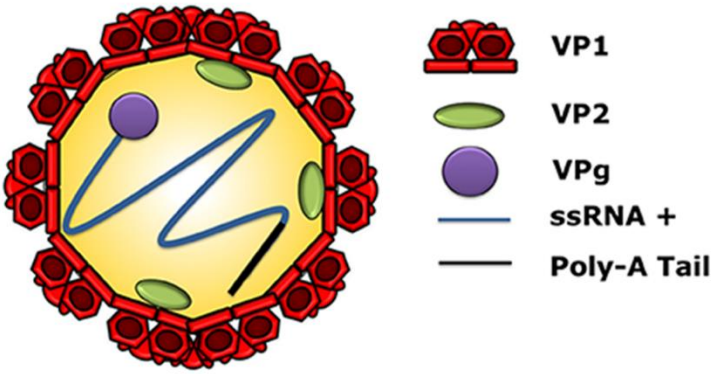

Figure 2. *Structure of NoV.*
NoV structure consists of the major capsid protein VP1 and the minor capsid protein VP2. VP1 is divided in the S and P domains. P is further subdivided in P1 and P2, being P2 found in the most external part, thus eliciting neutralizing antibodies. VP2 is found in the core virion along with viral genome. VP2 confers stability to the virion. Viral genome is covalently bound to VPg protein at the 5' end and polyadenylated at the 3' end [19]. This is a schematic representation and it's not in proportion.

The classification of NoVs is based on VP1 amino acid sequence diversity, and 10 genogroups have been described so far (GI to GX). The ones able to infect humans are GI, GII, GIV, GVIII and GIX, the two first ones responsible for most cases [20]. Genogroups are then subdivided into genotypes, where GII.4 is more prevalent, followed by GII.3 [21]. New GII.4 variants have emerged every 2 to 3 years since 1990, which include GII.4 US95/96 strain in 1995, GII.4 Farmington Hills in 2002, GII.4 Hunter in 2004, GII.4 Den Haag in 2006, GII.4 New Orleans in 2009, and GII.4 Sydney in 2012 [22]. Up to now, a total of 49 genotypes have been described [20].

At this moment there is no NoV vaccine available, which could be due to the extreme diversity presented by NoVs, the incomplete understanding of immunity to NoVs, and the lack of a robust cell culture system or animal model to replicate human NoVs [23–25]. Despite this fact, there are some NoV vaccine candidates, as HIL-214, previously known as Tak-214, firstly developed by Takeda Pharmaceuticals and then by HilleVax. It is a VLP-based bivalent, made of GI.1 and GII.4, and it has passed clinical phase 2b with promising results, since it can provide cross protection, and is also well tolerated [24,26].

1.2. Rotavirus and norovirus replication cycle

The first step in RV and NoV infection is the viral attachment to target cells, the mature enterocytes of the small intestine. In the case of RV, VP4 is proteolytically cleaved into VP5* and VP8*

subunits by trypsin, which enhances viral infectivity and facilitates virus entry into cells. The three subunits of the VP4 trimer remain associated with the virion after the cleavage. Once proteolysis has taken place, the spikes are well defined and appear dimeric protrusions (the third trimer subunit remains within the shell), contrary to the unproteolyzed spikes (not visible by standard cryo-electron microscopy), which leads to a lower infectivity. This indicates that the proteolysis of the VP4 spikes makes the viral entry more efficient [27–29]. After VP4 cleavage, RV attachment to host cells is mediated by the VP8* subunit, and it has been described that integrins [30,31], sialic acid (SA) [32], Hsc70 [33,34] and histo-blood group antigens (HBGAs) [35] act as viral receptors or co-receptors. Following binding, RV particles enter the cells by endocytosis or direct membrane penetration, leading to the release of DLPs in the cytoplasm [27] (Fig. 3). The transcription complex formed by the RdRp, VP1 and capping enzyme VP3 together with VP2 and VP6 generates capped positive single-stranded RNAs from each of the 11 double-stranded RNA genome segments, which are released to the cytoplasm from inside the DLPs. The transcripts are then either translated (early in the replication cycle) or used as templates for the synthesis of the double-stranded RNA genome (late in the replication cycle). NSP2 and NSP5 interaction results in the formation of cytoplasmic inclusions bodies, known as viroplasms. Such viroplasms concentrate the viral components required for genome assortment and replication and the assembly of viral particles. In these inclusions, several interactions between VP1, VP2, VP3, VP6 and NSP6 with the positive single-stranded RNA take place, which results in the assortment and packaging of the RNA into cores, where VP1 and VP2 trigger double-stranded RNA synthesis [36]. DLPs are then formed by the addition of the VP6 layer. DLPs bud from viroplasms into adjacent cellular membranes, where NSP4 is inserted and acts as an intracellular receptor for DLPs by interacting with VP6 [37]. DLPs are transiently enveloped. NSP4 serves as a viroporin, which creates pores and facilitates the increase of cytoplasmic Ca^{2+} levels required for viral particle formation [38]. DLPs then acquire the outer-capsid proteins VP7 and VP4. RV TLPs are released from non-polarized cells by lysis or by budding process in polarized cells. As for the function of NSP1, it antagonizes host interferon (IFN), which facilitates the evasion of immune responses [39]. NSP3 inhibits host protein translation [40,41].

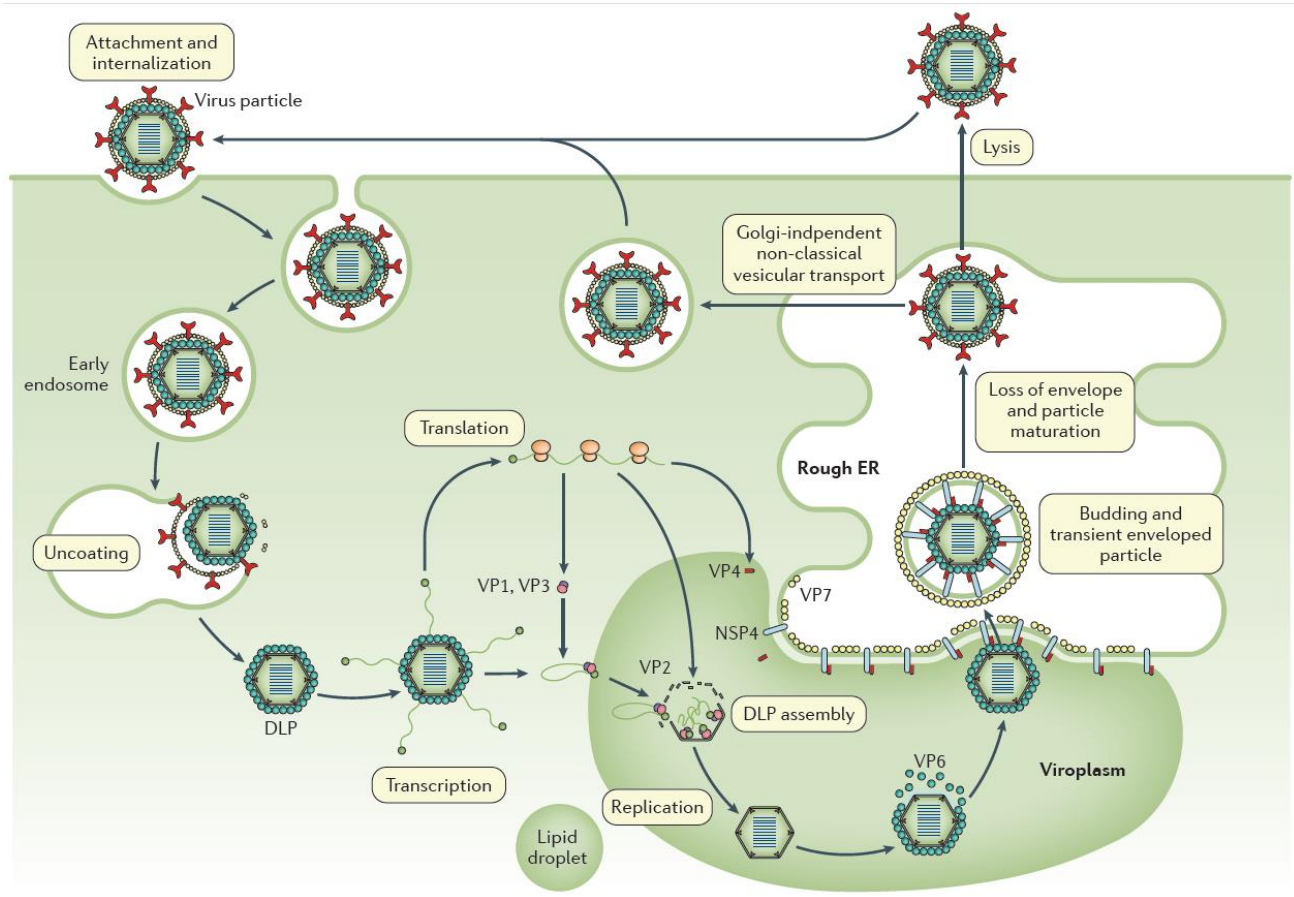

Figure 3. *Rotavirus replication cycle.*

Attachment of RV to host cells is mediated by the VP8* subunit. After binding, RV particles enter the cells through endocytosis or direct membrane penetration, releasing DLPs in the cytoplasm. The transcription complex, formed by RdRp VP1 and the capping enzyme VP3, with VP2 and VP6, generates capped positive single-stranded RNAs, which are released from the DLPs and are either translated or used as templates for the synthesis of double-stranded RNA genome. NSP2 and NSP5 form viroplasms that concentrate viral components required for genome assortment and replication. VP1, VP2, VP3, VP6 and NSP6 interactions in viroplasms lead to RNA assortment and packaging into cores, where VP1 and VP2 trigger double-stranded RNA synthesis. DLPs are formed by adding the VP6 layer, then bud from viroplasms into cellular membranes, with NSP4 acting as an intracellular receptor and also increases cytoplasmic Ca^{2+} levels. Then, DLPs are transiently enveloped, and then acquire the outer-capsid proteins VP7 and VP4. Finally, TLPs are released by lysis or budding processes. Adapted from [10].

In the case of NoVs, it is the P domain the one responsible for host cell interactions. P1 subdomain has moderate sequence diversity, while P2 has a highly variable amino acid sequence [42], which is the most exposed part of the particle and contains the receptor binding sites. The HBGAs have been described as human NoV receptors. Following viral attachment, NoVs particles are internalized by endocytosis or direct penetration (Fig. 4). Then, they are disassembled, releasing viral RNA in the cytoplasm. Once the VPg-linked RNA is released, VPg recruits host cell translation initiation factors [43], which results in the translation of the non-structural polyprotein and the VP1 and VP2 proteins. The protease NS6 is auto-cleaved, which later cleaves the rest of the NS proteins that have

specific functions in the replication and infection process [44]. After that, the positive single-stranded RNA is transcribed into negative RNA, which are used as templates for the synthesis of new positive genomic and subgenomic RNA by the action of RdRp. VPg, NTPase, and p48 participate in this process. Finally, it takes place the viral assembly, encapsidation and exit. The lack of human NoV replication models hinders the understanding of the complete process of the NoV replication.

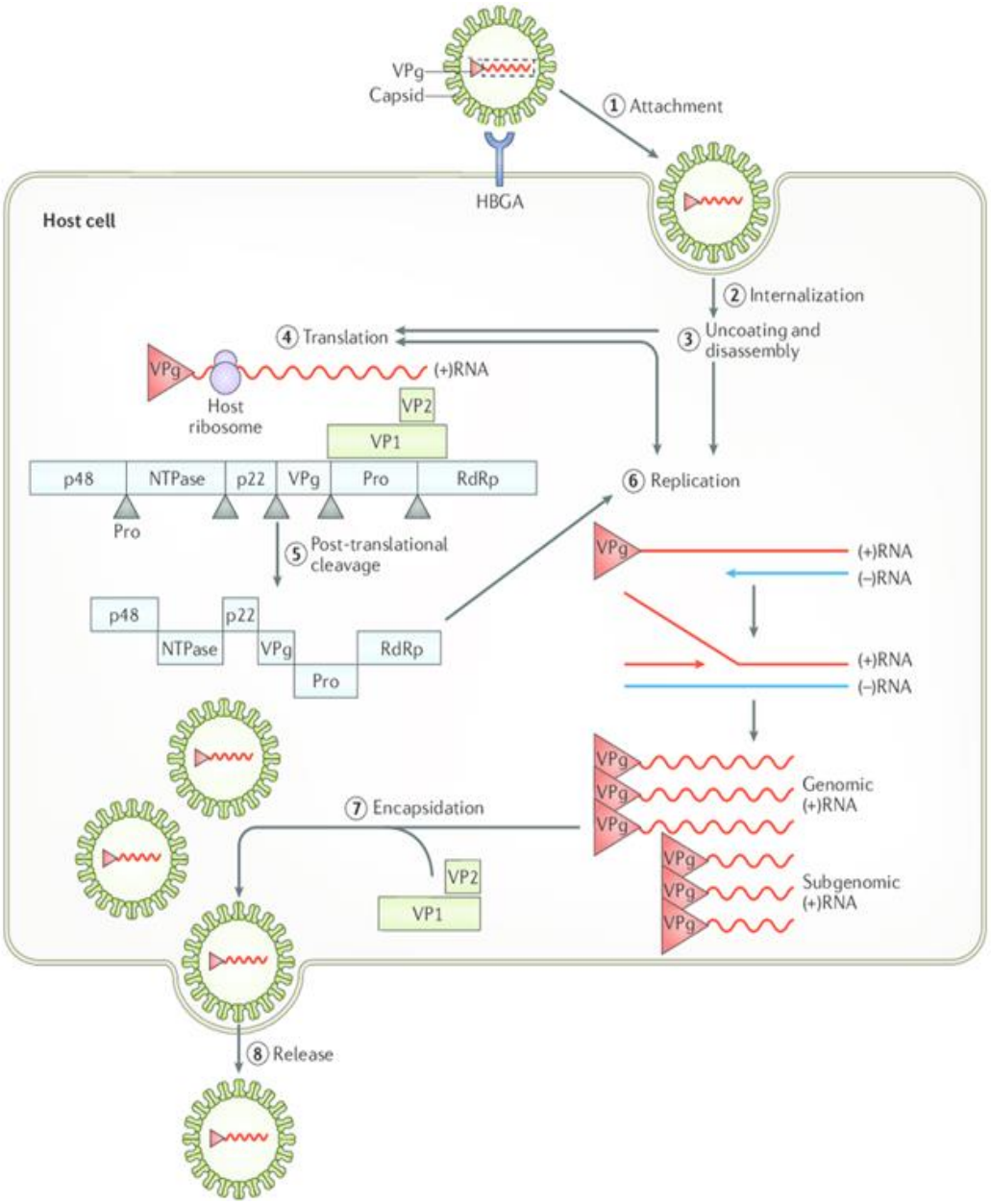

Figure 4. *Norovirus replication cycle.*

Following attachment to cellular receptors, NoV particles are internalized by endocytosis or direct penetration. Subsequently, disassembly of the particles releases viral RNA into the cytoplasm. The VPg recruits hots cell translation initiation factors, leading to the translation of the non-structural polyprotein and VP1 and VP2 proteins. The NS6 protease undergoes auto-cleavage, which later cleaves the remaining NS proteins. Then, the positive single-stranded RNA is transcribed into negative RNA, serving as templates for the synthesis of new positive genomic and subgenomic RNA by the RdRp enzyme, assisted by VPg, NTPase, and p48. Finally, viral assembly, encapsidation and exit take place [45].

1.3. HBGAs as rotavirus and norovirus receptors

In both, RVs and NoVs, HBGAs act as receptors to initiate viral infections, this implies that both viruses possess lectin activity. HBGAs are complex carbohydrates that not only are present on the surface of red blood cells but also in many other tissues, as mucosal surfaces of the respiratory, genitourinary and digestive tracts; as well as in the form of free oligosaccharides in some biological fluids, such as saliva, blood and milk [46].

The synthesis of HBGAs is carried out by stepwise addition of monosaccharides to precursors, by the action of glycosyltransferases coded by three major HBGA gene families. These three gene families are known as the secretor, Lewis and ABO families that code for an α-1,2 fucosyltransferase (FUT2), an α-1,3 or α-1,4 fucosyltransferase (FUT3) and two glycosyltransferases (A and B enzymes), respectively. The two precursors that can be modified by FUT2 and FUT3 enzymes are: type-1 precursor (galactose-β1-3-N-acetyl-glucosamine, known as lacto-N-biose (LNB)), and type-2 precursor (galactose-β1-4-N-acetyl-glucosamine, known as N-acetyl-lactosamine). FUT3 adds an L-fucose to the N-acetyl-glucosamine of type-1 and type-2 precursors with an α1-4 or α1-3 linkage, respectively, generating Lewis^a (Le^a) antigen in the first case, and Lewis^x (Le^x) in the second one. On the other hand, FUT2 adds a fucose to the precursors through an α1-2 linkage, thus generating type-1 and type-2 H antigens. Type-1 and type-2 H antigens can be further modified by FUT3, A or B enzyme. FUT3 adds an L-fucose to the N-acetyl-glucosamine of those antigens by α1-4 or α1-3 linkage, resulting in Lewis^b (Le^b) and Lewis^y (Le^y) antigens; A enzyme adds a N-acetyl-galactosamine to the galactose by α1-3 linkage, generating A type-1 and A type-2 antigens; and finally B enzyme adds a galactose to the galactose by α1-3 linkage, generating B type-1 and B type-2 antigens (Fig. 5) [46–48].

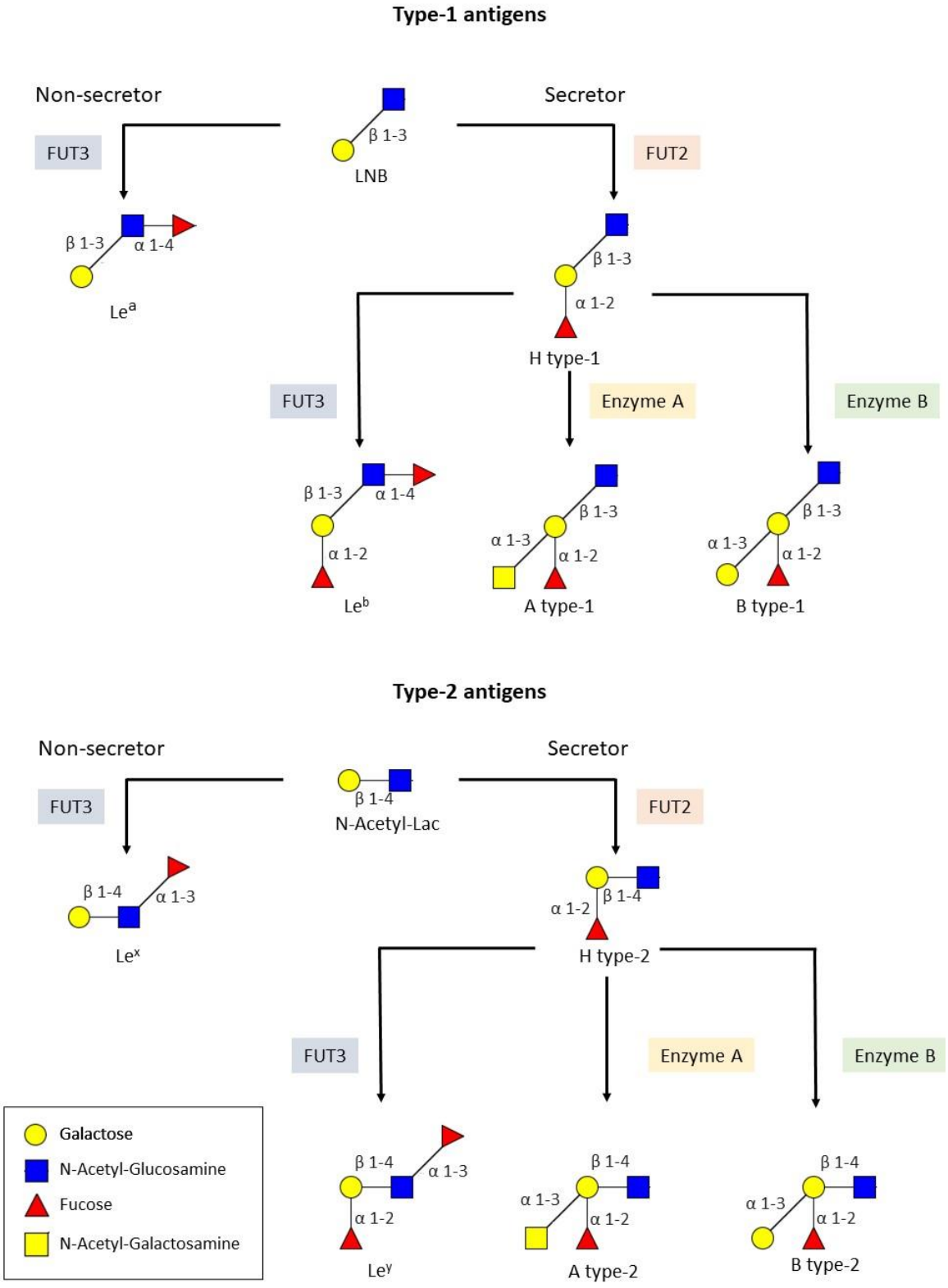

Figure 5. *Biosynthesis route of HBGAs.*

Type-1 and type-2 precursors are modified by either FUT3 that adds fucose in α1-3/4 to N-acetyl-glucosamine, or FUT2 that adds fucose in α1-2 to the galactose, to produce Lewis or H antigens. H antigens can be modified by FUT3, A or B enzymes, to produce Lewis, A or B bloods groups, respectively. LNB, lacto-N-biose; Le^a, $Lewis^a$; Le^b, $Lewis^b$; H type-1, H type-1 antigen, A type-1, A type-1 antigen; B type-1, B type-1 antigen; N-Acetyl-Lac, N-acetyl-lactosamine; Le^x, $Lewis^x$; Le^y, $Lewis^y$; H type-2, H type-2 antigen, A type-2, A type-2 antigen; B type-2, B type-2 antigen. Adapted from [48].

FUT2 and *FUT3* are polymorphic genes, which result in the absence or decreased amount of type-1 and type-2 H antigens in the case of *FUT2*, and the absence or decreased amount of Lewis antigens in the case of *FUT3*. Individuals who lack functional FUT2 are known as non-secretors, while the ones without FUT3 as Lewis negative individuals. Due to the role that HBGAs play as RV and NoV receptors, the presence or absence of specific antigens affects the viral ability to infect its host cells. As HBGA distribution varies widely between populations and ethnic groups, this is an important factor to consider regarding vaccine efficacy and protection in different populations [49–51].

1.3.1. Rotavirus and HBGAs

RVs bind HBGAs in a P genotype-dependent manner because it is the VP4 protein the one that interacts with the HBGAs (the viral lectin). Studying these recognition pattern provides new information about genetic susceptibility and RVV effectiveness among different populations.

P[4] and P[8] were reported to recognize Le^b and H type-1 HBGAs [52], but other authors found no interaction of the P[8] with the Le^b [53]. P[6] VP8* only binds H type-1 [52], while P[9], P[14] and P[25] were found to specifically bind A antigen [54–56]. P[11] binds type-2 precursor [57,58] and, as for P[19], it recognizes mucin core glycans with the GlcNAc-β1-6-GalNAc motif and the type-1 HBGA precursor [59].

Several studies have also been performed in order to elucidate the role of secretor status in susceptibility to RV infections. Studies conducted in Spain, USA and France concluded that 99-100% of patients infected with RVs were secretors and <1% non-secretors, while the proportion of non-secretors in control groups was 30% in Spain, 23% in USA and 19% in France [60–62]. In the Spanish and French studies all the individuals were infected with P[8] RV and in USA 90% with P[8], 9% with P[4] and 1% unknown. These studies indicate that positive secretor status was strongly associated with susceptibility to P[8] and P[4] genotypes, which aligns findings from other investigations [63,64]. As for Lewis positive or negative status, studies concluded that Lewis negative individuals are more susceptible to be infected with P[6] genotype [65–68]. Such differences in RV specificity could explain why RVV efficacy varies in different countries.

P[4] and P[8] RV infections predominate in Europe, North and Central America and Asia, where secretor individuals are more common (80% of secretors vs 20% of non-secretors in Caucasians) [69]. As for Sub-Saharan Africa, where Lewis negative individuals are more common (32% of Lewis negative individuals in Africa vs 6-8% in Europe), it is P[6] the predominant genogroup [70]. These differences in HBGA distribution and specificity of RV infection may be one of the reasons why RVVs are less effective in certain countries. A systematic review reported that vaccination in low mortality countries provides higher protection against severe RV AGE (more than 90%) as compared to high mortality ones (35-54%) in children followed up to 2 years after vaccination (Table 1) [71]. This could be explained by the fact that regions with high mortality rates have a higher prevalence of the P[6] genotype. Since the existing vaccines do not offer protection against this genotype, this results in an unprotected population against the circulating RV.

Table 1. *Vaccine efficacy depending on the mortality rate of countries in children followed up two years after vaccination.*

	Vaccine efficacy		
Vaccine	**Low mortality countries**	**Medium mortality countries**	**High mortality countries**
Rotarix	90%	77%	35%
RotaTeq	96%	79%	44%
Rotasiil	No data	No data	44%
Rotavac	No data	No data	54%

No studies were conducted in low and medium mortality countries for Rotasiil and Rotavac vaccines. Data obtained from Bergman *et al* 2021 [71].

1.3.2. Norovirus and HBGAs

The outermost part of the P domain, P2, acts as the as the viral lectin binding to HBGAs. ELISA-based binding assays, saliva binding assays or carbohydrate binding assays are normally performed to elucidate the recognition pattern of NoVs with HBGAs, which use P particles or VLPs (virus-like particles), that retain HBGA-binding function. These studies determined that the prototype Norwalk (GI.1) binds both A and H antigens, VA387 (GII.4) recognizes A, B and H antigens, MOH (GII.5) and Hiro (GII.12) binds to A and B and VA207 (GII.9) to Le^x and Le^y [47,72].

As for the relevance of secretor status in NoV infections, there is not a clear conclusion yet. Secretor status was found to be associated with susceptibility to GII.6 in a foodborne outbreak in Sweden. Among secretor individuals, 56% reported diarrhoea and/or vomiting, compared to 17% of non-secretors [73]. In another study, NoV predominantly infected children with secretor status, only 1.5% of infected children were non-secretors, compared to the 18% in the control group. The majority of genotypes were GII.4 Sydney (76%) and GII.17 (10.9%) [74]. Lopman *et al* concluded that all infections caused by GII.4 in a study conducted in Ecuador occurred in secretor children. However, infections with non GII.4 were higher in non-secretor individuals [75]. Reyes *et al* also concluded that the incidence of NoV GII was 4-fold higher in secretors than in non-secretors, but in the case of GI, the incidence was similar in both groups [76]. However, other study found the opposite results, where secretor status was associated with GI infections, but not with GII [77]. Another study of a foodborne outbreak in Sweden with GI.3 NoV reported that symptoms had the same frequency in secretors and non-secretors individuals [78]. Rodriguez *et al* found that salivary Ig-A titers against a mix of GI.1, GII.4 and GII.9 NoV P-particles were significantly higher in secretor-positive individuals [79]. These findings suggest, with some exceptions, that secretor individuals are susceptible to suffer from GII.4 NoV infection, whereas non-secretors are resistant to this genotype. However, non-GII.4 genotypes appear to infect people regardless their secretor status.

The parenteral NoV vaccine now being developed by HilleVax show that secretors and non-secretors had a similar total immunoglobulin response to a single dose of the vaccine [80].

1.3.3. Microbiota and host glycans

Not only RVs and NoVs take advantage of host glycans but also the microbiota. Up to 86% of the human gut microbiome codes for genes responsible for the cleavage of the carbohydrate moieties of mucins and human milk oligosaccharides, with 89% encoding genes to metabolize the resulting monosaccharides [81], since they use host glycans as a nutrient source. The mucins are highly glycosylated proteins, being MUC2 the one that represents the major soluble and gel-forming mucin at the small intestine and colon [82,83]. Mucin glycan degradation by the microbiota involves the action of glycosyl hydrolases (GHs), a group of enzymes that hydrolyse the glycosidic bonds between carbohydrates or between a carbohydrate and a non-carbohydrate moiety. Initially, they

target fucoses and sialic acid, present at the terminal location of the mucin oligosaccharides chains, which prevents the action of other GHs.

α-L-Fucosyl residues are commonly found at the end of glycoconjugates, such as blood group antigens, milk oligosaccharides, gastric and submaxillary mucins, and serum glycoproteins. The most relevant α-L-fucosidase enzymes belong to GH29 and GH95 families, which differ in their mechanism of action. A total of 98 and 18 have been characterized, respectively [84]. These enzymes are present in numerous members of the gut microbiota, including *Bifidobacterium bifidum* [85], *B. longum* [86,87], *Ruminococcus gnavus* [88] or *Akkermansia muciniphila* [89]. Three intracellular α-fucosidases from the GH29 family found in lactobacilli have been characterized, being AlfA, AlfB and AlfC [90]. The first one releases α1-6 fucose residues from some oligosaccharides with low efficiency. On the other hand, AlfB removes α1-3 fucose and AlfC α1-6 fucose of fucosyl-N-acetylglucosamine with high efficiency [90]. *B. bifidum* codes for an extracellular α1-2 fucosidase named AfcA, which belongs to the GH95 family. It showed complete activity on 2'-fucosyllactose, and partial on lacto-N-fucopentaose I and H type-1 antigen, all of them containing an α1-2 fucose [91]. *B. bifidum* also codes for AfcB, another extracellular enzyme with α1-3/4 fucosidase activity. This fucosidase was able to remove the fucose from the tested substrates containing α1-3/4 fucoses [85].

Sialic acid is another source of nutrients located at the ends of the mucin glycan chains, being N-acetylneuraminic acid (Neu5Ac) the most common form of sialic acid found in humans. Sialidase activity can be found in *Clostridium perfringens* [92], *R. gnavus* [93], *A. muciniphila* [94], and some strains of *Bifidobacterium* such as *B. bifidum*, *B. breve*, *B. dentium*, *B. longum*, *B. mongoliense* and *B. scardovii* [84,95,96]. They all express GH33 sialidases, also known as neuraminidases. In bacteria, the genes involved in the metabolism of sialic acids are usually found clustered as a Nan cluster. However, some bacteria have incomplete packages of enzymes for using sialic acid, since some of them encode the sialidase but lack de Nan operon required to consume the released monosaccharide [97], while others, as the pathogen *Clostridium difficile*, encode de Nan operon but not the sialidase [98].

Later, the rest of monosaccharides and oligosaccharides that compose the glycan moieties are available to be cleaved by exo- and endo-β-N-acetylglucosaminidases (GH84, GH85), β-galactosidases (GH2, GH20, GH42), α-N-acetylglucosaminidases (GH89), endo-β1,4-galactosidases (GH98) and α-N-acetylgalactosaminidases (GH101, GH129) [84].

1.4. Enteric viruses and microbiota

Enteric viruses, such as RV and NoV, infect the gastrointestinal tract, a complex ecosystem where host, bacteria, viruses, fungi and pathogens continuously interact. Although bacterial composition depends on the genetics, diet, and health status, among others, a core microbiome is shared between individuals. In adulthood, gut microbiota is predominated by *Bacillota* and *Bacteroidota* (former *Firmicutes* and *Bacteroidetes*), with lower abundances of *Pseudomonadata and Actinomycetota* (former *Proteobacteria* and *Actinobacteria*) [99]. The establishment of the microbiota begins during childhood, influenced by prenatal and postnatal factors (delivery mode, breastfeeding, use of antibiotics, etc.) [100]. RVs and NoVs have co-evolved with the bacterial gut microbiota, so some aspects of virus infectivity may be modulated by them, either by promoting inhibitory effects or infectivity through numerous mechanisms.

1.4.1. Bacterial inhibition of rotavirus and norovirus infections, *in vitro* and animal model studies

Due to their beneficial effects against enteric viral infections, bacteria play an important role in maintaining human health. The proposed mechanisms include bacterial binding to receptors, thus blocking viral attachment, as well as attachment to viruses which facilitates their elimination through faeces. Also, stimulating the host immune system, mucus secretion and changes in glycosylation pattern on the surface of target cells, along with others (Fig. 6) [2,48,101].

Many studies have demonstrated the role microbiota has in protection against RV and NoV infections. Segmented filamentous bacteria incubation with RV reduces infectivity *in vitro* and it also protects mice against RV infection [102]. The colonization of gnobiotic pigs with *Escherichia coli* Nissle 1917 resulted in a significant reduction in RV shedding titters by modulating an immune response [103–106] and also incubation of Caco-2 cells with such bacteria caused a 50% reduction in RV attachment [103]. HT29-MTX cells were incubated with bacteria-derived soluble factors from *Bacteroides thetaiotaomicron* and *Lacticaseibacillus casei*, which resulted in the blockage of RV infection by modifying the cell surface glycans [107]. Both Caco-2 and HT29-MTX are transformed cell lines widely used in the study of RV thanks to the expression of HBGAs on their surface and their resemblance to human gut, as later explained in section 1.6.1. Additionally, bacterial flagellin induces the production of IL-22 and IL-18, which prevent RV infection in mice [108]. *Ruminococcus gauvreauii*

can bind RV by HBGA-like substances in bacterial surface, which resulted in a 3-fold decreased RV replication in Caco-2 cells [109].

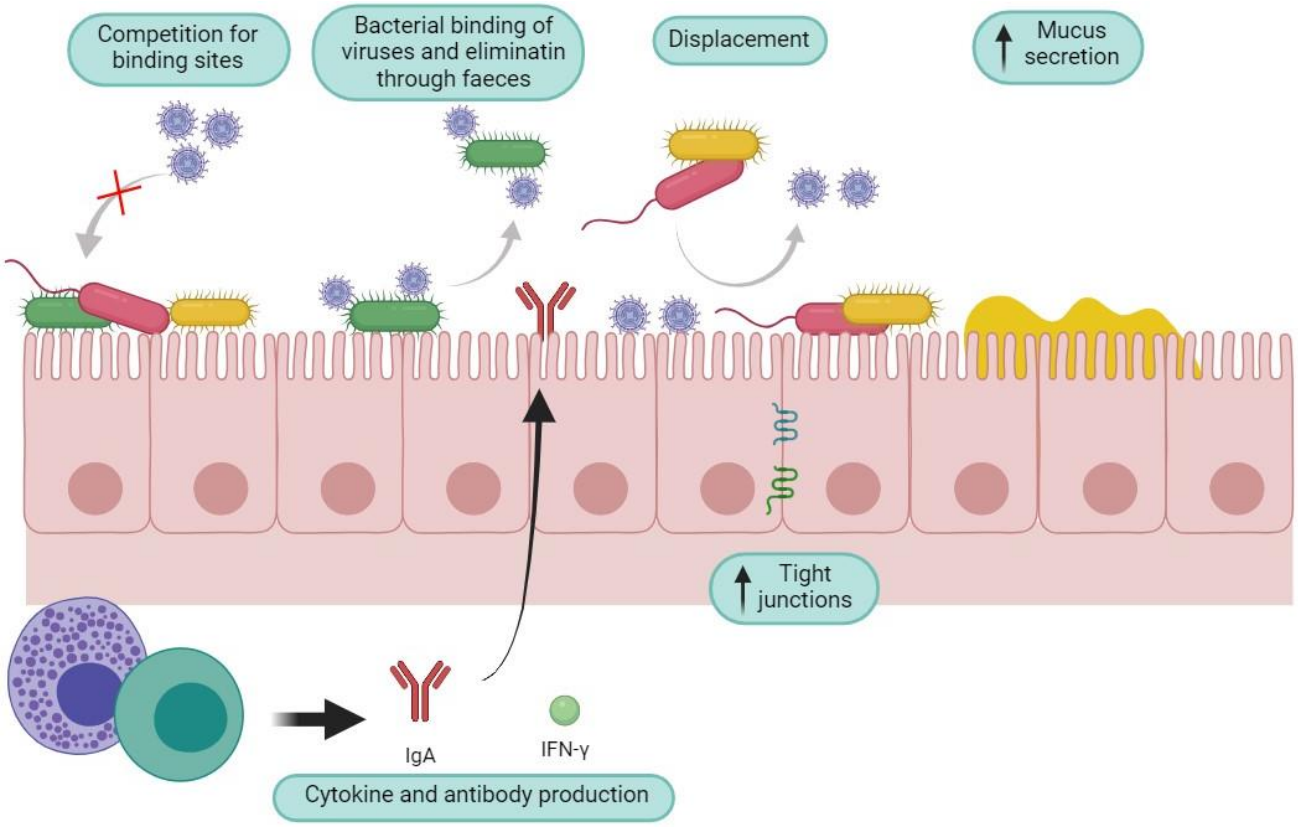

Figure 6. *Mechanisms by which microbiota inhibits viral infections.*
Microbiota can inhibit the replication of enteric viruses by a great variety of mechanisms, which include competition for binding sites, bacterial binding to viruses, displacement, mucus generation and stimulation of immune system, among others.

As for NoV, *L. case*i, *E. coli* Nissle 1917 and *Bifidobacterium adolescentis*, prevented the attachment of GI.1 VLPs or P-particles *in vitro* [110,111]. It also has been proven that a reduced virus faecal shedding was obtained when gnotobiotic pigs colonized with *Lacticaseibacillus rhamnosus* GG and *E. coli* Nissle 1917 were infected with NoV GII.3 and GII.4 genotypes [112].

1.4.2. Bacterial promotion of rotavirus and norovirus infection, *in vitro* and animal model studies

Intestinal microbiota is able not only to inhibit RV and NoV infection, but also promote it. Kuss *et al* [113] and Kane *et al* [114] were the first to demonstrate that microbiota can enhance viral infections by infecting germ-free and antibiotic-treated mice with poliovirus, reovirus and mouse

mammary tumour virus (MMTV). A decrease in viral infections was observed when compared to infections of microbially-colonized mice. They found that poliovirus binds lipopolysaccharides on the surface of bacteria, which significantly enhanced yield [113], as also does MMTV [114,115]. According to these findings, enteric viruses exploit intestinal microbes for replication and transmission.

Microbiota might facilitate RV and NoV infection through different mechanisms, that include stabilization of virions, promotion of virus attachment to host cells and alteration of antiviral immune response (Fig. 7) [2,48,101].

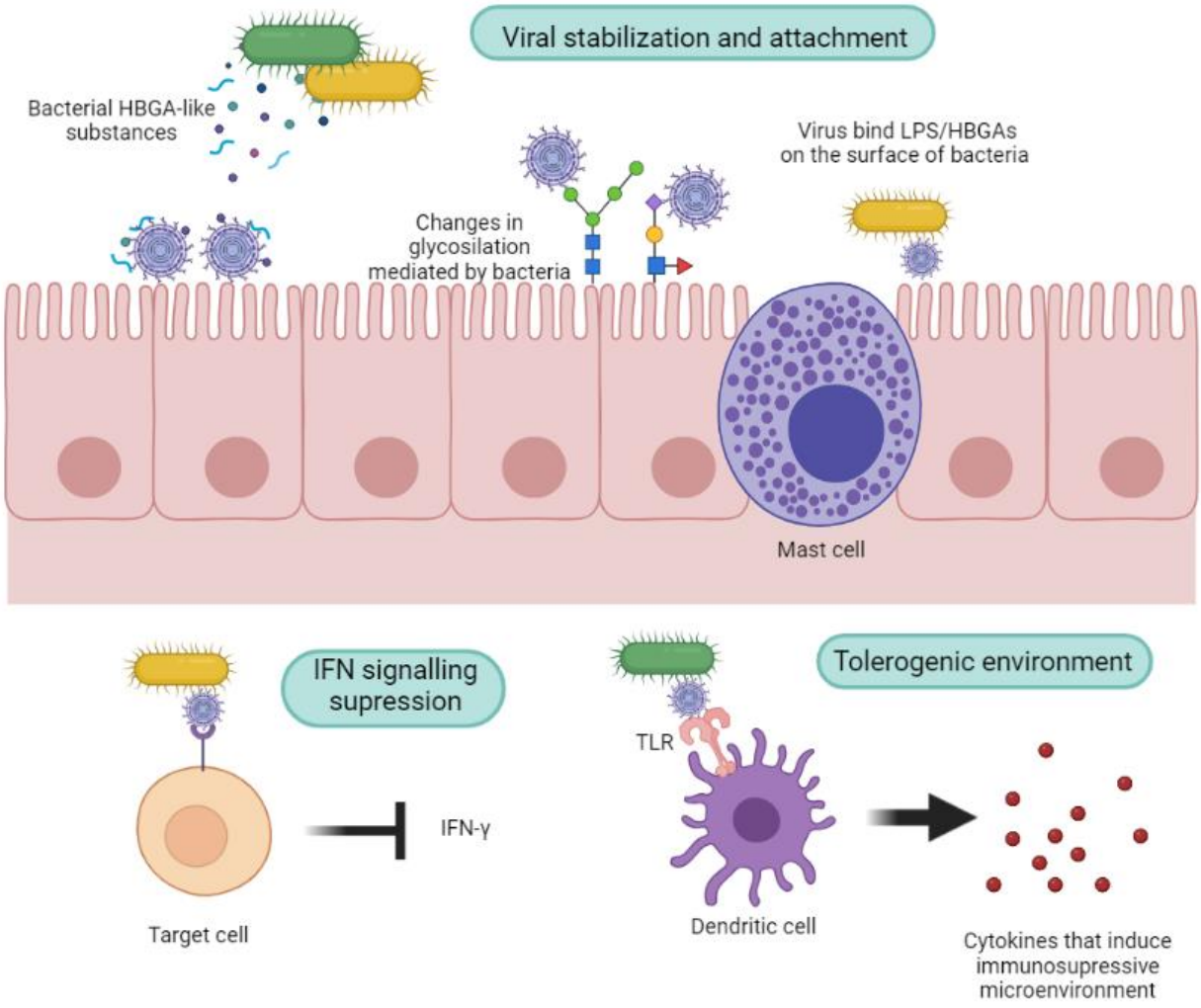

Figure 7. *Mechanisms by which microbiota promotes viral infections.*
Microbiota can promote the replication of enteric viruses by stabilizing virions and their attachment and modifying immune responses.

By infecting B cells with faecal samples with NoV GII.4, Jones *et al* found that filtered samples have a reduced infection when compared to unfiltered ones. It is possible that the virus attaches to the HBGA-like sugars present on bacteria's surfaces [116]. Some of the bacterial species that express

HBGA-like sugars are *Enterobacter cloacae*, *E. coli* and *Helicobacter pylori*. Also, incubation of filtered samples with synthetic H antigen or inactivated *E. cloacae* restored their infectivity, thus confirming that NoV interactions with HBGA-like substances could facilitate the infection of and attachment to B cells. It was also discovered that *H. pylori* could also promote NoV replication by modulating the expression of HBGA in the host, since the virulence factor CagA is related to the expression of HBGAs [117]. Additionally, it was found that NoV P-particles enhanced their attachment to HT29 cells when cells were pre-treated with lactic acid bacteria or when adding bacteria to cells with already attached P-particles (more than 4-fold increase). It was suggested that bacteria might prevent their release with washes and increase P-particle retention on cell surface. Rubio *et al* also found that when P-particles and bacteria were added at the same time to cells, it resulted in a reduction of P-particles attachment, which may be explained by the reduction of available P-particles to bind cells due to their interaction with bacteria in suspension [111]. It was also demonstrated that gnobiotic pigs with human gut microbiota transplantation resulted in increased GII.4 NoV shedding when compared to germ free gnobiotic pigs [118]. Finally, Eshaghi *et al* investigated the effect of *B. bifidum* in NoV VLPs attachment to oyster digestive tissue extract [119]. Oysters filtrate water, and in the case of contamination, they can accumulate NoVs thanks to the presence of HBGA-like carbohydrates on their intestines [120]. As for *B. bifidum*, it codes for two fucosidases with α1-2 and α1-3/4 activities [85]. It was found that the treated extract attracted significantly more VLPs than the untreated one [119].

Based on the above statements, it is clear that gut microbiota plays a dual role in RV and NoV replication through a wide range of mechanisms, instead of being only a protective factor for the host.

1.4.3. Microbiota in rotavirus and norovirus infection, human studies

Gut microbiota varies greatly among populations, which may be attributed to age, sex, diet, health status and antibiotic use. Additionally, different faecal microbiota profiles are also found in healthy individuals with different HBGA composition [121,122], highlighting the influence of host genetics on the intestinal microbiome composition. The modulation of the gut microbiota depending on the availability of fucosylated carbohydrates may be related to the ability of some intestinal bacteria to use L-fucose as a carbon source, thus facilitating their growth and that fucosylated HBGAs

can act as binding sites, promoting bacterial attachment and persistence in the gastrointestinal tract. The intestinal microbiota plays many specific functions, including nutrient metabolism, maintenance of structural integrity of the gut mucosal barrier, immunomodulation and protection against pathogens. The role of gut microbiota in immunomodulation have been proved using germ free mice, which exhibit underdeveloped mucosal immune tissue characteristics, such as defective formation of lymphoid organs, but restored after microbiota reconstitution [123]. Therefore, microbiota could also be affecting RVV response, apart from HBGA composition and RV specificity. Understanding the interplay between microbiota and RVV response could be relevant in improving vaccine efficacy.

Specific bacterial taxa have been associated with RVV responses. Harris *et al* found in Ghana that RVV responders, the ones with anti-RV IgA antibodies >20 IU/mL after Rotarix vaccination, are positively correlated with *Streptococcus bovis* and non-responders with members of the *Bacteroidota* phylum. Additionally, the enterobacteria-*Bacteroidota* ratio was significantly higher in responder infants [124]. Microbiota composition of Ghanaian children was compared to that of Dutch infants, who didn't receive RVVs but were assumed to be responders due to the seroconversion rates exceeding 90% in Northern European countries. The study found that Dutch infant microbiota composition was significantly more similar to Ghanaian responders than non-responders. Secretor status is unknown among these infants. They speculate that *S. bovis* may be immunostimulatory, acting as an adjuvant to the RVV. The same group performed a new study in Pakistan, observing higher levels of Gram-negative bacteria as *Serratia* and *E. coli* in Rotarix responders. When compared to Dutch infants, they were also more similar to Pakistan responders [125]. Another study conducted in Zimbabwe, where low Rotarix vaccine seroconverters were found, determined that *Bacteroides thetaiotaomicron* was the only bacterium associated with responders (high anti-RV IgA titer) [126]. Parker *et al* also compared intestinal microbiota of Rotarix responders and non-responders in India. Contrary to the previous results, they found no differences between both groups [127]. Differences in methodology could be responsible for such discrepancies between studies.

Fix *et al* performed a study with RotaTeq vaccine in Nicaragua. Responders, the ones with > 4-fold increase in RV-specific IgA titers, had higher abundance of *Pseudomonadata* and *Eggerthella*, while non responders had higher abundance of *Fusobacteria* and *Enterobacteriaceae*, but such differences were not statistically significant. Therefore, gut microbiota seems to have a limited impact on response to RotaTeq vaccination according to this study [128].

In the view of these results, Harris *et al* performed a new study with adults to investigate whether microbiota modulation by antibiotics had any effect on RVV response in adults. Three groups were formed: a group without antibiotic treatment, a group receiving vancomycin and another one receiving broad-spectrum antibiotics [129]. Treatment with vancomycin was aimed to reflect microbiota composition of responders according to their previous study [124], thus boosting anti-RV immune responses, since the treatment significantly depletes *Bacteroidota* phylum and increases *Pseudomonadata* [130]. As expected, treatment with vancomycin resulted in a depletion in the relative abundance of *Bacteroidota* and *Bacillota*, along with an increase in *Pseudomonadata*. The broad-spectrum treatment also caused such decrease in *Bacteroidota* and *Bacillota* but no the increase of *Pseudomonadata*. Although no significant differences were found among experimental groups in terms of IgA titers, vancomycin group showed an increased anti-RV IgA boosting (2-fold increase) by day 7. RV shedding the week after vaccination was more common in vancomycin and broad-spectrum treatments. Differences in the microbiota composition in faeces were evident between the groups and correlations between enrichment in *Bacteroidota* populations at the boost at day seven were observed. Additionally, several taxa, including *Prevotellaceae*, *Cloacibacillus everynsis*, and members of *Pseudomonadata* such as *Escherichia* and *Shigella* were associated with increased viral shedding [129]. This study shows how alteration of gut microbiota composition can impact RVV immunogenicity, as proved by RVV boosting on day 7 and increased viral shedding in vancomycin group as compared to the control.

St Jean *et al* also studied the effect of antibiotic use by children prior to completion of RVV series on RVV response. The most common antibiotic prescribed was penicillin. No negative impact on the effectiveness of RVV was observed. Indeed, they found that antibiotics may have improved the response to Rotarix vaccine. However, antibiotic treatment could reduce the duration of the vaccine-induced immunity, since children who took antibiotic experienced more RV diarrhoea as compared to the ones without such treatment even though they were associated with increased seropositivity [131]. Another research also investigated the effect of antibiotics on RV specific IgA responses in infants. The seroresponse rates 1 month after the last Rotarix or RotaTeq vaccination showed similar results between infants exposed or not to antibiotics in all studied groups. Also, antibiotic treatment did not affect neutralizing antibody responses [132]. Contrary to the general thought that antibiotic treatment may disrupt the gut microbiome and thus decrease immune

response to RVV, these studies demonstrate that vaccine effectiveness was not diminished by antibiotic treatment, and in some cases, even enhanced it.

All this data could help to improve the effectiveness of RVV, which could have a significant impact on reducing RV related-deaths in low-income countries.

As for NoV, it was found that abundancies of *Ruminococcus* and *Faecalibacterium* is inversely associated with salivary anti-NoV IgA levels. This suggests that such specific bacteria are associated with lower susceptibility to NoV infections [79]. Regarding HIL-214, NoV currently under development, there are not studies about the changes in microbiota after vaccination. Such studies would enhance vaccine efficacy in case it is necessary.

1.5. Antivirals, therapeutic strategy against rotavirus and norovirus

Although RVVs are accessible, RV was responsible for the death of 128,500 of children under 5 in 2016 [17]. Furthermore, there is no NoV vaccine available at the moment. In this regard, it would be extremely beneficial the development of a therapeutic strategy to treat RV and NoV infections. Currently, there are no commercial antivirals available to treat RV or NoV, so the diseases are mainly managed by treating dehydration. However, in the last years considerable progress has been made towards the development of antivirals.

As previously mentioned, Shi *et al* found that segmented filamentous bacteria interfere with replication of RV [102], which raises the idea of using specific bacteria to treat RV infections. However, despite some studies show the beneficial effects of some probiotics (*Bifidobacterium* and *Lactobacillus* mainly) in diminishing diarrhoea duration, defecation times or RV shedding [133–137], many others failed to find positive effects in the treatment of patients suffering from RV-related diarrhoea with the same bacteria [138–142]. The variations observed in clinical trials could be attributed to factors such as the number of subjects, the probiotic used, application methods, doses, and the approach used to evaluate the effects. In order to have more reliable results, standardized and controlled trial conditions are required to assess the efficacy of probiotics in viral AGE.

Different drugs have also been studied in the treatment of RV and NoV. The compound 7-deaza-2'-C-methyladenosine inhibits replication of RV, NoV and sapovirus, and it was demonstrated

that it inhibits transcription of RV genome [143]. Brequinar, leflunomide, gemcitabine, 6-thioguanin and ML-60218, were also able to reduce RV replication [144–147]. Tohmé *et al* and Netzler *et al* reviewed those and many others compounds able to diminish RV and NoV infections at different levels of the replication cycle [148,149]. They include attachment, entry and release inhibitors, polymerase inhibitors and immunomodulators among others. One of them is nitazoxanide, which has demonstrated broad-spectrum antimicrobial activity against a range of bacterial, protozoan and viral infections. It is currently approved by the FDA for treating *Giardia* and *Cryptosporidium* infections [150]. A randomized, placebo-controlled, double-blind clinical trial was conducted to evaluate its effectiveness in treating RV and NoV infections. Treatment resulted in a significant reduction in the duration of symptoms from 2.5 to 1.5 days when compared to control groups [151]. Despite the small sample size in the study (26 individuals with RV and 13 with NoV), leading to the need for cautious analysis of the data, nitazoxanide has promising results against RV and NoV infections. Other studies also investigated the effect of nitazoxanide in RV infections, revealing significant reductions of diarrhoea and hospitalization duration [152–154]. La Frazia *et al* studied the mechanism of action in an *in vitro* RV model, and they concluded that it hampers the NSP5-NSP2 interaction disturbing the viroplasm formation and stabilization, leading to reduced RV yields [155]. Additionally, nitazoxanide successfully treated immunosuppressed transplant patients infected with NoV [156,157]. However, some studies determined that such treatment is ineffective against NoV infections [158–160], so some new studies should be performed in order to elucidate the role of nitazoxanide in NoV replication.

1.6. Models to study rotavirus and norovirus

The mechanisms underlying RV and NoV replication as well as therapeutic strategies have been extensively studied *in vitro* and *in vivo*. Different strains, particles, cellular and animal models have been used.

1.6.1. Cellular and animal models to study rotavirus and norovirus

Different cellular models are used to study RV *in vitro*. They include MA-104, Caco-2, HT29 cells and human intestinal enteroids (HIEs). MA104 cells, an epithelial monkey kidney cell line, are

permissive to RV entry and replication. However, they do not present HBGAs in their glycocalyx. Caco-2 cells come from human colon carcinoma and they spontaneously differentiate 11 days after confluency, which leads to the expression of several morphological and functional properties characteristic of mature enterocytes. They start to polarize, acquiring apical brush border with microvilli, and tight junctions form between adjacent cells, apart from expressing most receptors [161], like HBGAs [162,163], transporters and enzyme activities typical of enterocytes. It is important to take into account that different culture conditions and number of passages could lead to different properties, so results may not be directly comparable between laboratories. As for HT29 cell line, it also expresses characteristics of mature intestinal enterocytes. This cell line can also differentiate 15 days after confluency. The main difference between HT29 and Caco-2 cells is that the first one can produce mucin at high levels [164]. These immortalized cell lines are easy to maintain. However, their main limitation is that they consist of a single epithelial cell population. This problem is solved with HIEs, also described as mini-guts or mini-intestines, which are produced from different regions of the small intestine from donors. After cultivation in differentiation media, they exhibit a similar cellular composition and biological and physiological properties to that of the human gastrointestinal epithelium. They include enterocytes, goblet cells and paneth cells. HIEs can be infected in 3D o 2D monolayer [165–168]. HIEs could be employed in personalized medicine approaches since they derived from individuals. However, this also leads to variability issues between cultures from different donors. Another disadvantage is that their maintenance is expensive, time consuming and requires specialized expertise.

A different situation is found in NoV replication *in vitro*. Human NoV cannot be cultivated in the immortalized cell lines described above, like MA104 or Caco-2 cells. Consequently, the investigation of the virus has been limited until the recent discovery of its ability to replicate in B-cells and HIEs. Firstly, Jones *et al* cultivated human NoV in B-cells. However, it yields a low level of replication [116]. A major breakthrough in NoV research occurred in 2016, when human NoV were successfully replicated in HIEs [169].

As for *in vivo* systems, mice and gnobiotic pigs are commonly used in the study of RV and NoV. It was described an adult mice model with depleted microbiota after antibiotic treatment which allowed RV and NoV replication in high titers [170,171]. Zebrafish larvae is also used as *in vivo* model to study NoV replication. This model breeds rapidly, up to 82% of the human disease-related genes

have at least one zebrafish orthologue, and also is transparent, which facilitates the study of NoV infections [172,173].

1.6.2. Viral strains and particles commonly used in rotavirus and norovirus experiments

Regarding RV, cell culture adapted strains as human Wa and simian SA11 strains are frequently used in the study of RV. Such strains have been adapted in MA104 after serial passaging. They have contributed to the understanding of pathogenesis, immune responses and antiviral treatments of RV.

In the study of NoV, VLPs and P-particles are used. The VLPs consist of self-assembled viral capsid protein VP1 without a viral RNA genome, so they are not infectious. In the absence of infection systems for human NoV, VLPs play a critical role in determining how NoV interacts with host cells and immune responses, as well as vaccine development. The expression of the P domain alone results in P dimers. Twelve of such P dimers form P-particles, which retain the ability to bind HBGAs. As VLPs, they are also used in vaccine development and virus-host interactions studies [174,175]. Additionally, murine NoV is a valuable tool for studying human NoV, since it is able to replicate in cell cultures [143]. Both have similar replication mechanisms, genome route of infection and environmental stability [176–178]. However, results may not directly be translated to human NoV since it belongs to the genotype V and does not show gastric symptoms in infected mice.

1.6.3. Possible translation problems with some viral strains and cellular models

Human RV and NoV have been investigated using the above explained models, which has resulted in a much better understanding of the mechanisms underlying viral replication, as well as vaccine development, which is based on such information. Nevertheless, many studies have used RV cell culture adapted strains and cell lines as MA104 cells, that lack HBGAs on their surface, which act as RV and NoV receptors or co-receptors, as well as murine or simian strains, as documented with some examples in Table 2. It is not surprising that they might behave differently to wild viruses that infect humans, so conclusions about human RVs and NoVs and its infection processes should be made with caution when employing such strains and cell lines.

Table 2. *Examples of studies that employed RV and NoV strains different from human ones, and cell lines without HBGAs on their surface.*

Virus employed	Cell lines employed	Purpose of the study	Reference
Murine RV EC, Rhesus	HT29, MA104	Antiviral compound	[102]
Murine NoV, SA11, ST3	HG23, MA104, NSP5-EGFP MA104	Antiviral compound	[143]
Wa, simian SA11	HT29, Caco-2, SW620, MA104	Antiviral compound	[179]
Simian SA11, murine D6/2	BHK-T7, MA104	Replication	[39]
Simian SA11	Caco-2	Antiviral compound	[180]
Simian SA11	MA104, NSP5-EGFP MA104	Antiviral compound	[181]
Adapted wild type Rhesus	MA104	RV-shedding model	[182]
Adapted wild human RV	REH	Kinetics	[183]
Wa, simian SA11	HT29, MA104	Antiviral compound	[184]

In blue, cell lines without HBGAs.

A better approach would be the use of wild viruses obtained from human RV^+ or NoV^+ faeces, and use them directly in infection experiments, without adapting, as well as P particles or VLPs in the case of NoV. Also, cell lines with HBGAs on their surfaces are recommended, such as differentiated Caco-2 cells, HT29, HIEs, among others in RV experiments to study the virus host interactions without excluding the relevant HBGAs.

2. HYPOTHESIS AND OBJECTIVES

2. Hypothesis and objectives

A key process of enteric viral infections along with receptor attachment is detachment. Respiratory viruses, including influenza virus (*Orthomixoviridae*) or SARS (*Coronaviridae*), which infect via the mucosa and bind to sialic acid beside the lectin activity, have their own GHs on their surface that facilitate detachment from receptors, enabling them to continue infecting host cells [185]. By contrast, enteric viruses such as RV and NoV do not present GHs to facilitate their detachment from HBGAs.

As previously mentioned, microbiota not only protect their host from viral infections but there is also evidence that they promote viral replication through various mechanisms. In addition, gut microbiota members possess a wide range of GHs that enable them to feed from host glycans present in the digestive tract, that include α-L-fucosidases, sialidases, exo- and endo-β-N-acetylglucosaminidases, β-galactosidases, α-N-acetylglucosaminidases, endo-β1,4-galactosidases, and α-N-acetylgalactosaminidases [85,86,88,92,93,186,187]. Fucoses are present on the external moiety of HBGAs and thus are susceptible to cleavage by bacterial fucosidases.

On the other hand, RVs and NoVs bind HBGAs in a genotype-dependent manner. There is evidence that secretor individuals have more incidence of infection by P[4] and P[8] RVs and GII.4 NoVs and thereby changes in HBGAs affect their replication [73,74,188,189].

Since RV and NoV recognize HBGAs of the gastrointestinal tract, which are modified by gut microbiota thanks to GHs, literature indicates that gut microbiota promotes RV and NoV infection [101,116,118] and the intestine is a complex environment where host, microbiota and pathogens continuously interact, it was hypothesised that bacterial GHs, more specifically, bacterial fucosidases, may play a key role in RV and NoV infection.

To test the present hypothesis, the main objective of the thesis was focused on the effect of bacterial fucosidases coded by intestinal microbiota members during RV and NoV infections. In order to achieve this objective, the following specific objectives were proposed:

1. To study the metagenome of infant faeces and search for non-characterized fucosidases by bioinformatic analysis.

2. To clone, purify and characterize the selected fucosidases.

3. To find RV and NoV clinical isolates able to replicate on dCaco-2 and HIEs, respectively.

4. To study the RV clinical isolates and cell culture-adapted RV strain Wa replication on cellular lines with different HBGA profile.

5. To study the effect of fucosidases on RV and NoV replication in cellular cultures, HIEs and mice.

6. To study the effect of a fucosidase inhibitor on RV and NoV replication in cellular cultures, HIEs and mice.

3. MATERIAL AND METHODS

3. Material and methods

3.1. Faecal samples and microbial DNA extraction

Stool samples were obtained from four exclusively breastfed infants between the ages of 1 and 3 months. The samples were collected in anaerobic jars with Oxoid AnaeroGen anaerobic atmosphere generation system sachets (Thermo Scientific), immediately stored at 4 °C and cryopreserved within the next 12 h. Cryopreservation media contained 80% BHI (Brain Heart Infusion, Pronadisa) 2X concentrated supplemented with 0.1% of cysteine and 20% skim milk (200 g/L). Faeces were diluted in cryopreservation media 1:2 (vol/vol) and stored in aliquots at -80 ºC. A pooled faecal sample containing one sample from each infant was used to isolate total DNA. The MasterPure Complete DNA and RNA purification kit (Epicentre) was employed following the manufacturer's instructions with some modifications. This included an incubation step with lysozyme (0.13 mg/mL) and mutanolysin (0.03 U/µL) at 37°C for 1 h right after adding the lysis solution, as well as a cell disruption step using 0.1 mm diameter glass beads (FastPrep 24-5 G Homogenizer, MP Biomedicals, CA, USA). The concentration of DNA was measured using a Qubit 2.0 fluorometer (Life Technology). The use of human samples was approved by the Ethical Committee for Human Research of the University of Valencia, with registration number H1544010468380. Written informed consent was obtained from a parent of each of the subjects.

3.2. Metagenomic analysis

A genomic DNA library was constructed using a TruSeq DNA library kit. The size of the amplicons was verified using a Bioanalyzer DNA 1000 chip from Agilent Technologies. The library was sequenced on a MiSeq Sequencer using a 2x300 bp paired-end run (MiSeq reagent kit v3), following the instructions provided by Illumina. The sequencing was performed by the Central Service of Research Support at the University of Valencia (Spain).

The raw reads generated by the MiSeq Sequencer underwent quality checks, adapter-trimming and filtering using the AfterQC [190] and FastQC version 0.11.8 (http://www.bioinformatics.babraham.ac.uk) tools. Metagenomic assembly was conducted using metaSPAdes [191]. For functional profiling of the sequenced metagenome, the RAST-MGRAST web

server [192,193] was utilized. The annotation of ORFs was performed using the Cluster of Orthologous Genes (COG) database [194]. To predict the genes encoding GHs belonging to the GH95 family defined by the CAZy database, the dbCAN2 meta server [195] was employed. SignalP 4.1 was used to predict the presence of signal peptides [196].

The CLUSTAL Omega sequence alignment program from EMBL-EBI [197] was used to calculate the percentage of amino acid identity matrix for the putative α-L-fucosidases. Multiple alignments of the α-L-fucosidase sequences were conducted using ClustalW and ClustalX version 2 [198] along with the analysis tool web services provided by EMBL-EBI [197]. Cluster analyses were performed using the unweighted pair group method with arithmetic mean (UPGMA).

3.3. Cloning of fucosidases

Ten potential α-L-fucosidase genes were amplified by PCR using Phusion high-fidelity DNA polymerase (Thermo Fisher Scientific). These genes were amplified from total DNA extracted from a combined faecal sample, using specific primers (Table 3). The resulting PCR fragments were digested with specific restriction enzymes and inserted into pQE80 L vectors with the T4 DNA ligase (Thermo Fisher Scientific), also digested with the same enzymes. This vector possesses the start codon ATG followed by a 6xHis-tag and the multiple cloning site, thus allowing the expression of 6xHis-tagged proteins. The restriction enzymes employed were *Bam*HI (G^GATCC), *Hind*III (A^AGCTT), *Pst*I (CTGCA^G), and *Sph*I (GCATG^C). The resulting plasmids pQEfuc18, pQEfuc19A, pQEfuc30, pQEfuc35A, pQEfuc35B, pQEfuc39, pQEfuc193, pQEfuc1584, pQEfuc2358, and pQEfuc5372 were used to transform *E. coli* DH10B by electroporation with a Gene Pulser apparatus (Bio-Rad), following manufacturer's instructions. The transformed *E. coli* were selected on Luria-Bertani (LB) agar supplemented with ampicillin at 100 µg/mL incubated at 37 ºC. Later, DNA sequencing was performed to confirm the correct sequence of the inserts, by Eurofins Genomics (http://www.eurofinsgenomics.com).

Table 3. *Primers used to amplify ten putative α-L- fucosidases from pooled faecal sample.*

Primer	Sequence (5' – 3')
Fuc18*Bam*HI	TTTTGGATCCTGTCAGAGTGTTTCGGCAC
Fuc18*Hind*III	TTTTAAGCTTCTATCGACACCCAATTTCCG
Fuc19A*Bam*HI	TTTTGGATCCCAACACACATTTGTACATAAAC
Fuc19A*Pst*I	TTTTCTGCAGTCACTTCTTGTTTTGTTTCGG
Fuc30*Bam*HI	TTTTGGATCCCAAACTAAGTCGTTGCACC
Fuc30*Hind*III	TTTTAAGCTTTCATCTTCTCTCACAATATAC
Fuc35A*Bam*HI	TTTTGGATCCACTACCGAAGACAATTTGCAT
Fuc35A*Pst*I	TTTTCTGCAGTCAGAAATATTCTACTTTTAGC
Fuc35B*Bam*HI	TTTTGGATCCCAAGAGAAAATAATTGTATGTC
Fuc35B*Hind*III	TTTTAAGCTTTTAATATATTGCGAAAGACTTTA
Fuc39*Bam*HI	TTTTGGATCCTGTGGACTGACGAAAGAAAAC
Fuc39*Hind*III	TTTTAAGCTTTCAAGGAGCTACGGTCAC
Fuc193*Bam*HI	TTTTGGATCCACACATATTGTTCAAAATCAATA
Fuc193*Hind*III	TTTTAAGCTTCTACTCCAATATAAGTTCTA
Fuc1584*Bam*HI	TTTTGGATCCCAAATCTCGGAAAAAGCATTTG
Fuc1584*Pst*I	TTTTCTGCAGTTATTTTGCCTCTACCTTCAG
Fuc2358*Sph*I	TTTTGCATGCATGATAAGCCTTGAAGAGATTG
Fuc2358*Hind*III	TTTTAAGCTTCTAAAAGCTGATGCGCAAAAC
Fuc5372*Bam*HI	CTGGGATCCCAAGATACCCTGCAAAATGAGACC
Fuc5372*Hind*III	ATTAAGCTTGGCTGCAGGTCGACCCTAGCTAGG

Underlined, recognition sequence of restriction enzymes.

3.4. Fucosidase obtention and characterization

3.4.1. Expression and purification of fucosidases

One clone of each fucosidase, PE179 (pQEfuc18), PE180 (pQEfuc19A), PE181 (pQEfuc30), PE182 (pQEfuc35A), PE183 (pQEfuc35B), PE184 (pQEfuc39), PE185 (pQEfuc193), PE186 (pQEfuc1584), PE187 (pQEfuc2358), and PE188 (pQEfuc5372), along with two α-L-fucosidases from *B. bifidum* with His-tags, AfcA and AfcB, provided by Takane Katayama [85,91], were expressed in *E. coli* BL21. The bacteria were grown overnight in a total volume of 5 mL of yeast extract tryptone

medium (2xYT) medium, supplemented with 100 µg/mL of ampicillin at 37 ºC with agitation at 250 rpm. The following day, the preinoculum was transferred to 1 L of 2xYT medium containing the mentioned antibiotics and incubated at 37 ºC with agitation until the OD_{600} reached 0.5 (≈4 h). Then, 0.1 mM IPTG was added to induce protein production and cultures were further incubated overnight at 18 ºC with agitation. Subsequently, the cells were harvested by centrifugation at 11,100 g for 30 min and resuspended in 15 mL of phosphate buffer saline 1X (PBS) containing 0.015 g lysozyme, 3 U DNase and PMSF 0.8 mM, followed by 30 min agitation at room temperature. Then, the cell lysates underwent 10 cycles of sonication, each lasting 30 seconds with 30 second intervals. Cell debris was removed by centrifugation at 40,000 g for 40 minutes and cell extracts were then purified by affinity chromatography with 5 mL HisTrap columns (Cytiva) using an Äkta Prime FPLC system (Cytiva). After washing the column with buffer A (PBS 1X pH 7), proteins were then washed with 5% and 10% of buffer B (PBS 1X Imidazole 500 mM pH 7), and finally eluted with 100% buffer B. Fractions of interest were analysed by 10% SDS-PAGE gels, and buffer B was changed with Amicon 30 kDa centrifugal units (Millipore). Finally, proteins were resuspended in PBS 1X containing 15% glycerol and kept frozen at -80 ºC. Proteins concentrations were determined by Bradford.

3.4.2. Fucosidases characterization

3.4.2.1. Characterization of the fucosidase activity on neoglycoproteins

Fucosidase activities to hydrolyse HBGAs were characterised by Western blot using the following neoglycoproteins (IsoSep), HSA conjugated to: LNFP I (H type-1), Le^a, Le^b, Le^x and Le^y. First, the specificity of the different primary antibodies and lectin employed was tested. Glycoconjugates were separated in a 12% SDS-PAGE gel and transferred onto nitrocellulose membrane for Western blot analysis. A total of 7 membranes were prepared. Subsequently, the membranes were blocked by incubating them with 5% skim milk in PBS 1X containing 0.05% of Tween 20 (PBS-T) for 1 h at room temperature. Later, membranes were washed three times with PBS-T and incubated with the primary antibodies or lectin for 1 h at room temperature (anti-H antibody [catalog no. 922102, BioLegend]; anti-Le^a antibody [catalog no. 922202, BioLegend]; anti-Le^b antibody [catalog no. SAB4700761, Sigma]; anti-Le^x antibody [catalog no. 912901, BioLegend]; and anti-Le^y antibody [catalog no. 912501, BioLegend]; anti-HSA antibody conjugated to horseradish peroxidase [HRP] [catalog no. ab8941, Abcam] or lectin [Ulex europaeus agglutinin conjugated to HRP; catalog no. L8146; Sigma]). Then,

membranes with primary antibodies non conjugated to HRP were washed 3 times and incubated with the secondary antibody anti-mouse-HRP in a 1/10,000 dilution in PBS-T. Finally, membranes were washed three times with PBS-T, and the immunoblots were developed with the Immobilon Western reagent (Millipore). Also, glycoconjugates were analysed by Coomassie.

After determining that each antibody and lectin only recognised their specific glycoconjugate, characterization of fucosidases by Western blot was performed. Each fucosidase was incubated with each glycoconjugate overnight at 37 ºC, in a reaction mixture of 25 µL, containing 5 µg of fucosidase and 1 µg of substrate in PBS 1X. Following the incubation, samples were separated in 12% SDS-PAGE gels and transferred onto nitrocellulose membranes for Western blot analysis, following the procedure explained above.

3.4.2.2. Characterization of the fucosidase activity on soluble oligosaccharides

The capacity of the fucosidases to hydrolyze natural fucosyloligosaccharides (Biosynth Carbosynth) was evaluated using H type-1, H type-2, Le^a, Le^b, Le^x, Le^y, blood group A trisaccharide (BG A), blood group B trisaccharide (BG B), 2'-fucosyllactose (2' FL), 3-fucosyllactose (3FL) and 6-fucosyl-N-acetylglucosamine (6FN) (Table 4). The reaction mixture (10 µL) containing 2 mM substrate in PBS 1X and 2 µg of enzyme was incubated at 37 ºC for 16 h. Following incubation, the reaction mixture was diluted 1/10 with deionized water and analysed by high-performance liquid chromatography using ICS3000 chromatographic system (Dionex) and a CarboPac PA100 column with pulsed amperometric detection. A gradient ranging from 10 to 100 mM NaOH for 30 min at 27 ºC with a flow rate of 1 mL/min was employed. The identification of reaction products was confirmed by comparing their retention times with those of standard carbohydrates.

Table 4. *Structure of glycans used in fucosidase characterization.*

Glycan	Structure	
LNFP I	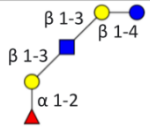	Fucose-α1-2-galactose-β1-3-N-acetyl-glucosamine-β1-3-galactose-β1-4-glucose
H type-1	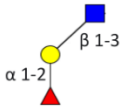	N-acetyl-glucosamine-β1-4-galactose- α1-2-fucose
Le^a	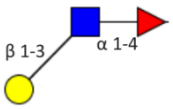	Galactose-β1-3-N-acetyl-glucosamine-α1-4-fucose
Le^b	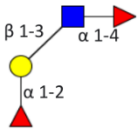	Fucose-α1-2-galactose-β1-3-N-acetyl-glucosamine-α1-4-fucose
Le^x	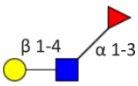	Galactose-β1-4-N-acetyl-glucosamine-α1-3-fucose
Le^y	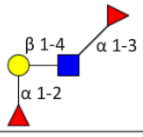	Fucose-α1-2-galactose-β1-4-N-acetyl-glucosamine-α1-3-fucose
H type-2	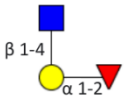	N-acetyl-glucosamine-β1-4-galactose- α1-2-fucose
BG A	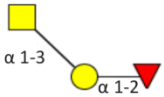	N-acetylgalactosamine-α1-3-galactose-α1-2-fucose
BG B	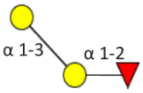	Galactose-α1-3-galactose-α1-2-fucose
2’ FL	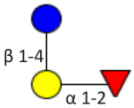	Glucose-β1-4-galactose-α1-2-fucose
3FL	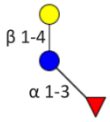	Galactose-β1-4-glucose-α1-3-fucose
6FN		N-acetyl-glucosamine-α1-6-fucose

LNFPI, lacto-N-fucopentaose I that includes the H type-1 antigen; Le^a, Lewis^a antigen; Le^b, Lewis^b antigen; BG A, blood group A trisaccharide; BG B, blood group B trisaccharide; H type-2, H type-2 antigen; Le^x, Lewis ^{x} antigen; Le^y, Lewis^y antigen; 2’FL, 2’-fucosyllactose; 3FL, 3-fucosyllactose; 6FN, 6-fucosyl-N-acetylglucosamine. Circle, glucose; yellow circle, galactose; blue square, N-acetyl-glucosamine; red triangle, fucose.

3.5. Fucosidase inhibitor characterization

To determine the half maximal effective concentration (EC50) of the fucosidase inhibitor 1-deoxyfuconojirimycin HCl (DFJ) (Biosynth), 10 µg of four fucosidases were incubated with increasing concentrations of DFJ (ranging from 0 to 1,000 nM) for 1 h at 37 ºC in a total volume of 100 µL in PBS 1X. The fucosidases employed were Fuc2358 and Fuc5372 from the metagenome study, and AlfB and AlfC, previously characterized in the laboratory [90]. Subsequently, the colorimetric substrate 4-nitrophenyl-α-L-fucopyranoside (*p*NP-Fuc) was added to the mixture at 1 mM. The p-nitrophenol released was measured at 405 nm 15 min later, using the spectrophotometer MultiSkan FC. Absorbance data was used to calculate the EC50 using drc package (version 3.0.1, [199]) in R version 4.1.2 running under macOS Big Sur 11.7.6. Plots were generated using ggplot2 (version 3.4.3). To test the specificity of DFJ, 10 µg of the lacto-N biosidase LnbB previously characterized in the laboratory were incubated with different concentrations of DFJ for 1 h at 37 ºC. Later, the colorimetric compound p-nitrophenyl β-D-galactopyranoside (*p*NP-gal) was added to the mixture at a concentration of 5 mM. After 15 min the absorbance was measured at 405 nm.

3.6. Human virus stool filtrates preparation

Faecal samples that tested positive by BD-MAX for RV and NoV were obtained from the Hospital Clínico Unversitario de Valencia. The G and P genotypes of RV samples were examined using a seminested PCR method following the protocols of the EuroRotaNet surveillance network [200]. All the selected RV^+ stool samples belonged to the P[8] genotype, as well as the G1, G9 and G12 genotypes. NoV genotypes were examined by RT-PCR. PCR products were purified with NZYGelpure kit (Nzytech) and sequenced upstream and downstream. Viral genogroup, genotype and variant were assigned by using the Norovirus Typing Tool and the Human Calicivirus Typing Tool [201]. All used samples belonged to the GII.4 genotype.

To prepare the stool filtrates, a previously described method [169] was followed with some adjustments. Initially, 0.5 g of RV^+ or NoV^+ stool was weighed and placed in a 15 mL conical tube, then diluted in 4.5 mL of TNC 1X buffer (20 mM Tris HCl pH8, 100 mM NaCl, 1 mM $CaCl_2$) in the case of RV or PBS 1X in the case of NoV. The presence of $CaCl_2$ in the TNC buffer allowed the correct conformation of the TLPs of RV. The solid components were disrupted using a 1 mL pipette, followed

by 30 seconds of vortexing. After a 5-minute incubation at room temperature, the samples were vortexed again for 30 seconds. Subsequently, they underwent three cycles of sonication for 30 seconds each (using a Branson Sonifier 250), with a 1-minute interval between each sonication. The output control was set at 7. Afterwards, the suspension was centrifuged at 4,500 g for 10 minutes at 4 ºC to eliminate debris. The supernatant was collected in a new 15 mL centrifuge tube and centrifuged at 4,500 g for 10 minutes at 4 ºC.

Next, the supernatant was sequentially filtered using syringe filters with pore sizes of 5, 1.2, 0.8, 0.45, and 0.2 µm (Merck and Whatman). The resulting 10% stool filtrate was aliquoted and stored at -80 ºC.

3.7. Rotavirus VP4 and VP7 sequencing

VP4 and VP7 of the RVs able to replicate in differentiated Caco-2, as well as that of Wa were sequenced by Sanger in Príncipe Felipe Institute, Valencia (Spain), using the primers listed in table 5 [202]. Sequence alignments were obtained using BioEdit software 7.0.5.3.

Table 5. *Primers used to sequence VP4 and VP7 of RV.*

Primer	Sequence (5' – 3')
VP4 forward	TGGCTTCGCCATTTTATAGACA
VP4 reverse	ATTTCGGACCATTTATAACC
VP7 forward	ATGTATGGTATTGAATATACCAC
VP7 reverse	AACTTGCCACCATTTTTTCC

3.8. Transformed cell lines experiments

3.8.1. Cell cultures maintenance

The cell lines Caco-2 and MA104 were cultured in minimum essential medium (MEM) supplemented with 1% penicillin and streptomycin (P/S), 1% glutamine, 1% non-essential amino acids, and 10% foetal bovine serum (FBS). HT29 and HT29M6 cells were grown in Dulbecco's modified

Eagle's minimum essential medium (DMEM) supplemented with 1% P/S, 1% sodium bicarbonate, and 10% FBS. All cell types were maintained in T75 flasks at 37 °C in a humidified atmosphere with 5% CO_2. The medium and supplements used were purchased from Gibco.

When the flasks reached 80-90% confluency, they were washed with 7 mL of DPBS (Corning) and detached using 1 mL of verseno trypsin (Lonza) for 10 minutes at 37 °C. The cells were then resuspended with 9 mL of complete medium, and 2 mL of the suspension were transferred back into each flask. A 10 µL sample was taken for cell counting and viability assessment, which was performed by diluting the cells 1:1 with trypan blue solution (Sigma) and using dual chamber counting slides and an automated cell counter (Biorad, TC20).

Subsequently, cells were seeded into 96-well plates with flat bottom, seeding 10^5 cells per well in a volume of 200 µL to ensure full confluency within 24 hours. For Caco-2 cells, differentiation occurred 11 days after confluency, and experiments were conducted 14 days after confluence. During those 14 days, the media was changed three times. If differentiation was not required, cells were infected on the following day. Cells were used until passage 30 to ensure genetic stability.

3.8.2. Infection of cell lines with human rotavirus

Once 96 well plates achieved confluency, and differentiation in the case of Caco-2, RV infection was performed. For each infection experiment, two or more plates were used if the replication was analysed by qPCR. One plate served as the 1-hour time point to assess viral adhesion, while the other plates were used to determine viral replication. Only one plate was necessary if impedance experiments were conducted.

Viral filtrates were thawed at room temperature and diluted 1:100 in complete medium, either MEM or DMEM (depending on the cell type), without FBS. The dilution was supplemented with 10 µg/mL of trypsin IX (Sigma) to activate the virus. The viral dilution was prepared in either 96-well plates with round bottoms (for volumes below 250 µL) or sterile crystal tubes (for volumes above 250 µL) and incubated at 37 °C for 1 hour.

Meanwhile, the cells were washed twice with complete MEM/DMEM without FBS. Subsequently, 180 µL of complete medium without FBS, supplemented with 1 µg/mL of trypsin IX,

were added to each well. After the viral activation period, 20 µL of the 1:100 viral dilution was added to the corresponding wells, resulting in a 1:1,000 dilution of the virus in a 200 µL infecting volume. The cells were infected for 1 hour at 37 °C with 5% CO_2. Following the incubation, the inoculum was aspirated and 100 µL of complete MEM/DMEM without FBS, supplemented with 1 µg/mL of trypsin IX, was added to each well. The plate designated as the 1-hour time point was frozen at -80 °C, while the other plates were further incubated at 37 °C with 5% CO_2 until the desired time point was reached.

For impedance experiments, Caco-2 cells were seeded in 96 wells xCELLigence E-plate (Agilent). After confluency and differentiation, infection experiments were conducted as explained above. After viral adhesion, plates were engaged into the xCELLigence RTCA SP [SP = single plate] instrument (Agilent) and incubated at 37 ºC for 72 h. Impedance values were recorded every 20 minutes.

Each experiment was performed in triplicate to ensure reliability and consistency of the results. The wild-type strain Wa was utilized in all experiments to study how a human G1P[8]cell culture-adapted virus replicated under the tested conditions.

3.8.2.1. Cellular treatments with fucosidases

In order to study the impact of fucosidases on viral replication, cells were treated prior to infection with the enzymes. These procedures included treatment with either AfcA, AfcB or both AfcA and AfcB simultaneously. For this purpose, cells were washed twice with 200 µL of complete medium without FBS. Then, 20 µg of each fucosidase were added to each well in complete medium without FBS in a total volume of 200 µL. Cells were incubated for 2 h at 37 ºC and 5% CO_2. After the incubation, cells were washed again twice with complete medium without FBS, and the infection was proceed as indicated before.

3.8.2.2. Viral treatment with fucosidase inhibitor

To investigate the effect of a fucosidase inhibitor in viral replication, DFJ was employed. It was diluted in mQ water. During RV activation, such inhibitor was added to the viral dilution at the desired concentrations and incubated for 1 h at 37 ºC. Then, viral infections were performed as explained above.

3.8.3. Immunofluorescence of differentiated Caco-2 cells with clinical RV

Caco-2 cells were seeded in 24-well plates containing a circular coverslip treated with poly-L-Lysine to allow cell attachment at a density of 10^6 cells per well in 2 mL of medium. The medium was changed once a week. Once the cells were differentiated, the infection process was initiated. Initially, the clinical RV V7 was activated in a 1:100 dilution in MEM medium without FBS, supplemented with 10 µg/mL trypsin IX. After incubating for 1 hour at 37 ºC and 5% CO_2, the cells were washed twice with MEM medium without FBS. For the infection, 500 µL of medium without FBS, supplemented with 1 µg/mL trypsin IX, were added to each well, along with 50 µL of the activated virus, in order to achieve a viral dilution of 1:1,000. The plate was then incubated for 1 hour at 37 ºC and 5% CO_2. Subsequently, the inoculum was removed, and 1 mL of medium without FBS, supplemented with 1 µg/mL trypsin IX, was added to each well. The plate was further incubated for 24 hours at 37 °C, under a humidified atmosphere with 5% CO_2. After the incubation period, the medium was aspirated, and the cells were washed twice with 1 mL of PBS 1X. To fix the cells, 500 µL of cold methanol was added to each well, and the plate was incubated at -20 ºC for 20 minutes. Following this, the cells were washed twice again with PBS 1X. For blocking, 500 µL of PBS 1X containing 5% BSA was added, and the plate was incubated for 30 minutes at room temperature. Subsequently, each coverslip was carefully lifted and placed facedown on top of a 50 µL drop of the primary antibody on a piece of parafilm in a 1:50 dilution in Dako solution. The primary antibody used was a mouse monoclonal α-VP6 obtained previously in the laboratory. The coverslips were incubated with the primary antibody for 2 hours at room temperature. After incubation, the coverslips were washed three times by gently scrubbing them in drops of PBS 1X. The same procedure was repeated for the incubation with the secondary antibody. In this case, α-mouse antibody labelled with alexa 488 at a concentration of 1:300 was used, mixed with DAPI at 300 nM in Dako solution. After 1 hour of incubation in darkness,

the coverslips were washed three times with PBS 1X and placed face down on a slide with a drop of fluorescent mounting medium (Dako). Then, the circular coverslips were covered with bigger squared coverslips and sealed with nail polish. Preparations were observed using a confocal microscope LEICA TCS-SP8.

3.9. Human Intestinal Enteroids experiments

3.9.1. HIEs 3D and 2D cultures preparation

Three different HIEs were employed. The intestinal epithelial cell line (InEpC) was purchased from Lonza (CC-2931), the jejunum J2 line was provided by Prof. Mary K. Estes (Baylor College of Medicine, Houston, TX) and fetal ileum FI124 lines was provided by Prof. Jason Spence (University of Michigan, Ann Arbor, MI). HIEs were maintained as undifferentiated 3D HIEs domes embedded in Matrigel in growth media (OGM). For 3D infections, HIEs were differentiated by adding differentiation media (ODM) to the wells 4 days after splitting. 5 days later, infections experiments were performed. For 2D infections, the undifferentiated 3D cultures were collected 7 days after splitting in DPBS with 0.5 mM EDTA and washed twice. The pellet obtained after centrifuging cells at 250g at 4 ºC for 5 min were resuspended in TryplE, a recombinant enzyme that dissociate HIEs into single cell suspension. During a 20 min incubation at 37 ºC, the cell suspension was vigorously resuspended every 5 min, and then cells were counted and pelleted by centrifugation. Subsequently, they were resuspended in OGM supplemented with Y-27632 and CHIR99021. The first one is an inhibitor of Rho-associated, coiled-coil containing protein kinase (ROCK), which blocks cell apoptosis. CHIR99021 inhibits the glycogen synthase kinase-3 (GSK-3) activity, thus promoting the Wnt pathway. The cells were seeded into collagen-coated wells of a 96-well plate at a density of 10^5 cells/well. Once a confluent monolayer was obtained after 2-5 days, HIEs were differentiated by adding ODM. After 5 days, infection experiments were performed.

Media was changed every other day. All media used in HIEs maintenance, differentiation and infection are summarized in table 6.

3.9.2. Infection of HIEs 3D with rotavirus and norovirus

On the infection day, 3D HIEs domes were collected in a 15 mL falcon tube treated with AARS (anti-adherence rinsing solution) and washed 3 times with CMGF- to remove Matrigel. Afterwards, HIEs were pelleted and resuspended in 2 mL of RV or NoV infection medium. A 100 µL aliquot was pelleted, resuspended in TryplE, incubated for 20 min at 37 ºC to obtain single cells, and counted. A total of $2 \cdot 10^5$ or $4 \cdot 10^5$ cells were used for each experimental condition in RV or NoV infections, respectively. The desired amount of HIEs was distributed in 15 mL tubes treated with AARS or low binding microtubes up to 2 or 1 mL of incubation media, respectively. In the case of RV infections, RV was trypsin activated and then added to the cells at the desired MOI. For NoV, the activation step is not required. During a 2 h incubation at 37 ºC and 5% CO_2, cell suspension was resuspended every 30 min with wide bore tips. Then, cells were washed 3 times with CMGF- and pelleted.

Table 6. *List of media used in HIEs maintenance, differentiation and infection.*

Media	Composition
CMGF-	Advanced DMEM/F12 + 2 mM GlutaMAX-1 + 10 mM HEPES + 100 U/mL P/S + 100 µg/mL Primocin
OGM	IntestiCult Organoid Growth Medium (STEMCELL) + 100 U/mL P/S + 5 µg/mL plasmocin
ODM	CMFG- + 50 ng/mL mouse recombinant EGF + 100 ng/mL mouse recombinant Noggin + 10 nM Lue15-Gastrin I + 500 nM A-83-01 + 1 mM N-acetylcysteine +1X B27 supplement + 1X N2 supplement + 5 µM DAPT
OGM for 2D HIEs	OGM + 10 µM Y-27632 + 10 µM CHIR99021
RV incubation medium	ODM + 0.25 mg/mL pancreatin
NoV incubation medium	ODM + 500 µM GCDCA + 2 µM Ruxolitinib

For infection in suspension, each tube was resuspended with the appropriate amount of ODM supplemented with 1 µg/mL trypsin for RV infection. 400 µL was necessary per condition. The 2 h time point was collected in tubes, while the remaining suspension was seeded in AARS treated 48 well plates, adding 400 µL of cell suspension per well.

For infection in domes, each tube containing the HIEs was resuspended in the appropriate amount of geltrex, with 25 µL per condition. The 2 h time point was again collected in tubes, while

the rest was added to prewarmed 24 well plates with 3 domes per well (total 25 µL/well). 500 µL of ODM supplemented with 1 µg/mL trypsin or NoV infection media was then added. For NoV infection, only infection in domes was carried out.

Lysis solution of the RNA extraction kit (RNAeasy mini kit, Qiagen) was added to the 2 h time points and aliquoted at -80ºC. Plates were incubated the desired time. Then, lysis solution was added to each well, and stored at -80 ºC.

3.9.2.1. NoV Infection of HIEs 3D with fucosidase treatments

It was also studied the effect of fucosidases in NoV infections of 3D HIEs before infection. After cell count and distribution in 15 mL tubes, 20 µg of each fucosidase was added per condition to each tube. After 2 h incubation at 37 ºC and 5% CO_2 with occasional mixing, cells were washed 3 times with CMGF-, resuspended in the correspondent infection media and proceed with the infection as explained above.

3.9.2.2. NoV infection of HIEs 3D with fucosidase inhibitor treatment

To study the effect of the fucosidase inhibitor DFJ, it was incubated at concentrations from 0 to 15 µM with the clinical NoV43 for 1 h at 37 ºC in ODM before infection. Then, viral infection proceeded as indicated before.

3.9.3. Infection of HIEs 2D culture with rotavirus and norovirus

To perform infection of 2D monolayers, media was removed from the wells and viral preparations were added at the desired MOI in a total volume of 100 µL. In the case of RV infections, RV was trypsin activated in ODM and then added to the cells. For NoV, no activation step is required, being resuspended in NoV incubation media. After 1 h at 37ºC and 5% CO_2, viral inoculum was removed and wells were washed 2 times with 100 µL of CMGF-. Finally, 200 µL of ODM supplemented with 1 µg/mL of trypsin or NoV incubation media was added to each well for RV or NoV infections,

respectively. The 1 hpi wells were collected with lysis buffer of the RNA extraction kit and stored at -80 ºC. The remaining timepoints were incubated the desired time at 37 ºC and 5% CO_2. Then, lysis solution was added to the wells and stored at -80 ºC.

3.9.4. HIEs viability assay

Fucosidases and fucosidase inhibitor DFJ toxicity was tested in HIEs. Once 3D HIEs were differentiated, collected, counted, and distributed in 15 mL tubes, the enzymes (10 and 20 µg/well) and inhibitor (concentrations ranging from 0 to 15 µM) were added. After an incubation step of 2 h at 37 ºC and 5% CO_2, cells were seeded in a 24 well plate, and cell viability was assessed following manufacturer's instructions, CellTiter-Glo® 3D Cell Viability Assay (Promega).

3.9.5. Immunofluorescence of 2D monolayers of InEpC and FI124 lines treated with fucosidases

InEpC and FI124 HIEs lines were seeded into 96 well-plates at a density of 10^5 cells/well. Once confluency was achieved after 3-5 days, ODM was added. 4 days later, each well was treated with 20 µg of AfcA, AfcB or both fucosidases simultaneously. Fucosidases were resuspended in ODM in a total volume of 200 µL/well and incubation took place for 2 h at 37 ºC and 5% CO_2. Afterwards, wells were washed twice with 200 µL of CMGF- and fixated with 100 µL of ice cold MeOH at -20 ºC for 20 min. Subsequently, cells were washed twice with 100 µL of PBS 1X and blocked with 100 µL of blocking buffer containing 3% BSA, 0.2% Triton X-100 and 1% goat serum for 30 min at room temperature. Once blocking was finished, cells were incubated with UEA-I lectin conjugated to fluorescein (Vector laboratories) at 1:1,000 and DAPI at 1:1,000 dilution for 1 h at room temperature in agitation and darkness. Finally, each well was washed twice with 100 µL of PBS and maintained in PBS. Cells were observed using Leica DMi8 inverted fluorescence microscope (Leica Microsystems).

3.10. RNA extraction, RT-qPCR and $2^{-\Delta\Delta Ct}$

The plates used in RV infections of transformed cell lines were thawed at 37 ºC, and subsequently the supernatant and cells were collected in a microcentrifuge tube. Following the

instructions provided with the Viral RNA extraction kit (Macherey Nagel), RNA was extracted from the collected samples.

To extract RNA from RV or NoV infections of HIEs, tubes containing infected cells and lysis buffer were thawed at room temperature. RNA was extracted following manufacturer's instructions (RNAeasy mini kit, Qiagen).

To determine the viral replication, qPCR analysis was conducted using an Exycler 96 instrument (Bioneer) in the case of transformed cell lines or QuantStudio 5 (AppliedBiosystems) in the case of HIEs. The qPCR master mix consisted of NZYSpeedy qPCR Probe Master Mix at a concentration of 1X (NZY), forward and reverse primers and a probe specific to RV or NoV at a concentration of 0.25 µM, forward and reverse primers and an Hypoxanthine phosphoribosyltransferase 1 (HPRT1) probe specific to the cells at a concentration of 1X (IDT), RT SSIII enzyme (20 U/sample, Invitrogen), and diethyl pyrocarbonate treated water (DEPC, Invitrogen). The following cycling conditions were applied: 30 minutes at 50 ºC, 10 seconds at 95 ºC and 45 cycles of 15 seconds at 95 ºC and 1 minute at 60 ºC. The replication of the virus was quantified using the $2^{-\Delta\Delta Ct}$ method. All primers and probes are sum up in table 7.

Table 7. *Primers and probes employed in qPCR.*

Primer	**Sequence (5' – 3')**
RV forward primer JVKF	CAGTGGTTGATGCTCAAGATGGA
RV reverse primer JVKR	TCATTGTAATCATATTGAATACCCA
RV probe JVKP	FAM-ACAACTGCAGCTTCAAAAGAAGWGT
NoV forward primer C0G2F	CARGARBCNATGTTYAGRTGGATGAG
NoV reverse primer C0G2R	TCGACGCCATCTTCATTCACA
NoV probe RING2	FAM-TGGGAGGGCGATCGCAATCT
HPRT-1 forward and reverse primers, and probe	Hs.PT.58v.45621572 (IDT)

3.11. Mice infections

3.11.1. Viral stocks and liposome preparations

Mice were infected with the cell culture adapted RV Wa and a human NoV from a clinical sample.

As for Wa stock, 10 confluent MA104 T150 flasks (approximately $1.5 \cdot 10^7$ cells/flask) were infected with activated Wa at a M.O.I of 1. After 7 days of incubation at 37 ºC and 5% CO_2, supernatants were centrifuged at 5,500 g for 15 min at 4 ºC to remove cell debris. The resultant supernatant was again centrifuged at 100,000 g for 2 h at 4 ºC in a Himac R25ST-0507 rotor coupled to a Himac CR-30N centrifuge. The pelleted viruses were resuspended in TNC 1X overnight at 4 ºC. The following day, viruses were ultracentrifuged in a sucrose gradient (30-70%) in a SW41 rotor coupled to a Beckman L80 ultracentrifuge at 150,000 g for 4 h at 4 ºC. The 30-70% fraction was collected and pelleted again in the SW41 rotor coupled to a Beckman L80 ultracentrifuge at 150,000 g for 4 h at 4 ºC. Finally, Wa was resuspended in TNC 1X.

NoV stock was prepared by resuspending 1 g of a positive GII.4 Sydney 2012 faeces with 9 mL of PBS 1X. After 5 min of vigorous mixing and vortex, the sample was centrifugated at 15,000 g for 20 min at 4 ºC to remove bacteria and cell debris. The supernatant was then ultracentrifuged at 150,000 g for 2 h at 4 ºC in the SW41 rotor coupled to a Beckman L80 ultracentrifuge. The pelleted virus was resuspended in 10 mL of PBS and stored at – 20 ºC.

Both viruses were titrated by qPCR. The quantified plasmids containing the RV or NoV qPCR target sequence were diluted in nuclease free water obtaining 10-fold dilutions. The standard curve was generated using 10^2 to 10^{10} copies of plasmid DNA by RT-qPCR in duplicates using the primers of table 7. By extrapolating the data of the standard curve, RV and NoV quantities of the viral stocks were calculated. The mice were orally inoculated with 10^{10} genome copy equivalent (GCE) of each virus.

Fucosidase AfcA was administered to mice in liposomes. The enzyme-containing lipid vesicles were fabricated with the solvent casting method. A mixture of 0.45 g of phospolipon POPC (Lipoid) and 12 mg of cholesterol (Acofarma) as surfactant were solved in 50 mL of methanol. The solution was then distilled using a rotatory evaporator (BUCHI) for 12 h at 55 ºC and 250 bar. The resulting

lipidic layer was reconstituted with 5 mg of liophilized AfcA solved into 10 mL of PBS 1X for 1 h at 30 ºC. Mice were treated with 50 µg of enzyme, in a volume of 150 µL.

All viruses and enzymes were administered orally with an intragastric tube.

3.11.2. Infection experiments

Groups of six C57BL/6 mice between 6 and 8 weeks old were used in the study. After reception, mice were acclimated in the animal facility for 1 week. All groups received antibiotic cocktail containing 1 g/L ampicillin, 1 g/L metronidazole, 1 g/L neomycin, and 0.5 g/L vancomycin in drinking water *ad libitum* to deplete mice gut microbiota, which was changed every 3 days during the course of the whole experiment, as described before [170]. Mice were fed a purified-defined germ-free diet (AIN-93G, Envigo, Barcelona, Spain). Three weeks after the beginning of the antibiotic treatment, infection experiments were carried out. The use of the mice was approved by the Ethical Committee of the University of Valencia and the General Direction of Livestock and Fisheries of the Ministry of Agriculture, Rural Development, Climate Emergency, and Ecological Transition, with registration number 2022 VSC PEA 0290.

A total of three set of experiments were conducted, with each of them further divided in two groups, one group infected with RV and the other with NoV (Fig. 8).

Set 1: Two groups of mice were treated with 50 µg of fucosidase AfcA once a day for 2 days and then infected the following day with RV or NoV.

Set 2: Two groups of mice were infected with RV or NoV along with 20 mM of fucosidase inhibitor DFJ.

Set 3: Two groups of mice were infected with RV or NoV as controls.

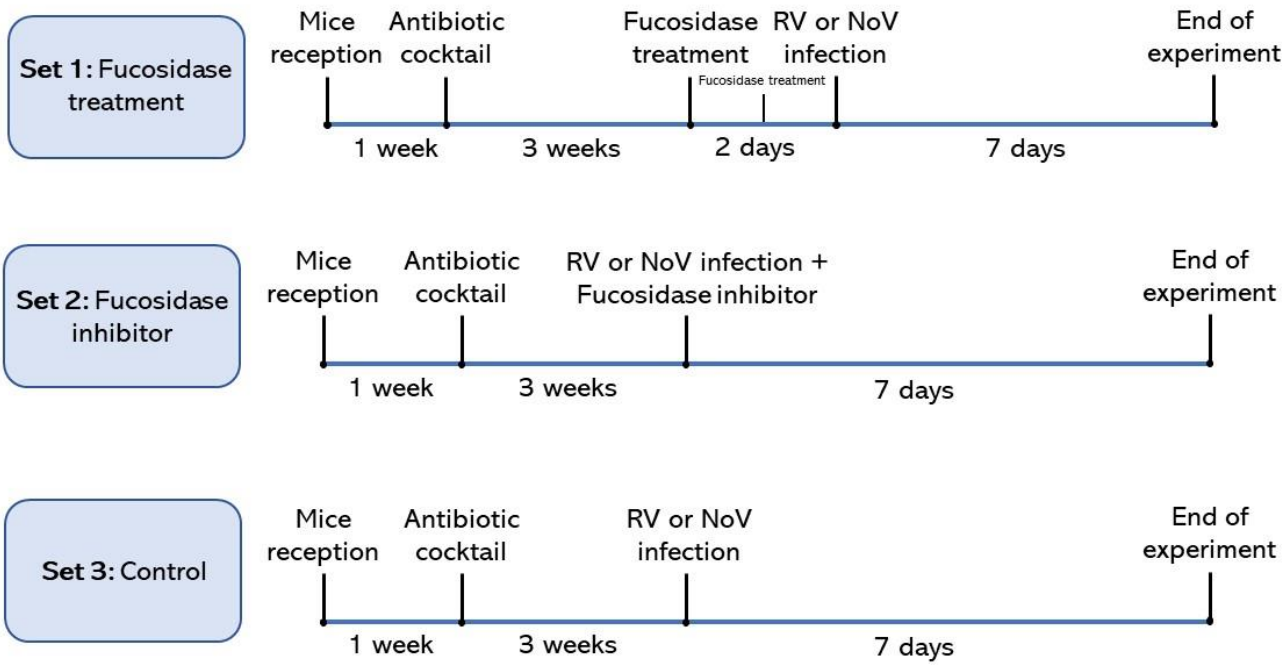

Figure 8. *Mice intervention.*
Schematic representation of the experimental procedure for the three sets of experiments.

Faeces were collected daily from the day of the viral infection and continued for 7 days. They were stored at -20 ºC. After that, mice were euthanized with 2% isoflurane and blood samples collected, as well as the spleen of 1 mouse per group stored in RNAlater for further analysis (Sigma).

3.11.3. Quantification of RV and NoV from stool samples by RT-qPCR

RNA was extracted from faecal samples with the Viral RNA extraction kit (Macherey Nagel). First, faeces were weighted in order to finally normalized the results depending on faeces quantity. After that, 700 µL of the lysis solution was added to the ≈80 mg of stool samples, which were then sonicated for 45 sec using a Branson Sonifier 250, with output set at 2. Later, samples were incubated at 70 ºC for 5 min and centrifugated at 21,000 g for 5 min. RNA from the supernatant was then extracted following manufacturer's instructions.

RNA was diluted 1/10 and then the RT-qPCR was performed using the StepOne 48 wells thermocycler (AppliedBiosystems), with primers and probes corresponding to RV and NoV of table 7. The standard curve was generated by serial end-point dilution, amplifying 10-fold dilutions of the quantified plasmid containing the RV or NoV target sequence by RT-qPCR in duplicates.

3.12. Statistical analysis

Graphs are represented as means ± SEM. Statistical differences were determined with the GraphPad Prism 8.0.1 software, using the unpaired t-test to compare the means between two distinct groups. A p value ≤ 0.05 was considered significant.

4. RESULTS

4. Results

4.1. Identification of glycosyl hydrolases from infant faecal microbial metagenome

A total of 60,354 sequences with predicted proteins with known functions were identified from the faecal microbial metagenome with the RAST-MGRAST server [192,193]. Using the COG database [194], various types of enzymes involved in the degradation of HMOs were found, including β-galactosidases, β-N-acetylhexosaminidases, α-sialidases and α-L-fucosidases. The most prevalent glycosidases were putative β-galactosidases (COG1874, COG2723, and COG3250) which comprised 224 enzymes from the GH35, GH42, GH2 and GH1 glycosyl hydrolase families of the CAZy database. β-galactosidases were followed by β-N-acetylhexosaminidases (COG3525) since 42 enzymes belonging to the GH20 were identified. As for α-L-fucosidases (COG3669), 36 of them were found, which belonged to GH29 family. When using dbCAN2 server [195], 27 putative α-L-fucosidases were identified, where it was also found some of the other major family of α-L-fucosidases GH95. Finally, there were identified also seven sialidases (COG4692 and COG4409) from the GH33 family.

4.2. Sequence analysis and biochemical characterization of GH29 α-L-fucosidases

22 out of 36 ORFs that coded for putative α-L-fucosidases showed a complete coding sequence. The amino acid sequence from those genes were subjected to BLAST searches against the nr database, finding the most significant matches (>98% identity) with α-L-fucosidases annotated in bacterial genomes of *Bacteroides thetaiotaomicron*, *Bacteroides caccae*, *Ruminococcus gnavus*, *Phocaeicola vulgatus* (formerly *Bacteroides vulgatus*), *Phocaeicola dorei* (formerly *Bacteroides dorei*), and *Streptococcus parasanguinis*.

An amino acid identity matrix of these sequences revealed four clusters of enzymes with sequence identities higher than 69% (Fuc1584/Fuc1821, Fuc144/Fuc584/Fuc1327, Fuc11/Fuc19B/Fuc47 and Fuc18/Fuc59/Fuc289/Fuc499) which suggest that enzymes within the same cluster might share similar substrate specificities. Moreover, upon comparing these sequences with previously characterized α-L-fucosidases, it was found that Fuc11 and Fuc21 exhibited 99% identity with BT_2970 and BT_2192 from *B. thetaiotaomicron* [203] respectively. Similarly, Fuc29 and

Fuc144 demonstrated 99% and 87% identity respectively with the α-L-fucosidase ATCC_03833 from *R. gnavus* [204] and BF3242 from *Bacteroides fragilis* [205].

Fuc18, Fuc19A, Fuc30, Fuc35A, Fuc35B, Fuc39, Fuc193, Fuc1584, Fuc2358 and Fuc5372 were selected for further analysis, since to the best of our knowledge, no proteins homologous to these α-L-fucosidases had been characterized to date. SignalP 4.1 [196] predicted the presence of signal peptides in all the selected α-L-fucosidases, except for Fuc2358. Raw Sequence data files are available in the NCBI Sequence Read Archive (SRA, http://www.ncbi.nlm.nih.gov/sra) under Bioproject number PRJNA814838. The sequences of the genes encoding the α-L-fucosidases characterized here have been deposited at the GenBank database under the accession numbers ON170361 to ON170370.

4.3. Purification of fucosidases

The ten selected fucosidases from the metagenome study (Fuc18, Fuc19A, Fuc35A, Fuc1584, Fuc193, Fuc39, Fuc2358, Fuc5372, Fuc30 and Fuc35B) as well as the AfcA and AfcB fucosidases (provided by Dr Katayama) were purified as indicated in material and methods. The purified enzymes were analysed by SDS-PAGE in 10% polyacrylamide gels and stained with Coomassie blue (Fig. 9). Each one of the fucosidases migrated at the expected molecular weight (Fuc18 70.36 kDa, Fuc19A 53.65 kDa, Fuc35A 52.14 kDa, Fuc1584 76.1 kDa, Fuc193 53.19 kDa, Fuc39 68.03 kDa, Fuc2358 57.98 kDa, Fuc5372 50.88 kDa, Fuc30 52.15 KDa, Fuc35B 49.63 kDa, AfcA 205 kDa, AfcB 152.26 kDa). It can be observed that all proteins were obtained with a purity higher than 80% since some contaminants or degradation products can be observed in each preparation.

4.4. Fucosidases characterization

Activity characterization was conducted for all enzymes, comprising those obtained in the metagenome analysis as well as AfcA and AfcB. The analysis involved the incubation of the enzymes with the different neoglycoproteins at 37 ºC overnight. The glycans conjugated to HSA were LNFP I, Le^a, Le^b, Le^x, Le^y, whose structures are shown in table 4. During the incubation process, the enzymes targeted and removed the specific fucose residues from the glycoconjugate, thus the primary

antibody will not recognize the sugar. The activity of the enzyme was confirmed then by the loss of signal in the Western blot.

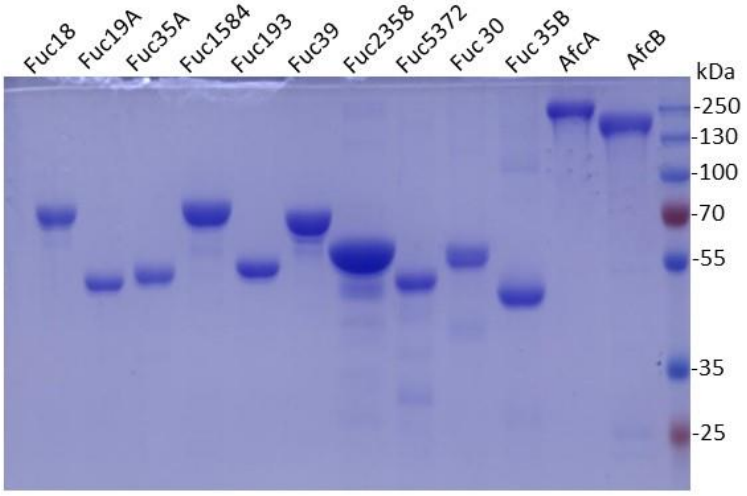

Figure 9. *Purified fucosidases from infant gut microbiome, with AfcA and AfcB.*
Coomassie of 5 µg of each α-L-fucosidase obtained. On the right, the molecular mass (kDa).

First, the specific affinity of the primary antibodies and lectins was confirmed (Fig. 10). An anti-H antibody was used to detect LNFP I, which recognized the H1 structure fucose-α1-2-galactose-β1-3 N-acetyl glucosamine. Also, the UEA-I lectin that recognized the α1-2 fucose in the H2 structure fucose-α1-2-galactose-β1-4 N-acetyl glucosamine that is present in the Le^y antigen was employed. With these two recognition proteins, fucosidase α1-2 activity was detected. The presence of the glycoconjugates in all the membranes was confirmed by a final incubation step of each of them with the anti-HSA antibody. Each antibody recognised only their respectful glycoconjugate, except for anti-Le^b, which also showed a weak signal in the lane of Le^a. This observation can be attributed to the fact that Le^b and Le^a share the same structure, except that Le^b has an α1-2 linkage that binds the fucose to the galactose, so the antibody is able to recognise Le^a, although less efficiently.

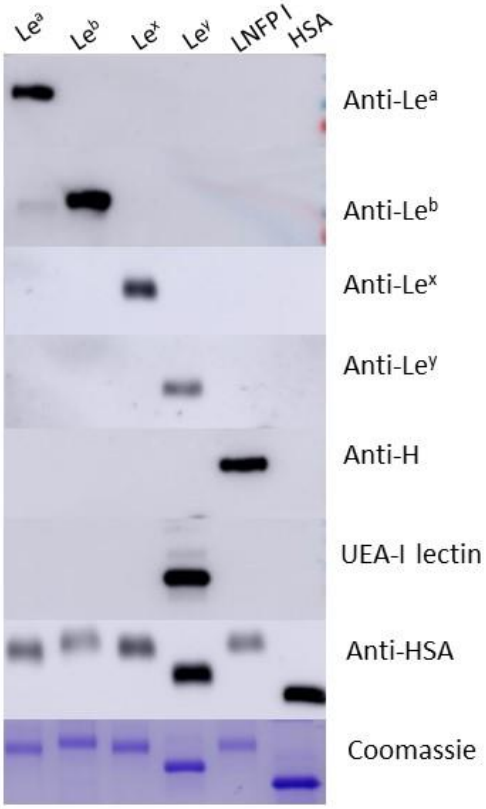

Figure 10. *Specificity of primary antibodies and lectin by Western blot.*
The figure shows the specificity of the primary antibodies and lectin employed in the characterization of the α-L-fucosidases by Western blot. The Western blots and Coomassie were used to confirm the presence of the glycoconjugates. LNFP I, lacto-N-fucopentaose I; Le^a, Lewis ^{a}; Le^b, Lewis ^{b}; Le^x, Lewis ^{x}; Le^y, Lewis ^{y}; anti-Le^a, anti-Lewis^a primary antibody; anti-Le^b, anti-Lewis^b primary antibody; anti-Le^x, anti-Lewis^x primary antibody; anti-Le^y, anti-Lewis^y primary antibody; anti-H, anti-H type-1 antigen primary antibody; UEA-I lectin, *Ulex Europaeus* agglutinin I lectin; anti-HSA, anti-human serum albumin antibody.

Once it was stablished that each antibody and the UEA-I lectin recognized their specific sugar, the activity of the fucosidases were studied by Western blot analysis (Fig. 11). AfcA had α1-2 activity, as observed by the absence of signal of the anti-H antibody and UEA-I lectin glycoconjugates. It was also the only fucosidase with this enzymatic function. Regarding AfcB, it released the α1-3/4 fucoses from all the sugars containing them, thereby confirming the documented activity of AfcA and AfcB [85,91]. Fuc19A displayed α1-3 but no α1-4 activity. However, it didn't release the α1-3 fucose present on Le^y. In contrast, Fuc35B exhibited α1-4 and not α1-3 activity, but it didn't cut the fucose present on Le^b. Fuc18 and Fuc39 showed α1-3/4 activity. Nonetheless, they were unable to completely remove the signal of anti-Le^y, and also anti-Le^b in the case of Fuc39, Fuc35A, Fuc1584,

Fuc193, Fuc2358, Fuc5372 and Fuc30 released minimal amounts of fucose present in the tested glycoconjugates. The control included only glycoconjugates.

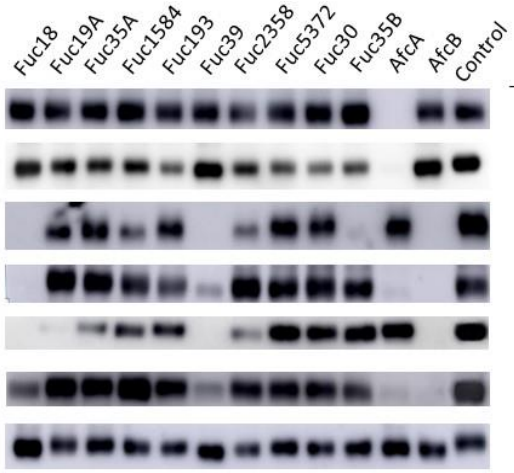

Glycoconjugate	Antibody / Lectin	Linkage detected
LNFP I	Anti-H	α1-2
Le^y	UEA-I lectin	α1-2
Le^a	Anti-Le^a	α1-4
Le^b	Anti-Le^b	α1-2 and α1-4
Le^x	Anti-Le^x	α1-3
Le^y	Anti-Le^y	α1-2 and α1-3
Le^y	Anti-HSA	None

Figure 11. *Characterization of fucosidases by Western blot.*
Glycoconjugates were incubated with the α-L-fucosidases overnight and later blotted and incubated with their specific antibody. Absence of signal indicates the removal of the fucose from the glycoconjugate detected by the antibody or lectin. LNFP I, lacto-N-fucopentaose I; Le^y, Lewis ^{y}; Le^a, Lewis ^{a}; Le^b, Lewis ^{b}; Le^x, Lewis ^{x}; anti-H, anti-H type-1 antigen primary antibody; anti-Le^a, anti-Lewis^a primary antibody; anti-Le^b, anti-Lewis^b primary antibody; anti-Le^x, anti-Lewis^x primary antibody; anti-Le^y, anti-Lewis^y primary antibody; anti-HSA, anti-human serum albumin antibody.

To further characterize the 10 enzymes identified after the metagenomic analysis, the hydrolysis of various non conjugated fucosyloligosaccharides (Table 4) was measured by Dionex [187]. With this method, the products generated during their hydrolysis were analysed and the presence of a peak at the same migration time than fucose was used to study it release, indicating that the enzyme has the specific fucosidase activity required to cut the oligosaccharide present in the reaction. Some differences were found when compared to Western blot since the enzymes had higher activity against the free substrates than against the glycoconjugates. The results (Table 8) showed that Fuc18, Fuc39 and Fuc 35B were able to release α1-3/4 fucose from all tested substrates, but the last one less efficiently. Fuc19A and Fuc1584 released α1-3 fucoses from Le^x, Le^y and 3FL, while only α1-4 fucose from Le^a but not from Le^b. Fuc1584 also displayed α1-6 activity. Fuc35A displayed partial α1-2, α1-3 and α1-6 fucosidase activity. As for 2358, it was able to remove fucose from all the tested substrates, except for Le^b, BG A and BG B, thus possessing α1-2, α1-3, α1-4 and α1-6 activity. Fuc30 presented α1-6 fucosidase activity. Fuc5372 showed partial α1-2 fucosidase activity. Finally, Fuc193 did not remove fucose from any tested substrate efficiently.

Table 8. *Characterization of fucosidases from the metagenome study by Dionex.*

		Percentage of hydrolysis									
Substrate	**Linkage detected**	**Fuc18**	**Fuc19A**	**Fuc35A**	**Fuc1584**	**Fuc193**	**Fuc39**	**Fuc2358**	**Fuc5372**	**Fuc30**	**Fuc35B**
H type-1	α1-2	0	0	0	0	0	0	81	2	0	0
Le^a	α1-4	100	74	66	84	14	100	100	0	0	100
Le^b	α1-2 and α1-4	100	14	8	27	0	100	32	0	0	72
Le^x	α1-3	100	100	100	100	36	100	100	0	0	82
Le^y	α1-2 and α1-3	100	100	73	94	22	100	100	0	0	62
H type-2	α1-2	0	0	74	0	8	0	100	77	0	0
BG A	α1-2	0	0	0	0	0	0	3	40	0	0
BG B	α1-2	0	0	0	0	0	0	3	43	0	0
2' FL	α1-2	2	0	96	0	8	0	100	100	0	0
3FL	α1-3	100	79	54	85	8	100	90	10	0	98
6FN	α1-6	0	0	73	100	15	0	100	11	100	0

In blue, percentage of hydrolysis between 70-90. In green, percentage of hydrolysis between 91-100. H type-1; H type-1 antigen; Le^a, $Lewis^a$ antigen; Le^b, $Lewis^b$ antigen; Le^x, Lewis ^{x} antigen; Le^y, $Lewis^y$ antigen; H type-2, H type-2 antigen; BG A, blood group A trisaccharide; BG B, blood group B trisaccharide; 2'FL, 2'-fucosyllactose; 3FL, 3-fucosyllactose; 6FN, 6-fucosyl-N-acetylglucosamine.

Among all tested enzymes, Fuc2358, Fuc35A and Fuc5372 showed partial α1-2 fucosidase activity. However, those did not present any activity against the glycoconjugates, being AfcA the only fucosidase able to function on those. As for α1-3/4 activity, Fuc18, Fuc39, Fuc 35B and AfcB had the ability to release fucose from all the tested sugars containing them. However, only AfcB released the α1-3/4 fucose residues found in the glycoconjugates. Consequently, AfcA and AfcB were selected for further experiments to ensure effective α1-2 and α1-3/4 activity on both cell and animal models, since these two showed complete activity on the glycoconjugates by Western blot analysis. As HBGAs do not possess α1-6 fucoses, fucosidases with α1-6 activity were not selected.

AfcA activity was also confirmed by immunofluorescence of 2D HIEs, using the lines InEpC and FI124 (Fig. 12, Fig.13). 2D monolayers were incubated with AfcA, AfcB or AfcA and AfcB simultaneously. Later, they were incubated with the lectin UEA-I conjugated to fluorescein and DAPI. It can be observed that the presence of AfcA causes the loss of the UEA-I lectin signal in both HIEs lines **(**Fig. 12d,j, Fig. 13d,j), which means the removal of the α1-2 fucoses recognized by the lectin.

Signal remains intact when no treatment is performed (Fig. 12a, Fig, 13a) or treatment with AfcB (Fig. 12g, Fig. 13g).

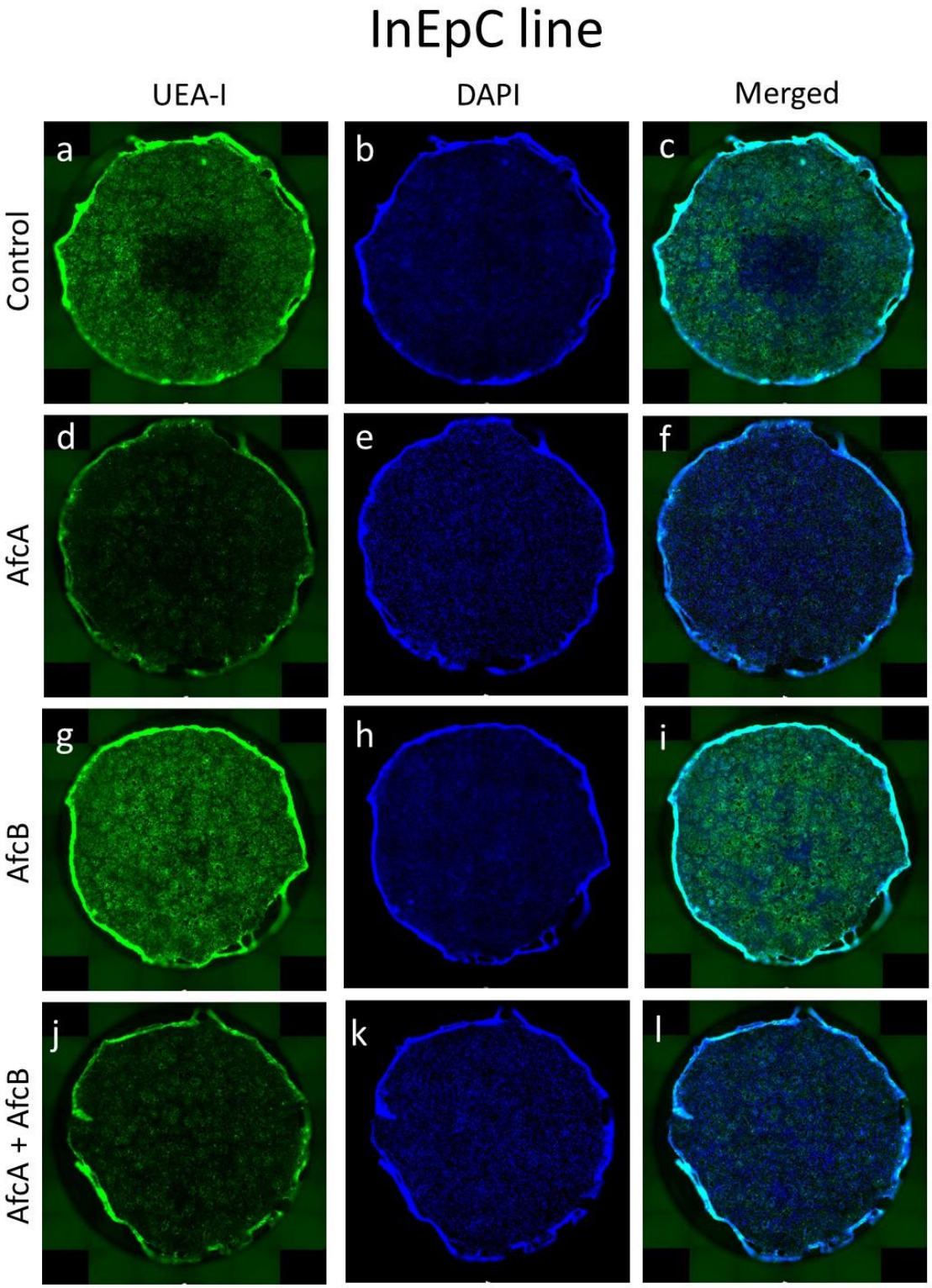

Figure 12. *Incubation of 2D HIEs of the InEpC cell line treated with the fucosidases AfcA and AfcB with UEA-I and DAPI.*

InEpC HIEs were incubated with a)-c) no enzyme, d)-f) AfcA fucosidase, g)-i) AfcB fucosidase or j)-l) AfcA and AfcB fucosidases simultaneously. After fixation and blocking, lectin UEA-I (green) and DAPI (blue) were added to detect α1-2 fucoses and cellular nucleus, respectively. Merged images are also shown. InEpC, intestinal epithelial cells.

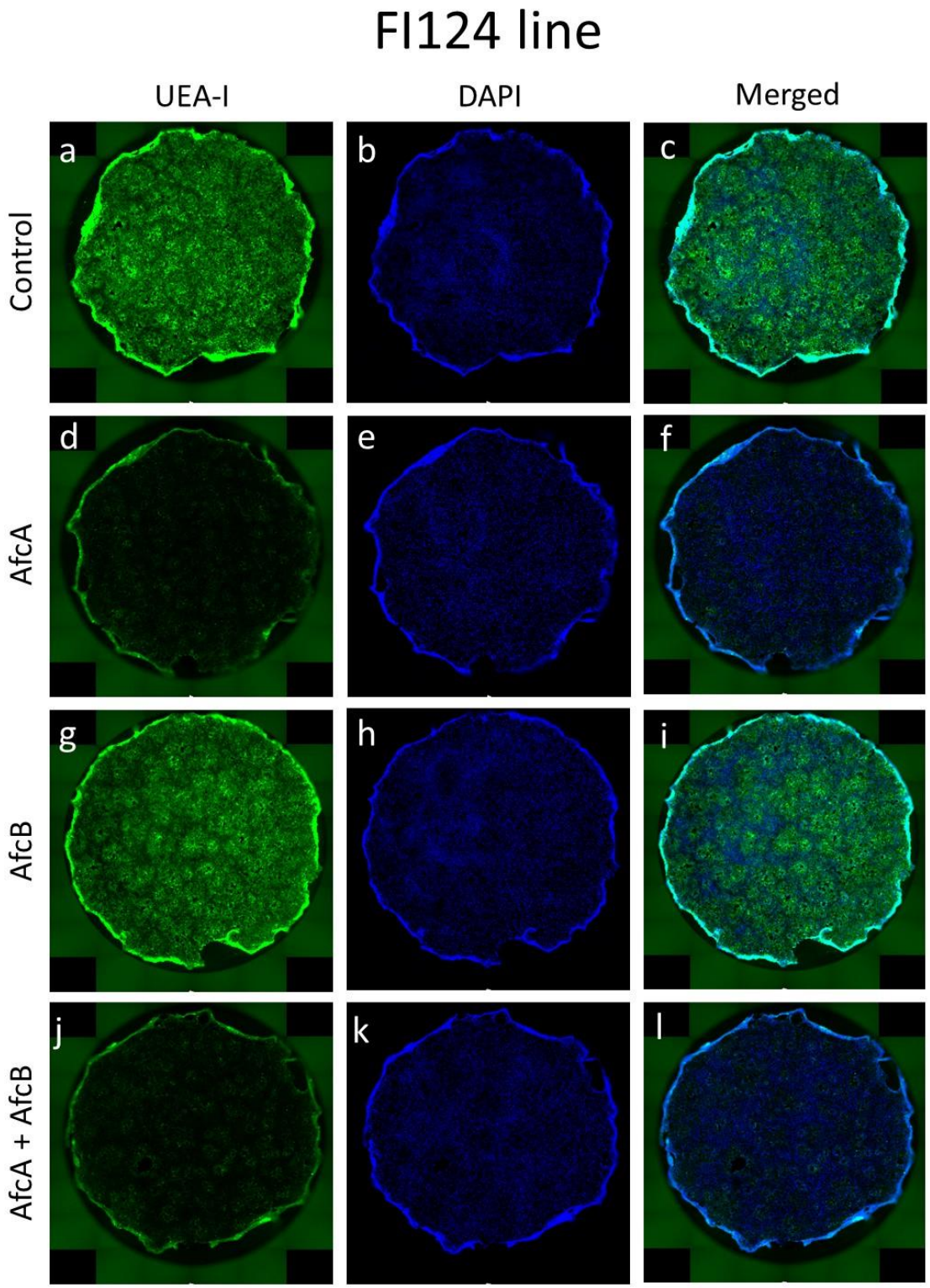

Figure 13. *Incubation of 2D HIEs of the FI124 cell line treated with the fucosidases AfcA and AfcB with UEA-I and DAPI.* FI124 HIEs were incubated with a)-c) no enzyme, d)-f) AfcA fucosidase, g)-i) AfcB fucosidase or j)-l) AfcA and AfcB fucosidases simultaneously. After fixation and blocking, lectin UEA-I (green) and DAPI (blue) were added to detect α1-2 fucoses and cellular nucleus, respectively. Merged images are also shown. FI124, fetal ileum 124.

4.5. Clinical rotaviruses screening

A total of 41 RV$^+$ stool filtrates were prepared and used to infect dCaco-2 cells for 72 hpi. After RNA extraction, the fold increase is analysed by $2^{-\Delta\Delta Ct}$. A fold increase >3 was considered viral replication. 4 clinical isolates showed ability to replicate in dCaco-2 under tested conditions, called RV7, RV18, RV39 and RV41 (Fig. 14). Also, dCaco-2 cells were infected with the cell-culture adapted RV strain Wa. Some of the viruses didn't attach to the cells (e.g. RV8, RV19 or RV20, not shown) and others did not replicate efficiently (fold increase <3). Finally, RV7 and RV39 were selected to continue further experiments, since RV18 and RV41 showed high variability when the infection experiments were repeated. No cytopathic effect was detected in any infection experiment.

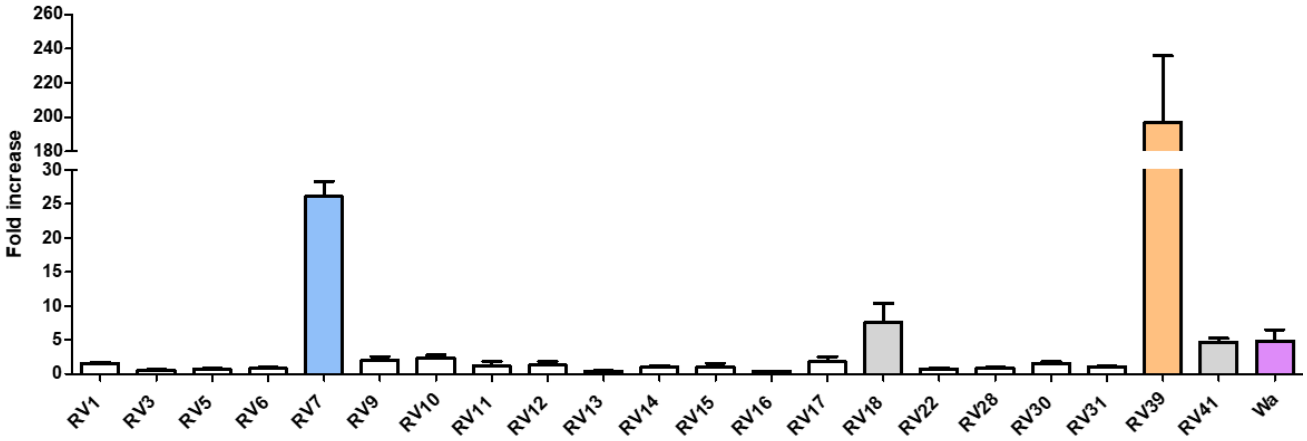

Figure 14. *Viral replication of RV$^+$ stool samples and the culture-adapted RV strain Wa in dCaco-2 cells at 72 hpi.* A total of 41 RV$^+$ stool samples were prepared and used to infect dCaco-2 cells, along with Wa for 72 hpi. A fold increase >3 was considered efficient viral replication. Viral preparations that did not attach to cells are not shown. RV, rotavirus; dCaco-2, differentiated Caco-2; hpi, hours post infection.

The sequences of the VP4 (Fig. 15) and VP7 (Fig. 16) of the selected clinical isolates and the Wa strain were obtained. RV7 and RV39 are G9P[8] while Wa is G1P[8]. The VP4 sequences of RV7 and RV39 are identical. Regarding VP7, there are two nucleotide variations between the clinical isolates at the positions 638 and 641. When comparing VP4 sequences of Wa strain with the ones from RV7 and RV39, a total of 55 mismatches are found. As for VP7, it can be observed a total of 212 mismatches with RV7 and 210 with RV39.

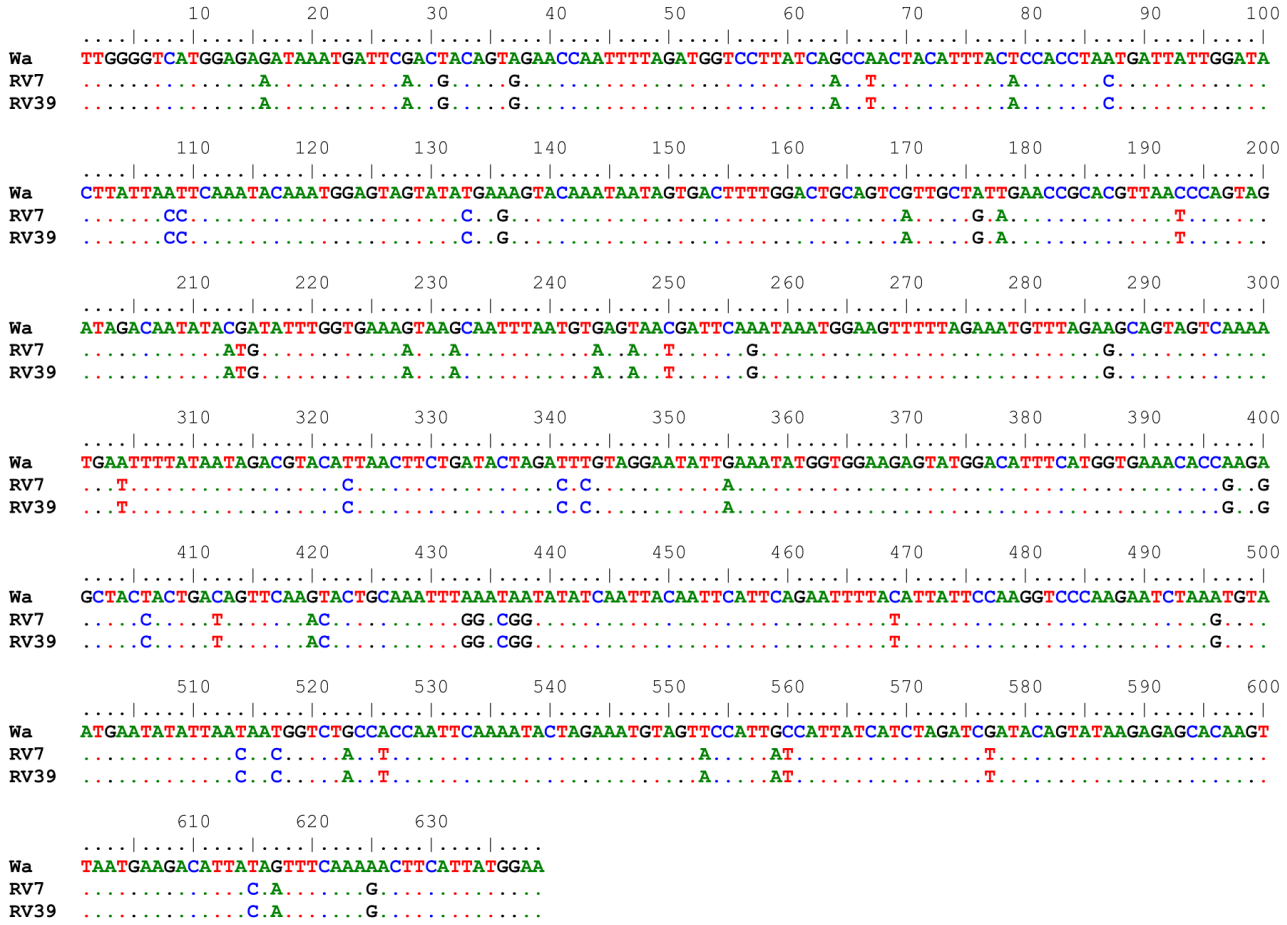

Figure 15. *VP4 sequences of Wa strain and clinical isolates RV7 and RV39.*

Three aligned VP4 sequences of the clinical isolates RV7, RV39 and the cell culture-adapted Wa strain are presented. Sequence alignments were obtained with Bioedit software version 7.0.5.3.

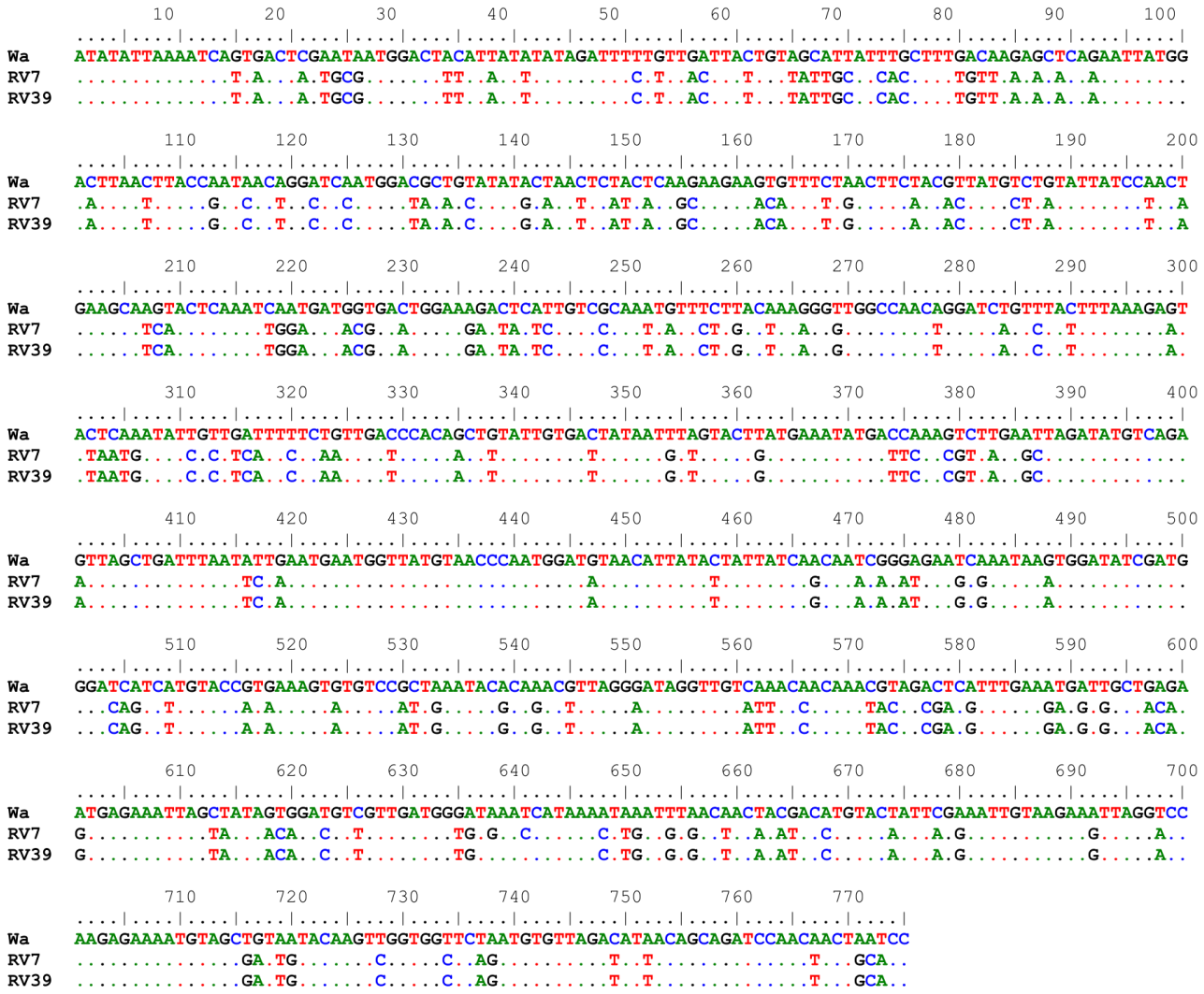

Figure 16. *VP7 sequences of Wa strain and clinical isolates RV7 and RV39.*
Three aligned VP7 sequences of the clinical isolates RV7, RV39 and the cell culture-adapted Wa strain are presented. Sequence alignments were obtained with Bioedit software version 7.0.5.3.

4.6. Clinical rotaviruses and Wa time course

In order to obtain the maximum viral replication, dCaco-2 cells were infected with the selected clinical isolates as well as with Wa at different time points (24, 48, 72 and 96 hpi) (Fig. 17). RV7 showed the highest replication 96 hpi (p value=0.0238). As for RV39, the highest replication was detected at 72 hpi (p value=0.0067). Although Wa replication did not yield significant differences at the analysed time points replication was similar at 48, 72 and 96 hpi. RV7, RV39 and Wa did not show statistical differences between 72 and 96 hpi. For these reasons 72 hpi was the selected time point for further experiments.

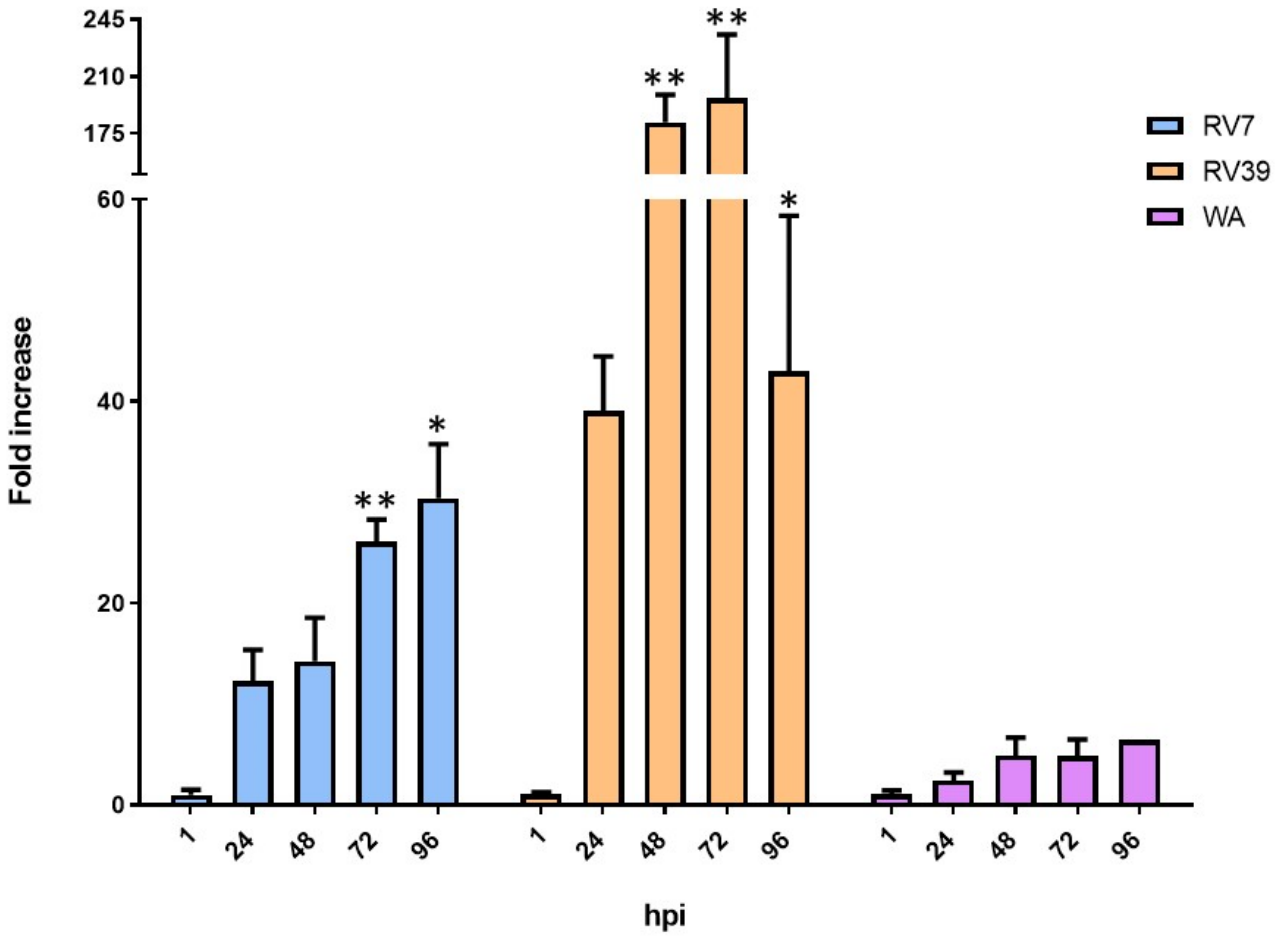

Figure 17. *Time course of RV7, RV39 and Wa in dCaco-2.*
DCaco-2 were infected with the selected RV isolates RV7 and RV39, as well as with the cell culture-adapted Wa strain for 1, 24, 48, 72 and 96 hpi. RV, rotavirus; dCaco-2, differentiated Caco-2; hpi, hours post infection. p values ≤ 0.05 are represented as *, p values ≤0.01 are represented as **.

Time course experiments were also performed in 3D HIEs. Once stablished, differentiated 3D HIE cultures were infected with RV7 to optimize RV replication. The infection was carried out in drop or suspension format. The tested MOIs were 100, 10 and 1 and the infected cells were collected after 2 hpi, 24 hpi, 48 hpi and 72hpi. Only the MOI 100 yielded data for all the time points by qPCR. To analyse the data, the value 1 was assigned to the total amount of virus that attached to the cells at 2 hpi in drop the format, so it can be compared where the viral production is higher (Fig. 18). In the suspension experiment, the fold increase rose sequentially until day 2, observing a decrease at day 3. In the drop experiment, the highest yield was obtained at 24 hpi, decreasing in days 2 and 3. Overall, the highest viral quantities were obtained by infecting the cells in suspension and incubating them for 2 dpi.

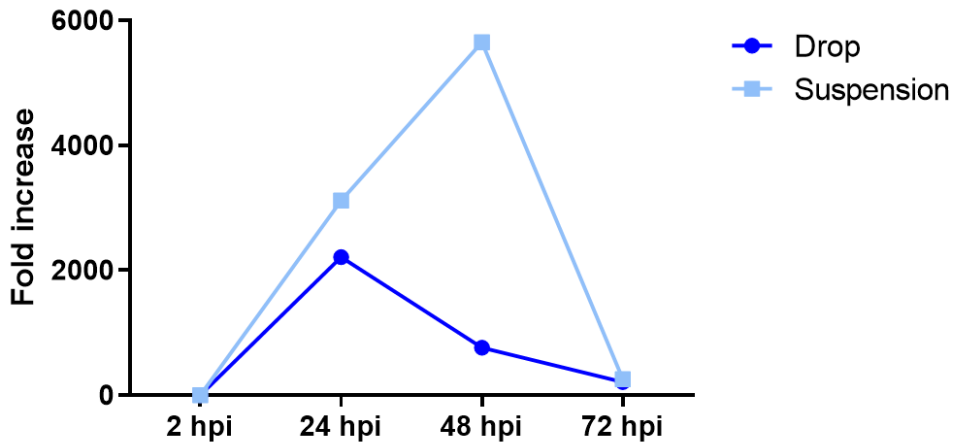

Figure 18. *Fold increase of RV7 after infection of 3D HIEs.*
3D HIEs were infected with RV7 with MOI 100 in drop and suspension formats for 2, 24, 48 and 72 hpi. Hpi, hours post infection.

In the view of these results, differentiated 3D HIE were also infected with RV39 and Wa in suspension format for 2 hpi, 24 hpi and 48 hpi with a MOI of 100 (Fig. 19). For RV39, the highest fold increase occurred at 48 hpi. However, in the case of Wa, neither attachment nor replication were observed under the tested conditions, despite studying an MOI of up to 1,000.

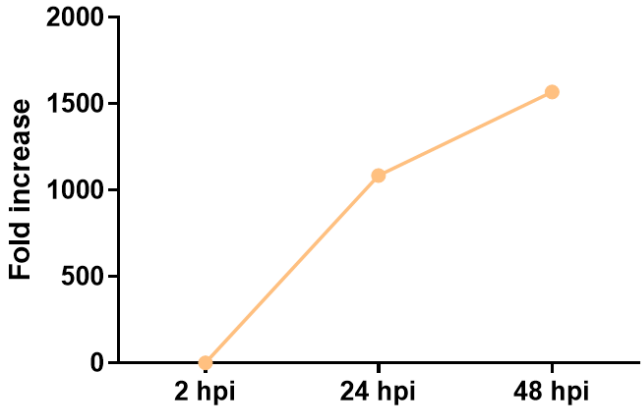

Figure 19. *Fold increase of RV39 after infection of 3D HIEs.*
RV39 was used to infect 3D HIEs in suspension with a MOI of 100 for 2, 24 and 48 hpi. Hpi, hours post infection.

4.7. Immunofluorescence of differentiated Caco-2 cells infected with a clinical rotavirus

Clinical RV7 was also used in an immunofluorescence experiment, in which dCaco-2 cells were infected. Anti-VP6 primary antibody and DAPI were used to stain the virus and the cell nuclei, respectively. In the figure 20, it can be observed dCaco-2 cells infected with RV7.

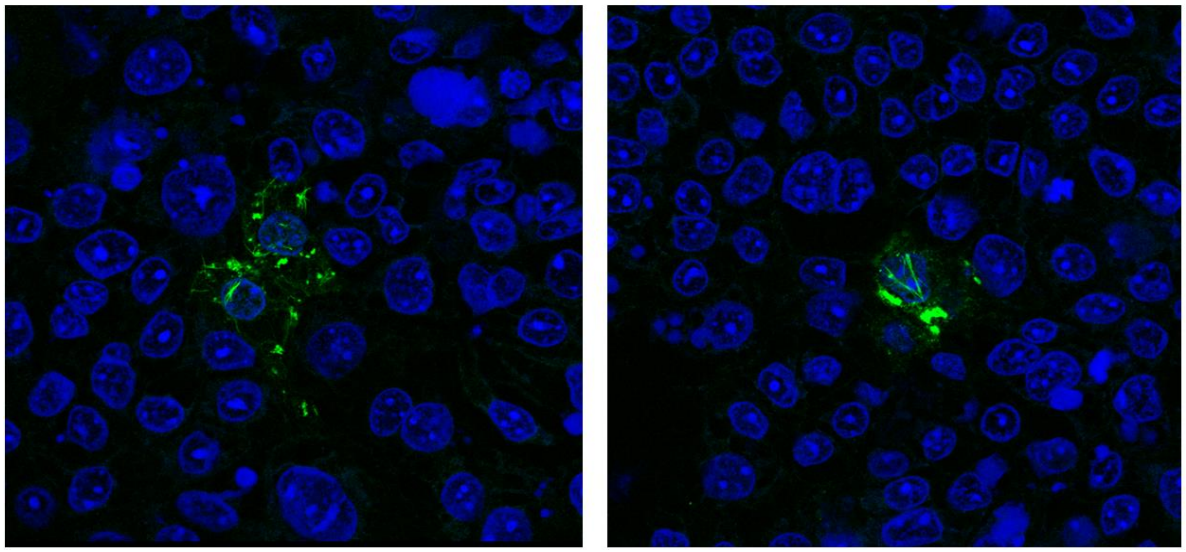

Figure 20. *Immunofluorescence of dCaco-2 cells infected with the RV7 filtrate for 24 h observed at 40X.*
In blue, cell nucleus stained with DAPI, in green, RV7 VP6 protein. DCaco-2, differentiated Caco-2.

4.8. Infection of cell lines with different HBGA composition

To investigate variations in viral replications between clinical isolates and a cell-culture adapted strain, cell lines with different HBGAs composition were infected with RV7, RV39 and Wa. As cell lines with HBGAs, dCaco-2, HT29, HT29 M6, 2D HIEs (J2 cell line) and 3D HIEs (InEpC cell line) were employed. UCaco-2 and MA104 served as cell lines without HBGAs. The results (Fig. 21) showed that the replication of clinical isolates was higher in those cell lines that express HBGAs on their surface (dCaco2, HT29, HT29 M6 and HIEs) as compared to uCaco-2 and MA104, where fold increases lower than 5 were obtained. In contrast, Wa replicated more efficiently in MA104, a cell line lacking HBGAs. Moreover, it did not attach to HT29, HT29 M6 and 3D HIEs, further supporting its preference for cell lines without HBGAs.

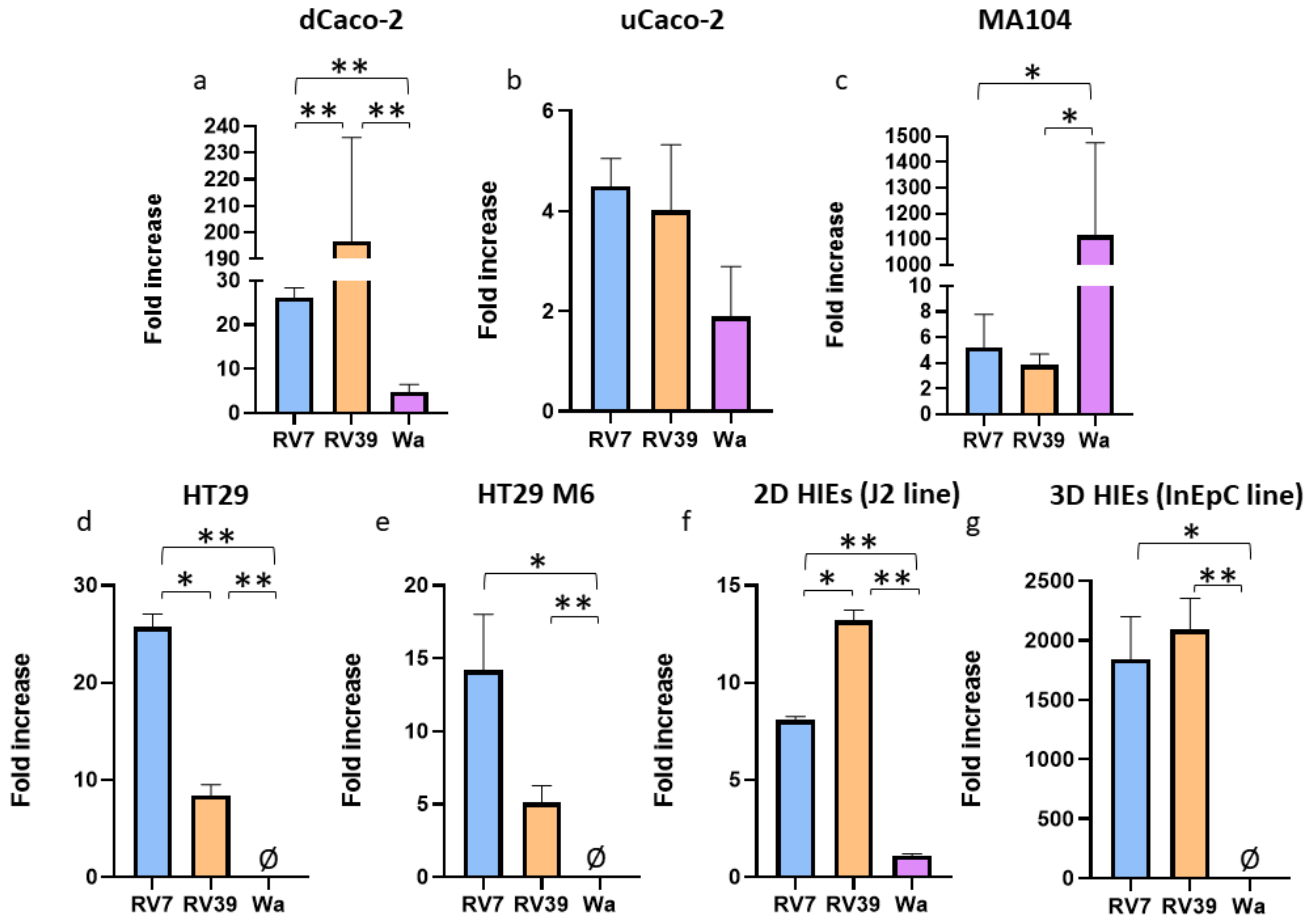

Figure 21. *Viral replication at 72 hpi of clinical isolates RV7, RV39 and the cell culture-adapted RV strain Wa in cell lines with different HBGAs composition.*

Viral replication of RV7, RV39 and Wa was studied in a) dCaco-2, b) uCaco-2, c) MA104, d) HT29, e) HT29 M6 cells, f) 2D HIEs (J2 cell line) and g) 3D HIEs (InEpC cell line). Hpi, hours post infection; RV, rotavirus, dCaco-2, differentiated Caco-2; uCaco-2, undifferentiated Caco-2; HIEs, human intestinal enteroids; Ø, no viral attachment. p values ≤ 0.05 are represented as *, p values ≤0.01 are represented as **.

4.9. Role of fucosylated HBGAs in the infection of differentiated Caco-2 cells with clinical rotaviruses and Wa

Since it was observed that HBGAs are relevant for the infection of wildtype RVs, it was investigated the relevance of the fucose present in the receptors. The experimental approach involved two treatments: a first step of fucosidase treatment to the cells for 2 h followed by RV infection, or alternatively, fucosidase inhibitor treatment of the viral stocks during activation.

The toxic screening performed to study the toxicity of the fucosidase inhibitor and the fucosidases on 3D HIEs of the InEpC line (Fig. 22) confirmed the absence of toxicity in the tested compounds. The cells that received no treatment were assigned a survival rate of 100%. When HIEs were incubated

with the compounds and enzymes at different concentrations, the percentage of survival remained closed to 100% in all tested conditions. Therefore, any decrease in replication that could be observed in experiments is not attributable to a toxic environment.

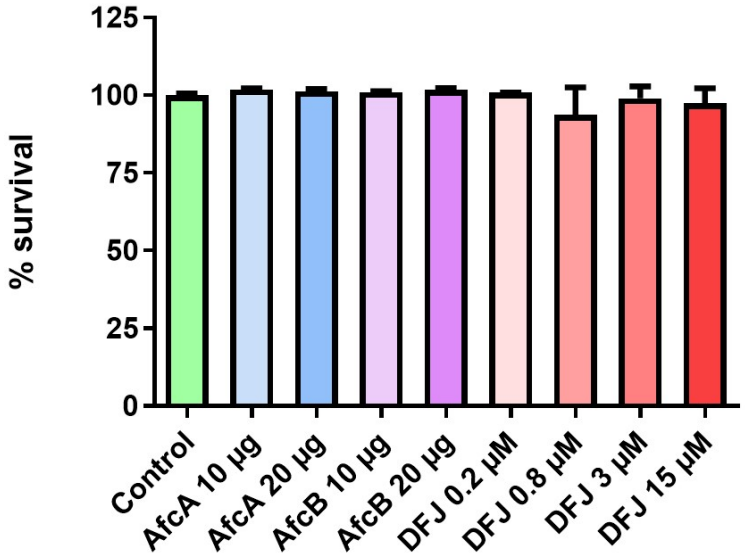

Figure 22. *Toxicity of fucosidases and DFJ on 3D HIEs.*
The figure shows the percentage of survival of 3D InEpC HIEs after 2 h incubation with the fucosidases AfcA and AfcB, and the fucosidase inhibitor DFJ at different concentrations for 2 h. DFJ, 1-deoxyfuconojyrimicin.

4.9.1. Fucosidase treatment

Cells were treated with the previously characterized fucosidases, AfcA and AfcB. For 2 h, cells were treated with AfcA to remove α1-2 fucoses, with AfcB to remove α1-3/4 fucoses, or with both simultaneously, to then proceed with the viral infection. 100% of adhesion was assigned to the controls. The results (Fig. 23a) showed an increase in RV7 adhesion when α1-3/4 fucoses were eliminated, but not when only α1-2 fucoses were removed. Treatment with both enzymes caused an increase in adhesion for RV7, but with no significant differences. Adhesion of Wa was increased when cells were incubated with AfcA and AfcB, but not significant data was obtained when cells were treated alone with the latest fucosidase (Fig. 23g). Adhesion of RV39 didn't seem to be affected by the enzymes (Fig. 23d).

Regarding the replication, it was analysed in two different ways. In the viral yield analysis (Fig. 23b, e, h), viral quantities can be compared, since in the calculation of the fold increase by the $2^{-\Delta\Delta Ct}$ method the value 1 was given to the total amount of virus that attached to the cells when no treatment was performed (control of adhesion). Later, the 100% of viral yield was assigned to the

control at 72 hpi. Since all the treatments are compared to the same reference value, it can be easily detected variations in viral amounts. In this case, results were similar for both RV7 and RV39. Treatments with either AfcA or AfcB yielded equivalent outcomes, resulting in a 2.6-fold for RV7 and a 1.9-fold for RV39. When the treatment was performed with both enzymes, the maximum viral quantity was achieved (5.8-fold for RV7 and 2.8-fold for RV39). In the case of RV7, significantly more virus is produced in all the treatments, while AfcA and combined treatment of AfcA and AfcB resulted in significant differences for RV39. As for Wa, AfcB treatment resulted in an increased viral yield (2.13-fold).

As for the viral replication analysis, each condition at 72 hpi was compared to the same condition at 1 hpi (Fig. 23c, f, i) for the calculation of the fold increase, so it can be studied how the virus replicates depending on the treatment performed. Later, 100% of replication was assigned to the control at 72 hpi. Again, similar results were obtained for both clinical isolates. Clinical RV replication was similar when no treatment or treatment with AfcB was carried out, indicating that the removal of α1-3/4 fucoses from the cell surface does not affect the replication itself. Regarding AfcA treatment, the removal of α1-2 fucoses significantly improved the replication (4.2-fold for RV7 and 3.6-fold for RV39). Treatment with both enzymes simultaneously produced similar findings than treatment with only AfcA for RV7 and RV39 (5.5-fold increase for RV7 and 3.4-fold increase for RV39).

Regarding the cell culture-adapted strain, Wa attached significantly more when combined treatment with AfcA and AfcB was applied. It was also detected an increased when cells were treated with AfcB without significant results. As for the viral yield, it was detected a 2.12-fold after cellular treatment with AfcB. Finally, no statistically significant data was obtained in Wa replication.

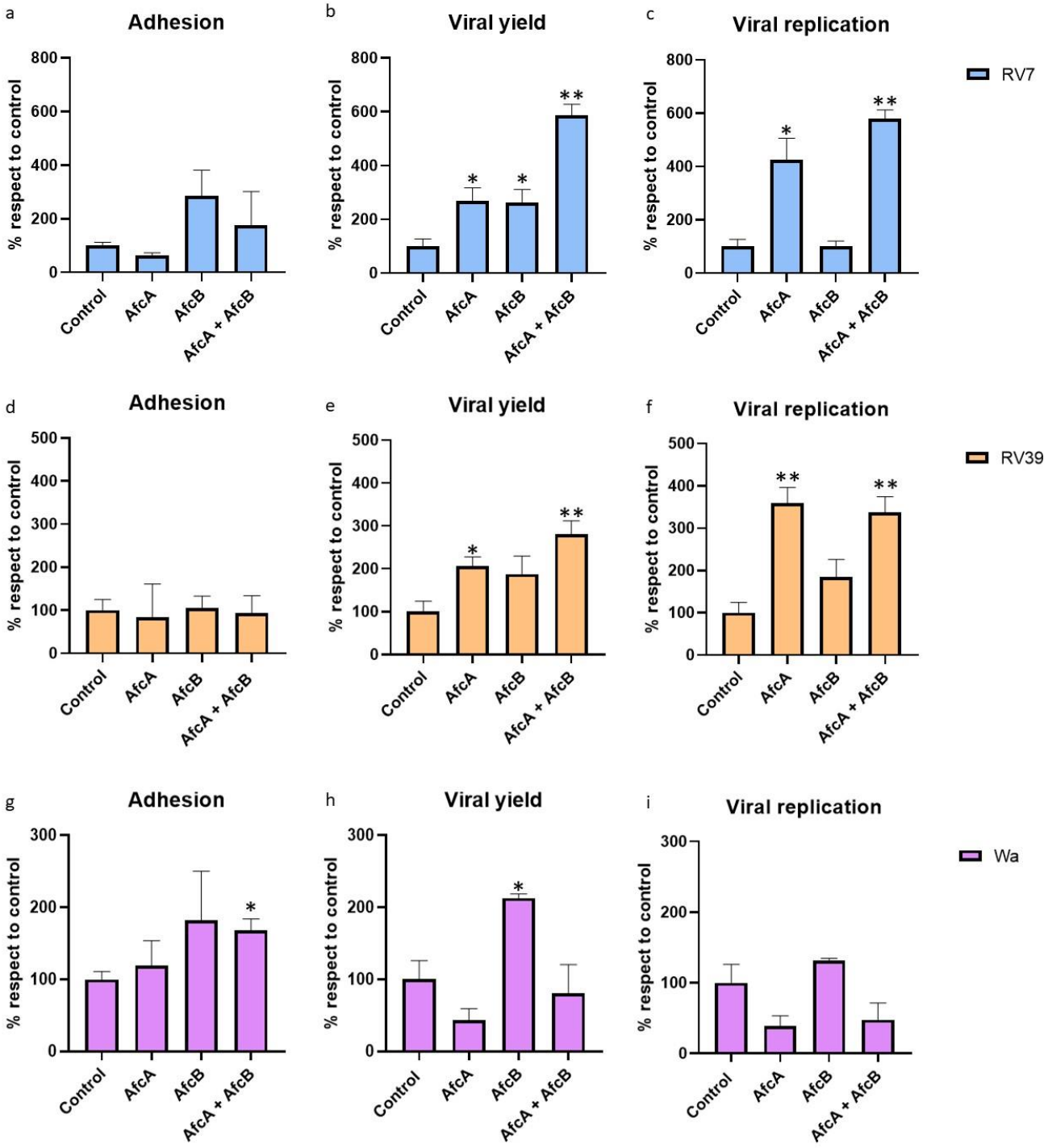

Figure 23. *Effect of the fucosidases AfcA and AfcB on infection of RV7, RV39 and Wa on dCaco-2 cells.*
Graphs show the percentage respect to control of a) d) g) adhesion, b) e) h) viral yield and c) f) i) viral replication of RV7, and RV39 and Wa in dCaco-2 pretreated with the fucosidases AfcA and AfcB alone or simultaneously. dCaco-2, differentiated Caco-2. p values ≤ 0.05 are represented as *, p values ≤0.01 are represented as **.

Based on these results, it can be concluded that the removal of α1-3/4 fucose affects the initial stages of clinical RVs replication by enhancing adhesion, while the removal of α1-2 fucoses

enhances later stages of replication. This explains why the total amount of virus is higher when both fucosidase activities are present in the case of clinical RVs. For Wa, AfcB also seemed to improve viral attachment, but the replication itself was not enhanced by AfcA.

4.9.2. Fucosidase inhibitor treatment

After studying how the presence of fucosidases affects RV replication, it was investigated the effect of a fucosidase inhibitor, DFJ. It was hypothesised that fucosidases may be present in viral stocks, since their origin was faeces that are rich in bacterial glycosidases [187,206]. First, it was calculated the EC50 of DFJ in four α-L fucosidases, two from the metagenome study (Fuc2358 from *S. parasanguinis* and Fuc5372 from *P. dorei*), and two produced by *L. casei* BL23 (AlfB and AlfC). The assay was performed using the colorimetric substrate *p*NP-fuc (Fig. 24a-d). The fucosidase activity of the enzymes was reduced 99.04% in the case of Fuc2358 (EC50=117.58 ± 5.05 nM), 97.32% for Fuc5372 (EC50=33.03 ± 6.65nM), 94.01% for AlfB (EC50=169.18 ± 14.84 nM) and 98.96% for AlfC (EC50=246.83 ± 23.57 nM), thereby proving its inhibitory properties of the DFJ on the fucosidases. The inhibitor was also incubated with the lacto-N-biosidase LnbB (Fig. 24e). Its activity was reduced a 10% after 1 h incubation with DFJ, with a EC50 of 731.07 ± 1,487.6 nM, which confirms the specificity of the compound.

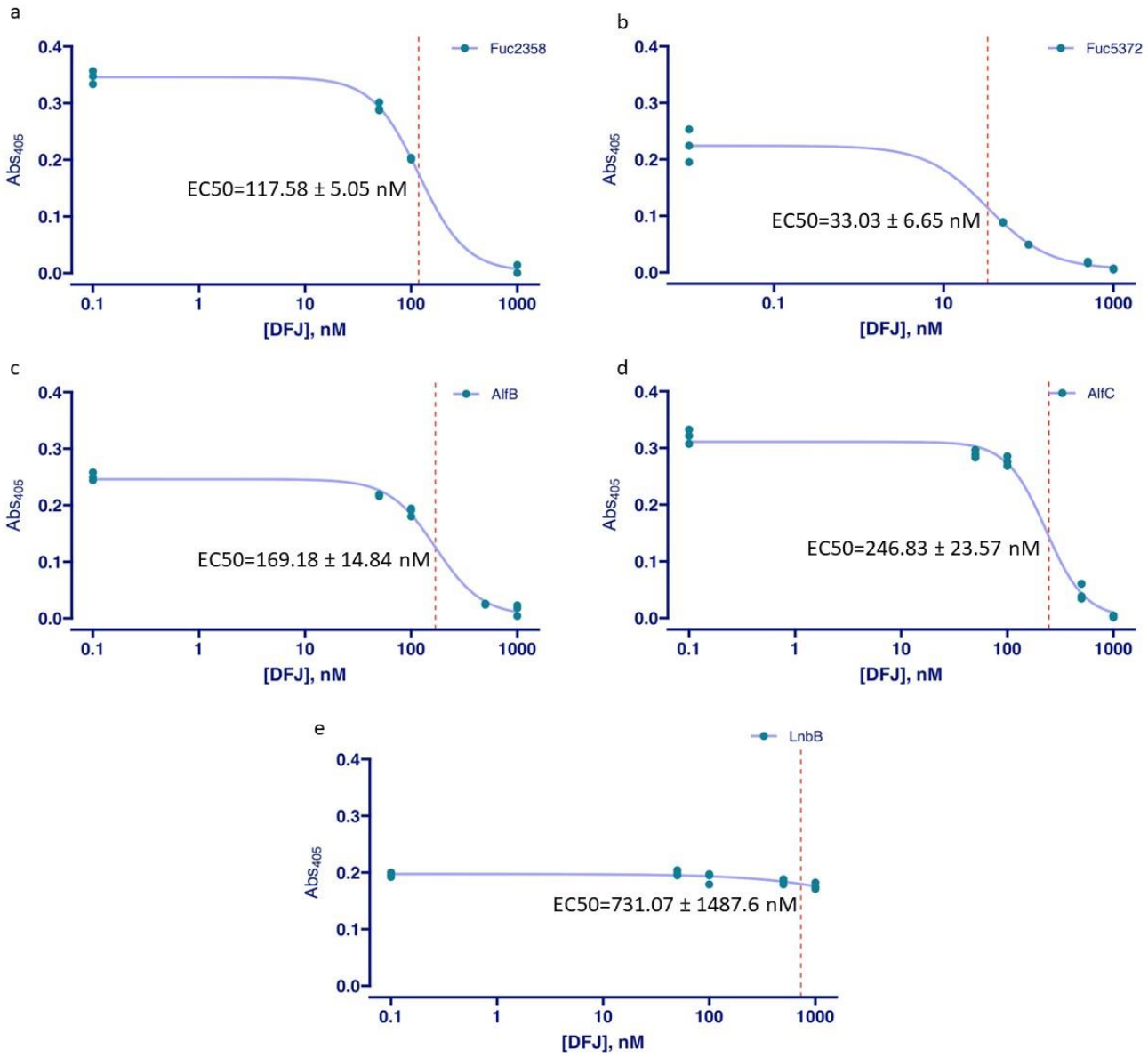

Figure 24. *EC50 of DFJ on the fucosidases Fuc2358, Fuc5372, AlfB and AlfC, and lacto-N-biosidase LnbB.*
Graphs show the EC50 of the fucosidase inhibitor DFJ on the fucosidases Fuc2358 and Fuc5372 from the metagenome study, AlfB and AlfC from *L. casei*, and the lacto-N-biosidase LnbB. Enzymes were incubated with DFJ concentrations ranging from 0 to 1,000 nM. The absorbance of the colorimetric substrate *p*NP-fuc in the case of fucosidases and pnp-gal for the lacto-N-biosidase was measured at 405 nM. DFJ, 1-deoxyfuconojyrimicim; *p*NP-fuc, 4-nitrophenyl-α-L-fucopyranoside; *p*NP-gal, p-nitrophenyl β-D-galactopyranoside.

Later, the effect of DFJ on RV replication was tested on dCaco-2. During RV activation, the fucosidase inhibitor was added, so the enzymes present on viral stocks would be deactivated. RV7 and Wa were treated with the fucosidase inhibitor at 500 nM (Fig. 25), more than 20 times the maximum EC50 obtained previously with the different fucosidases. Viral replication of RV7 and Wa was decreased a 51.63% and 94.87% respectively, by the inhibition of fucosidases, indicating that the activity of those enzymes is relevant for RV replication.

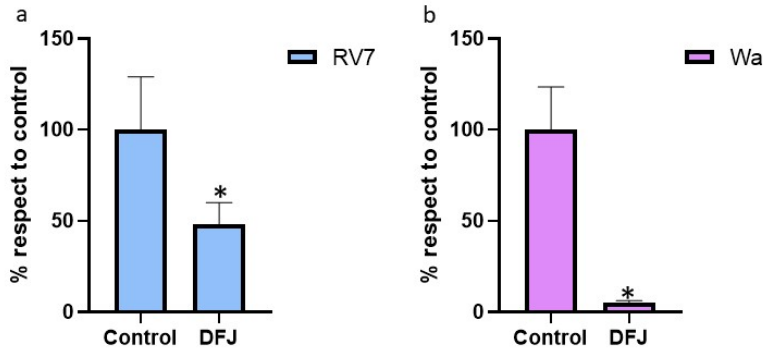

Figure 25. *Effect of the fucosidase inhibitor DFJ on the replication of the clinical isolate RV7 and Wa in dCaco-2.*
Graphs show the replication of a) RV7 and b) Wa treated with the fucosidase inhibitor at 500 nM for 2h in dCaco-2 72 hpi. DFJ, 1-deoxyfuconojyrimicin; dCaco-2, differentiated Caco-2. p values ≤ 0.05 are represented as *.

Later, RV7 and Wa were treated with increasing concentrations of the inhibitor (Fig. 26), obtaining the highest inhibition at 800 nM. In this case, the EC50 of RV7 was 395.94 ± 78.67 nM and that of Wa 67.72 ± 11.87 nM.

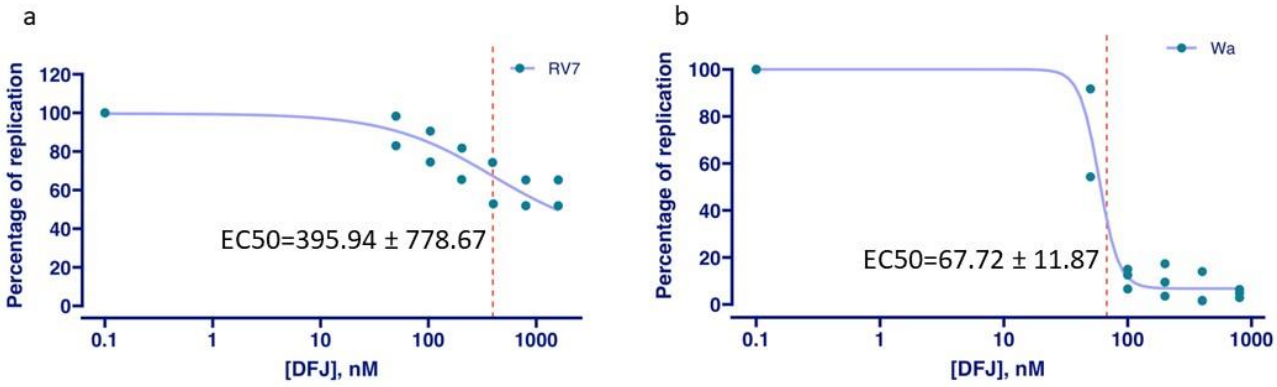

Figure 26. *EC50 of DFJ on RV7 and Wa viruses.*
Figure shows the EC50 of the fucosidase inhibitor DFJ on RV7 and Wa viruses during infection of dCaco-2.

The effect of the DFJ was also studied by impedance, which measures the cell monolayer integrity. In that experiment, dCaco-2 cells were infected with RV7 and Wa that were previously treated with the inhibitor. The results (Fig. 27) showed that the cell index was significantly higher when the viruses were treated with DFJ, which means that the integrity of the monolayer is higher, since less cells detached or lost thigh junctions due to viral replication. Cell index is lower for both viruses when no treatment is performed, thereby RVs replicated more. After 20 h, no detectable changes were observed.

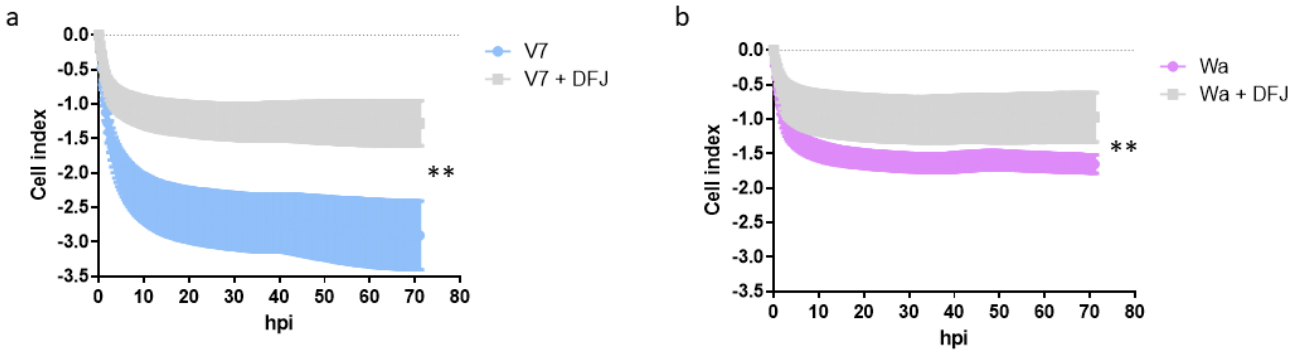

Figure 27. *Cell index obtained by impedance after infection of dCaco-2 with RV7 and Wa treated with the fucosidase inhibitor.*

Figures show cell index data every 20 min of the infection of dCaco-2 for 72 hpi with a) RV7 and b) Wa treated with the fucosidase inhibitor DFJ at 800 nM. DFJ, 1-deoxyfuconojyrimicin; dCaco-2, differentiated Caco-2; hpi, hours post infection. p values ≤ 0.01 are represented as **.

The same results were obtained in dCaco-2 cells by qPCR and impedance when viral stocks were treated with a fucosidase inhibitor prior to infection, where viral replication decreases when fucosidases are inactive, which highlights the relevance of such enzymes during RV replication. These findings are consistent with the previous experiments, where the cellular treatment with fucosidases results in an enhanced replication. The inhibition of fucosidases does not completely hinder RV replication, suggesting the involvement of other factors that play a relevant role in RV replication.

4.10. Role of fucosylated HBGAs in the infection of human intestinal enteroids with clinical noroviruses

Later, HIEs from the InEpC line were infected with clinical NoVs. HIEs were split once a week and used to obtain differentiated 3D HIE domes or 2D HIE monolayers (Fig. 28). 3D HIEs grow from day 0 to day 7 after passage, presenting a cystic morphology, which consists of a lumen surrounded by epithelial cells (Fig. 28a, b, c, d). Once they were differentiated, borders became brighter and thicker (Fig. 28e, f, g). When 3D HIEs were seeded in 96 well-plates to form a 2D monolayer, confluency was achieved 2-5 days later (Fig. 28h).

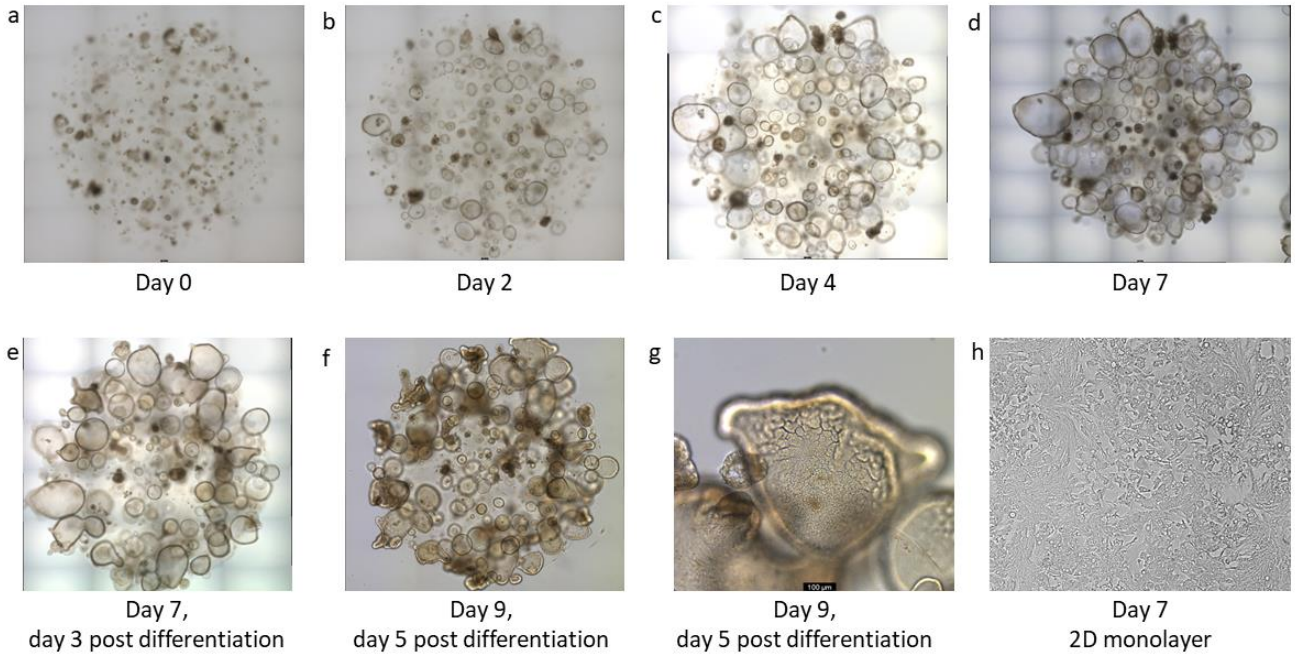

Figure 28. *Progression of 3D InEpC HIEs growth embedded in Matrigel from day 0 to day 9 after passage, and 2D monolayer of FI124 HIEs.*

Images show the growth of a 3D HIEs dome on a) day 0, b) day 2, c) day 4 and d) day 7 after passage. On day 4, some wells were differentiated, and it can be observed the growth of a 3D HIEs differentiated dome on a) day 7 after passage, day 3 post differentiation, f), g) day 9 after passage, day 5 post differentiation. Figure h) shows a confluent 2D monolayer of FI124 day 7 after seeding.

4.10.1. Infection optimization

A total of five NoV^+ stool filtrates were prepared and tested in 3D HIEs, named NoV43, NoV44, NoV45, NoV46 and NoV47, all of which belonged to GII.4 2012 Sydney genotype. The infection was performed in domes, colleting timepoints at 2 hpi and 48 hpi. Two of the five NoV samples replicated in 3D HIEs under the tested conditions, specifically NoV43 and NoV44 (Fig. 29). NoV43 exhibited a fold increase that almost arrived to 2,000 while NoV44 fold increase was less than 100. Due to reproducibility problems and lower fold increase, NoV43 was chosen for further experiments.

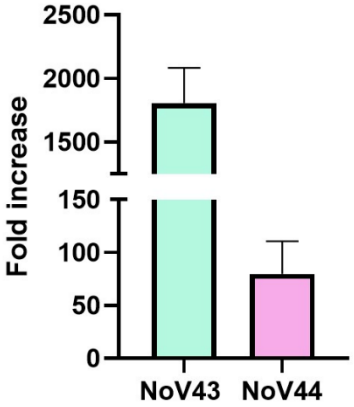

Figure 29. *Fold increase of NoV43 and NoV44 after infection of 3D HIEs.*
NoV43 and NoV44 infected 3D HIEs at 2 dpi in drop format with MOI of 100.

4.10.2. Fucosidases treatment

3D HIEs InEpC were also treated with the fucosidases AfcA and AfcB, followed by the infection of NoV43 (Fig. 30). Results indicated that removal of α1-2 fucosidases by AfcA significantly increases viral attachment, while AfcB treatment caused a reduction (Fig. 30a). As for the viral yield, significantly less viral particles were produced when cells were treated with AfcB or with both enzymes (Fig. 30b). Regarding viral replication, fucosidase treatment caused a reduction, with a significant reduction obtained with AfcA or AfcA and AfcB treatment (Fig. 30c). Data indicates that, contrary to results obtained in RV experiments with dCaco-2 cells, removal of α1-2 and α1-3/4 fucoses from the surface of HIEs results in a decrease viral production and replication.

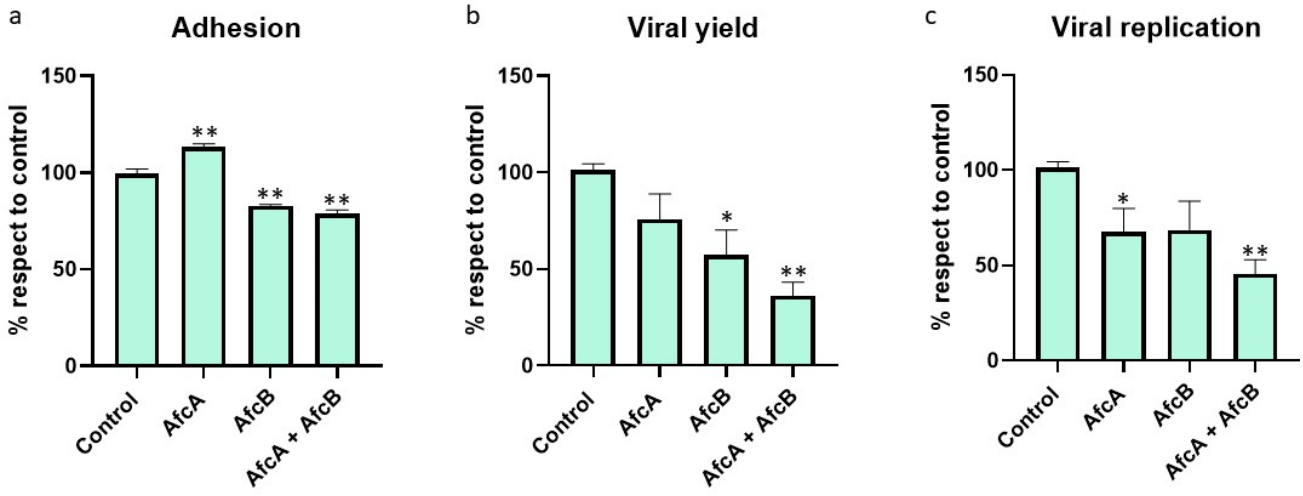

Figure 30. *Effect of the fucosidases AfcA and AfcB on infection of NoV43 in 3D HIEs.*
Graphs show the percentage respect to control of a) adhesion, b) viral yield and c) viral replication of NoV43 in 3D HIEs of the InEpC line pretreated with the fucosidases AfcA and AfcB alone or simultaneously. HIEs; human intestinal enteroids. p values ≤ 0.05 are represented as *, p values ≤0.01 are represented as **.

4.10.3. Fucosidase inhibitor treatment

Differentiated 3D HIEs were infected with the clinical NoV isolate previously treated with the fucosidase inhibitor. When NoV43 was treated with the DFJ at 2 µM concentration, viral replication in 3D HIEs decreases drastically (Fig. 31). 3D HIEs were also infected with NoV43 incubated with different concentrations of DFJ in order to calculate the EC50, which resulted to be 54.79 ± 95.19 nM.

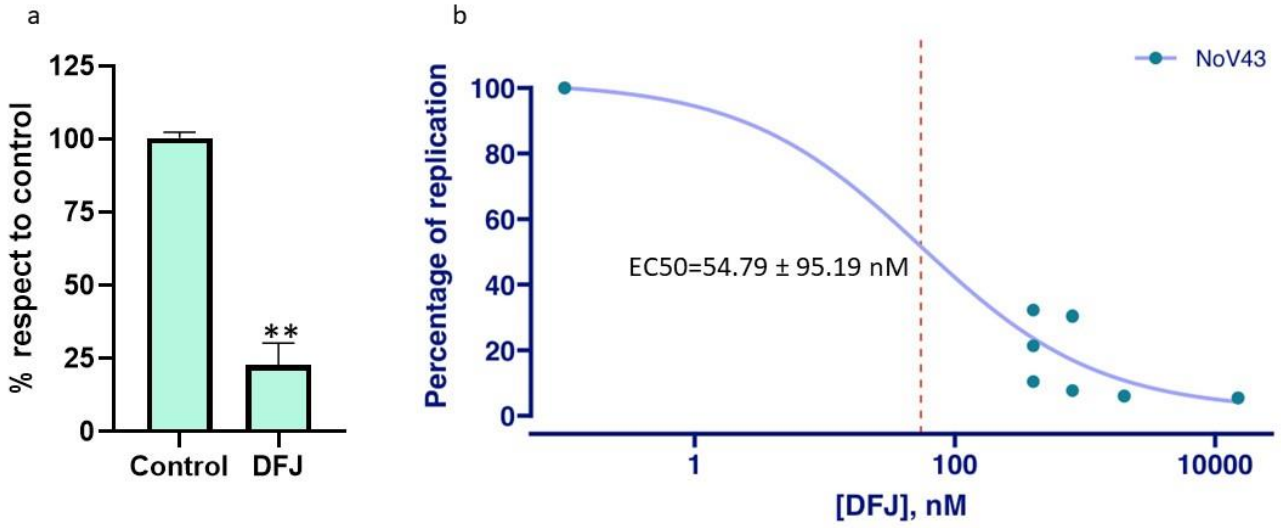

Figure 31. *Influence of the fucosidase inhibitor DFJ on NoV43 replication on 3D HIEs.*
Figure shows a) the replication of NoV43 treated with the fucosidase inhibitor DFJ at 2 µM in the 3D HIEs model of the cell line InEpC, and b) EC50 of NoV43. HIEs; human intestinal enteroids. p values ≤ 0.01 are represented as **.

4.11. Role of fucosylated HBGAs in the infection of mice with rotavirus and norovirus

Due to the observed influence of the treatments in dCaco-2 cells and HIEs, mice experiments were carried out. To infect mice, Wa was produced in cell culture, human NoV was obtained from a positive stool sample, and liposomes containing AfcA were generated. The capacity of AfcA to remove α1-2 fucoses was confirmed after the lyophilization process (Fig. 32a) and also after the production of liposomes (Fig. 32b). Lyophilized enzyme was resuspended in the appropriate amount of PBS. Both lyophilized enzyme and liposomes were incubated with LNFP I for 24 h. The incubation of the lipidic vesicles took place in the presence of triton, which facilitated the release of the enzyme by disrupting the lipidic membrane. The following day, samples were separated by SDS-PAGE, transferred to a membrane, and incubated with the anti-H antibody. In the case of the lyophilized enzyme (Fig. 32a), it was confirmed its activity by the absence of signal when incubating the membrane with the anti-H

antibody, as also occurs with AfcA without lyophilize. The figure 32b shows that the enzyme also retained its activity after the formation of the liposomes.

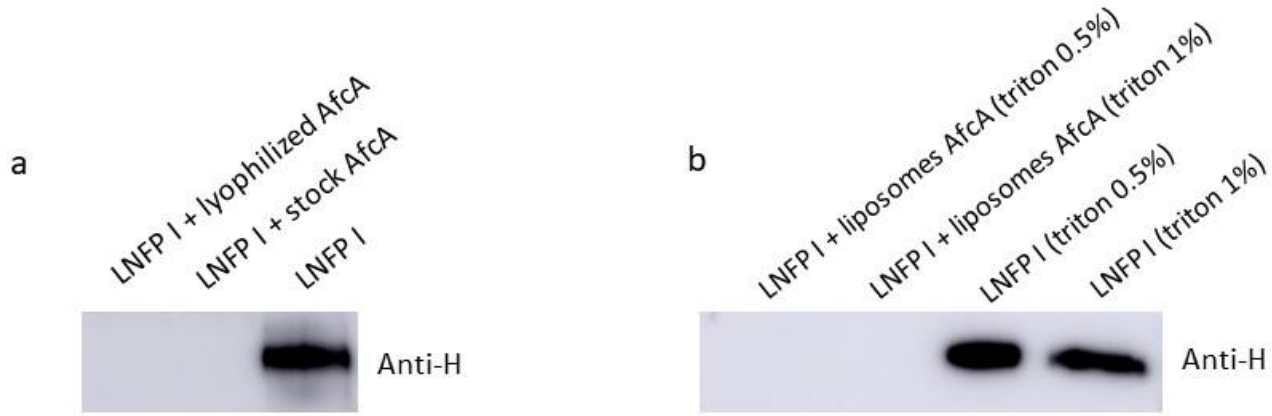

Figure 32. *Confirmation of fucosidase activity of lyophilized AfcA and liposomes containing AfcA.*
AfcA fucosidase activity to hydrolase α1-2 fucoses was evaluated after a) lyophilization and b) liposomes formation by Western blot. Following an incubation step with LNFP I, the resulting membrane was incubated with anti-H antibody to confirm the absence of signal. Anti-H antibody, H type-1 antigen primary antibody.

Once viral stocks and liposomes were prepared, mice experiments were conducted according to the schedule of section 3.11.2. First, control animals were analysed to determine the days on which viral particles were detectable in the faeces of the mice (Fig. 33). As for Wa strain, both 1 and 2 dpi exhibited the same copies of RV copies, $1 \cdot 10^6 \pm 3.6 \cdot 10^5$ copies/g. The viral copies gradually decreased from day 2 until day 4, finding none on day 5. Regarding NoV, viral particles increased from day 1 ($9.49 \cdot 10^4 \pm 1.47 \cdot 10^4$ copies/g) to day 2 ($1.71 \cdot 10^5 \pm 7.17 \cdot 10^4$ copies/g), when the maximum amount was obtained. It decreased up to day 5, when no viral RNA was found.

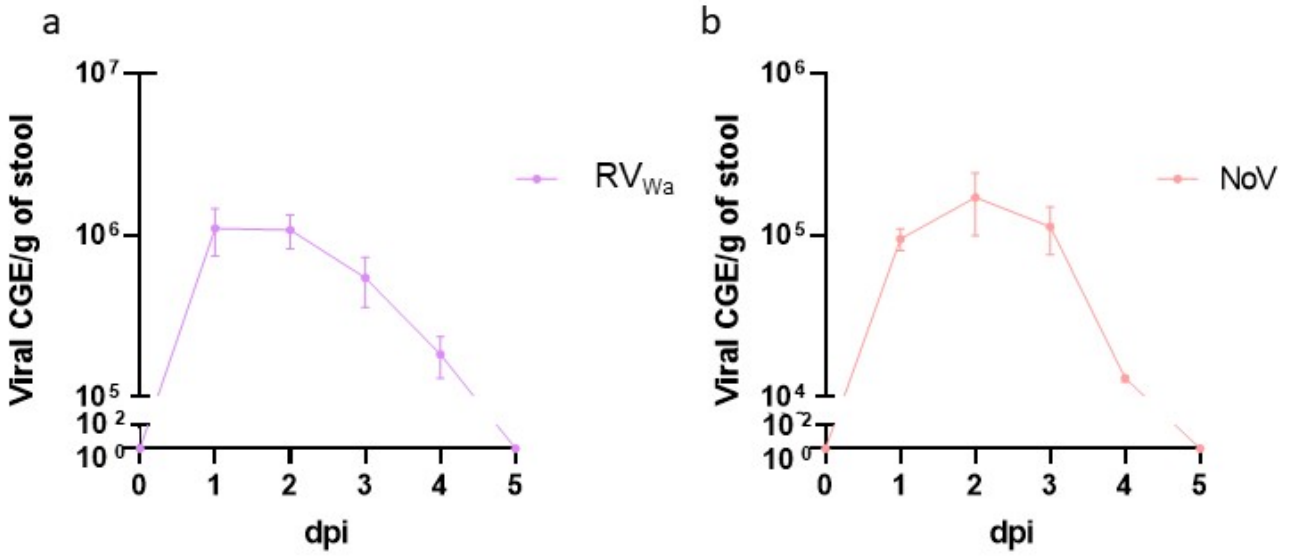

Figure 33. *Viral shedding of mice infected with Wa strain and GII.4 2012 NoV in mice.*
Mice were infected with a) RV Wa and b) GII.4 2012 NoV for 10 days, collecting faeces every day to analyse viral shedding. Dpi, days post infection.

4.11.1. Fucosidase treatment

AfcA treatment was administered to mice before the infection, thus following the same procedure as for dCaco-2. The results of RV-infected mice (Fig. 34a) showed higher viral shedding in the fucosidase treated mice, with significant differences detected at 1, 2, 5 and 6 dpi. Viral shedding was also higher at 3 and 4 dpi, although no statistical differences were detected. Interestingly, AfcA treatment resulted in a longer infection. Figure 32 shows that Wa was detected from 1 dpi to 4 dpi. However, in mice treated with AfcA, virus was also detected at 5 and 6 dpi. Similar results were obtained for NoV infection (Fig. 34b). Mice treated with AfcA prior to infection had significantly higher viral copies at 1 and 4 dpi, and higher but not significant at 2 and 3 dpi. In this case, the infection did not last longer than in control mice.

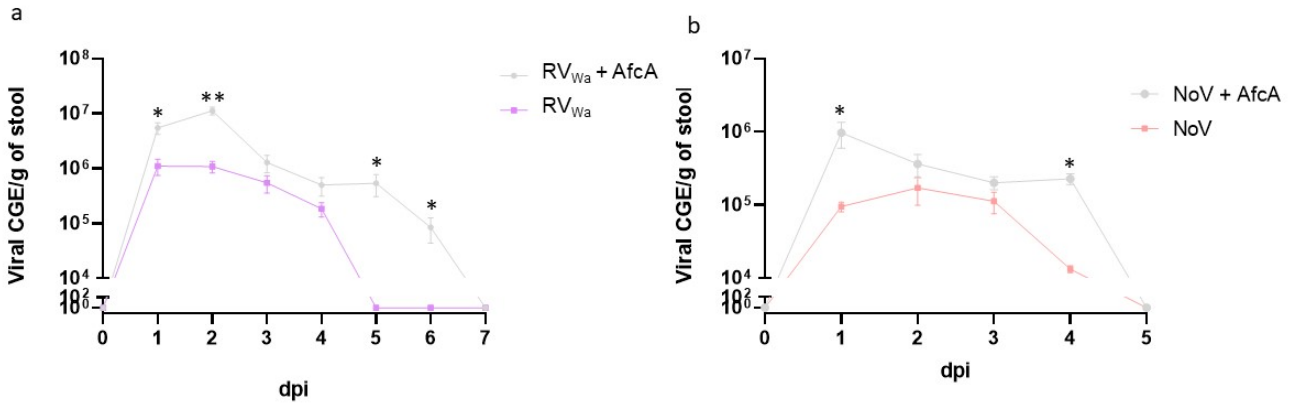

Figure 34. *Viral shedding of mice infected with Wa strain and GII.4 2012 NoV previously treated with AfcA.*
Mice were treated for 2 days with the fucosidase AfcA and later infected with a) Wa and b) GII.4 2012 NoV (grey lines). Control results are also shown (coloured lines). Dpi, days post infection. p values ≤ 0.05 are represented as *, p values ≤0.01 are represented as **.

4.11.2. Fucosidase inhibitor treatment

To further confirm the role of fucosidases in RV and NoV infectivity, the fucosidase inhibitor DJF was also studied in mice. When mice were infected with RV or NoV together with the inhibitor, there were no significative differences during the 3 first days after infection, even if a reduction in viral shedding could be seen, especially in NoV (Fig. 35). More interestingly, the viral shedding was significative lower at day 4 in the mice infected with RV (Fig. 35a). Similarly, the mice infected with NoV shed viruses only for three days instead of four, showing a shorter shedding period (Fig. 35b).

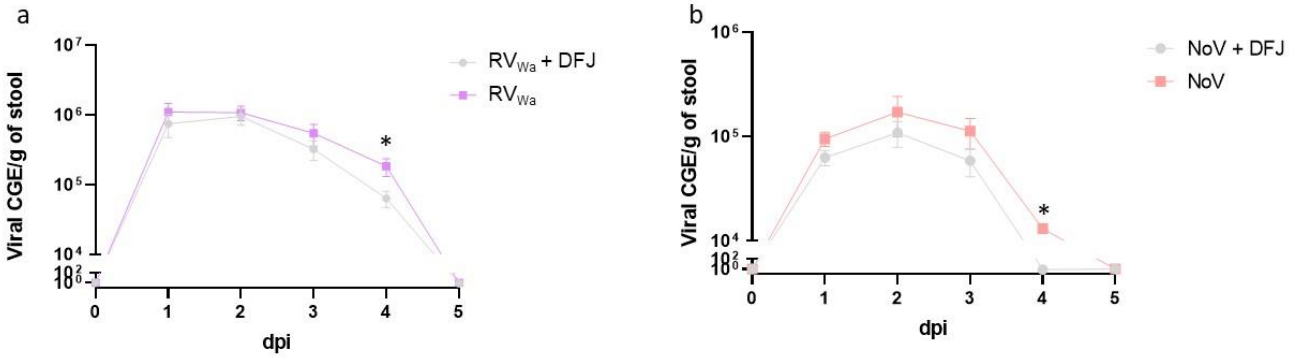

Figure 35. *Viral shedding of RV Wa and NoV GII.4 2012 treated with the fucosidase inhibitor.*
Mice were infected with a) RV Wa and b) NoV GII.4 2012 treated with the fucosidase inhibitor (grey lines). Control results are also shown (coloured lines). Dpi, days post infection. p values ≤ 0.05 are represented as *, p values ≤0.01 are represented as **.

The antiviral effect of the fucosidase inhibitor in mice was also consistent with the results obtained in dCaco-2 for RVs and in HIEs for NoVs, where the incubation of the compound with the viral stocks reduced replication.

5. DISCUSSION

5. Discussion

RV and NoV are the main responsible for viral gastrointestinal infections worldwide, commonly characterized to cause diarrhoea, vomiting, malaise, fever, and dehydration, leading to the death of the patients in the most extreme cases and they are transmitted through the faecal-oral route. The introduction of RVVs has reduced RV incidence considerably. However, it's been estimated that RV caused more than 258 million episodes of diarrhoea and 128,500 (104,500-155,600) deaths among children under 5 in 2016, with 104,733 (83,406-128,842) deaths occurring in sub-Saharan Africa [17]. After RVV introduction, NoV is recognized as the leading cause of AGE in all age groups. In 2016, it caused a total of 218,800 (170,900-277,200) deaths, with 212,500 (164,800-270,800) occurring in low and middle-income countries [207]. These data might even underestimate the true values since in low-income countries accurate techniques used to detect RV and NoV are frequently not available, and also most of the diarrhoeal cases remain aetiologically unknown. The same occurs for the mild cases that don't require hospitalization or emergency room visits in developed countries.

Both RV and NoV bind to HBGAs located on the surface of host cells to initiate the infection process [35,47,72]. Nevertheless, owing to the variations that *FUT2* and *FUT3* genes present, individuals can be secretor or non-secretor, as well as Lewis-positive or negative individuals. Since RVs and NoVs interact with HBGA in a genotype-specific manner, individuals' susceptibility to these infections varies based on their specific HBGA profiles [49–51]. Secretor status is reported to be a cause of P[8] and P[4] RVs and GII.4 NoVs susceptibility [74,75,188,189,208].

RVVs have less efficacy in low-income settings (Table 1), which may be explained by the HBGAs distribution, RV genotypes, and microbiota composition, among others. The complete understanding of such facts would help improve vaccines and thereby, reduce RV-related deaths.

As for NoV, five of the ten described genogroups can infect humans (GI, GII, GIV, GVIII and GIX) [20]. Among them, the GII.4 variants have caused all six major NoV pandemics of AGE in the last two decades, being the last pandemic variant, GII.4 Sydney 2012, the one that has dominated ever since [21,22]. Due to the absence of a cell line model able to replicate NoV until recently [169], its study has been hindered, and so, the development of a vaccine. The vaccines most advanced in clinical trials are based on VLPs [24,26], which have shown to be safe in adults and infants, but also P-particles [209,210] and adenovirus vector-based vaccines [211] are under development. The

implementation of a NoV vaccine would drastically reduce its related deaths, with the greatest impact on low-income countries.

On the other hand, there are no antivirals commercially available to treat RV or NoV infections. However, nitazoxanide, which has FDA approval for treating *Giardia* and *Cryptosporidium* [150], has promising results in the treatment of RV and NoV [151–153,156]. Nevertheless, other studies have not reported any improvement in NoV infections [158–160].

It is also important to highlight that, in terms of RV and NoV research, cellular lines or strains that differ from target cells or wild-type viruses are used (Table 2). While these investigations have undoubtedly enhanced the comprehension of RV and NoV binding and replication mechanisms, and even contributed to vaccine development, among others, extrapolating those data to human RVs and NoVs should be made with caution since such findings may differ from what takes place in natural human infections. That is why the present work employs cellular and animal models with host cells similar to the human gut, as well as wild type human RVs and NoVs.

Since RV and NoV continue to cause hundreds of thousands of deaths worldwide, it is imperative to keep working on antivirals and vaccine development. To do so, it is important to investigate their infection mechanisms. In the present work, we focused on the role of GHs enzymes produced by microbiota members in RV and NoV attachment and replication. In particular, the role of fucosidases, given that fucoses are the outermost monosaccharide present on HBGAs (Fig. 5), for what clinical RV and NoV isolates were prepared and used in the infection of different cellular and animal models. Not only clinical isolates were used in the study of RV replication, but also the cell culture-adapted strain Wa, which belongs to the G1P[8] genotype.

With that aim, it was performed a metagenome study of infant faeces to find non-characterized α-L-fucosidases produced by intestinal microbiota. Putative GHs such as β-galactosidases, β-N-acetylhexosaminidases, α-sialidases, and α-L-fucosidases were identified. Out of the total 36 α-L-fucosidases found in the metagenomic analysis, 10 were selected for characterization, being Fuc18, Fuc19A, Fuc30, Fuc35A, Fuc35B, Fuc39, Fuc193, Fuc1584, Fuc2358, and Fuc5372. Thus, it can be observed how the GH activity in general and the fucosidase activity in specific, is commonly found on microbiota. That activity that is used by the bacteria to feed themselves will also modify the local glycosylation profile affecting to the HBGAs that serve as NoV and RV attachment factors and consequently affect viral infections.

Along with these 10 fucosidases, AfcA and AfcB were also used. These two enzymes are produced by *B. bifidum* JCM 1254 and were previously characterized by Dr Katayama [85,91]. *B. bifidum* is a commensal bacterium frequently detected in the stool of breast-fed infants [212,213], attributed to the presence of human milk oligosaccharides [214,215]. *B. bifidum* is also present in the adult life, since it can metabolize mucins, where AfcA and AfcB participate. AfcA and AfcB were not found in the metagenomic study, which could be attributed to the use of only 4 samples.

Enzyme characterization was performed by Dionex (Table 8) and Western blot (Fig. 11). Glycoproteins conjugated to HSA were employed in the Western blot method, where the absence of signal determine the hydrolytic activity of the fucosidases. By Dionex, free oligosaccharides were used, and hydrolytic activity was assessed by analysing the reaction products, where the presence of fucose would confirm the enzymatic reaction. Both methods are widely used in enzyme characterization thanks to their sensitivity. However, they yielded similar but not identical results. By Western blot analysis, only two enzymes from the metagenomic study showed partial α1-3/4 fucosidase activity, Fuc18 and Fuc39, and none α1-2. On the other hand, six of the ten selected fucosidases showed complete or partial α1-3/4, and three α1-2 fucosidase activity by Dionex. Such difference in results was attributed to the better accessibility of fucoses on the free oligosaccharides, which might not be accessible in the neoglycoproteins due to the steric impairment. We only focused on enzymes with complete activity, being AfcA and AfcB by Western blot, and Fuc18 and Fuc39 by Dionex. Since complete fucosidase α1-2 activity was only detected on AfcA, this enzyme was selected for further experiments. AfcB was able to hydrolyse substrates with less accessible fucoses (i.e., neoglycoproteins, conjugated to HSA), while the fucosidases from the metagenomic analysis only the most accessible ones (i.e., free oligosaccharides). To ensure proper fucosidase α1-3/4 activity on the surface of host cells in cellular and animal models, much more complex than free oligosaccharides, AfcB was selected for further experiments.

After successfully producing and characterizing AfcA and AfcB, a screening to find human RVs able to replicate without previous cell culture adaptation steps took place. The selected faeces were positive to P[8] (33) and to P[4] (8) genotypes, since secretor positive status is associated with susceptibility to P[8] and P[4] genotypes [64,188,189,208,216] and thus infection of wild type RVs from those genotypes depend on HBGA composition. Both Caco-2 and HT29 are suitable cellular models to study RV replication *in vitro*. However, it was decided to work with dCaco-2 cells due to previous laboratory experience, they spontaneously differentiate after confluency and grow faster

under tested conditions. Viral replication was analysed as fold increase, in which the total amount of virus present at the studied time point is compared to the total amount of virus that attached to cells 1 hpi, normalizing the results based on the number of cells in each well using the HPRT 1 gene. Out of the total 41 clinical isolates evaluated on dCaco-2, only 4 replicated (RV7, RV18, RV39 and RV41), being all four P[8] RVs (Fig. 14). The low rate of positive samples observed might be due to the presence of contaminants in the faeces that inhibit viral replication, as co-infection with other viruses or bacteria. Although the presence of bacteria in the viral stocks was prevented due to the filtration steps, the storage of faeces from collection to preparation of the filtrate stocks may have affected the viability of RVs as well, since some of the faecal samples were stored for a long period of time. Finally, RV7 and RV39 were used in subsequent experiments due to their robustness in replication after several independent experiments.

The VP4 and VP7 sequences of RV7 and RV39 revealed identical sequences for VP4 and had only two nucleotide variations for VP7, which shows the high conservation of VP4 and VP7 proteins in the circulating P[8] RVs. Nevertheless, VP4 and VP7 proteins from Wa exhibit differences from those found in clinical isolates, where multiple mismatches were detected along the sequences. These differences between circulating RVs and Wa could be attributable to the adaptation of Wa to replicate in MA104. MA104 cells have a kidney origin that differs from those found in the intestinal tract, which are the natural RVs target. Differences in sequences and thus in VP4 and VP7 proteins may have an impact on attachment and replication during infection experiments.

After studying the appropriate infection conditions, we compared the replication differences of the clinical isolates RV7 and RV39 and the cell culture-adapted strain Wa on various cell lines. These included uCaco-2, dCaco-2, HT29, HT29 M6, MA104, 2D HIEs from the J2 line and 3D HIEs from the InEpC line, which differ on the presence of HBGAs on their surface among others. We speculated that, as the Wa has been adapted in MA104, cell line lacking HBGAs on its surface, it might present different ability to bind to HBGAs than circulating RVs, and thus it might behave differently than clinical isolates. Indeed, it has been previously demonstrated that the VP8* from the Wa strain has a weaker recognition of the H-type-1 and the precursor type-1 antigens than the VP8* of a clinical isolate with almost identical sequence to the ones utilized here [53]. Once Caco-2 cells spontaneously differentiate after achieving confluency, they express HBGAs on their surface, used by clinical RVs as receptors to initiate viral infections. Previous studies indicate that Le^b, Le^x, Le^y, H-type 1 and H-type 2 antigens are more abundant in the cellular glycocalyx in dCaco-2 when compared to uCaco-2

[162,163,217]. However, not all those investigations reported the presence of the same antigens, which could be due to the different techniques and antibodies employed. It is worth noting that Caco-2 cells were isolated from a blood type O secretor and Lewis positive individual [162,218], indicating the expression of secretor and Lewis antigens in these cells, with the exception of A and B blood antigens. On the other hand, HT29 cells were isolated from a blood type A secretor and Lewis positive donor [218,219], thus expressing secretor, Lewis and type A HBGAs. Although HT29 and HT29 M6 cells also differentiate after achieving confluency when media composition is changed, and thus presenting characteristics more similar to human intestine, they already express HBGAs constitutively in an undifferentiated state [219], reason why differentiated HT29 were not used. The main difference between HT29 and HT29M6 is the secretion of mucus by the last one, representing an environment more analogous to the human intestine. As for MA104, although these cells do no express HBGAs, they are permissive to RV replication. HIEs used for 2D infections belong to the J2 line, which were isolated from a secretor and Lewis positive individual [220,221]. Finally, the specific HBGAs expressed by InEpC HIEs which were used for 3D infections remain unknown. However, we detected the expression of type-2 H antigen by incubating untreated HIEs with the UEA-I lectin (Fig. 12), thus confirming the presence of HBGAs.

The results of the *in vitro* infection experiment indicate that clinical strains replicated better in those cell lines with HBGAs on their surface when compared to uCaco-2 and MA104, while the opposite occurred for Wa (Fig. 19). RV7 and RV39 replicated more efficiently on dCaco-2 (fold increase > 25) and HIEs (fold increase > 1,500) than in uCaco-2 and MA104 (fold increase <5). The same occurred for RV7 on HT29 and HT29 M6 (fold increase >13). On the other hand, Wa showed the highest replication on MA104, cell line where it had been adapted, achieving a fold increase of 1,115.26 ± 360.29. These findings indicate that clinical isolates, that is, human circulating RVs, infect more efficiently cell lines with HBGAs on their surface, more alike to the intestinal environment. In contrast, Wa, the cell culture-adapted RV widely used in experiments, replicates better in MA104 and poorly in the other cell lines tested, not even attaching to HT29, HT29 M6 and 3D HIEs. Here we state the significance of HBGAs in the infection of clinical RV isolates, while they are not as relevant for Wa, due to its adaptation to the MA104 cell line, which lacks these carbohydrates. As result, conclusions obtained using cell culture-adapted strains should be considered with caution. For RVs, the use of non-cell culture adapted viruses in experiments is not common, since the majority of RV

studies performed include cell culture-adapted strains or adapted wild type RVs, as sum up in table 2.

Once it was characterized the replication of RVs with clinical origin in cellular models that express HBGAs, the role of fucosidases was determined in dCaco-2 cells. The monolayers were treated with fucosidases prior to infection. AfcA removes α1-2 fucoses attached to galactose and AfcB α1-3/4 fucoses attached to N-acetyl-glucosamine, and also are not toxic to cells (Fig. 28). It was also stablished that AfcA is able to remove α1-2 fucoses from the surface of 2D HIEs (Fig. 13) as evidenced by the absence of signal when incubated with the UEA-I lectin. This suggests its proper activity on dCaco-2, and also that of AfcB. The 2 h treatment completely remove the fucose signal on HIEs, although it was not studied whether fucoses regenerate over time. However, we hypothesised that this might be the case due to the expression of α-fucosyltransferase by dCaco-2 cells to produce HBGAs [222].

Contrary to the expected, the treatment with fucosidases for 2 h on dCaco-2 before RV infection resulted in an increased replication, obtaining comparable results with both non-cell culture adapted viruses (RV7 and RV39). The highest viral yield was obtained when cells were treated with both enzymes simultaneously, while treatment with either AfcA or AfcB yielded similar data (Fig. 20b, e). These results indicate that the removal of α1-2 fucoses by AfcA results in an increased replication (Fig. 20c, f), while the activity of AfcB provokes an increased viral attachment to cells, since the viral replication is the same than when no treatment is performed (Fig. 20c, f) but the final viral yield is higher (Fig. 20b, e). It was also noted for RV7 in the analysis of adhesion (Fig. 20a, d), but not statistically significant data is obtained. Interestingly, when the cell culture-adapted Wa strain was employed, an increase in viral yield was found when the AfcB was utilized. Previous results from the laboratory showed that the Lewis fucose (fucose-α-1-4-N-acetyl-glucosamine) impairs the binding of the H-type 1 antigen and its precursors to the binding pocket of the VP8* [53]. Since the binding of the VP8* of the Wa strain is weaker, this removal seems to benefit viral attachment and higher viral titter after 72 hpi. Furthermore, it is well established for influenza viruses that the hemagglutinin and neuraminidase activities must be in balance to ensure a maximum replication [223]. Since contrary to influenza viruses, RVs do not carry their own fucosidase, they might be taking profit of the fucosidase activity provided by the microbiota members. Taking this into account, our results seem to indicate that for RV Wa that has a weaker lectin activity (that is, the capacity of viral particles to bind carbohydrates) the AfcA will exceed the optimum fucosidase activity required for an optimal

replication, while in the case of higher affinity lectins (V7 and V39) the addition of the α1-2 fucosidase activity balances the attachment/detachment process promoting viral replication *in vitro*.

In the present thesis, infections were also performed to elucidate if the bacterial fucosidases AfcA and AfcB influenced NoV replication in 3D HIEs. One human viral sample belonging to the GII.4 Sydney 2012 was able to infect 3D HIEs satisfactorily. Our results showed significant decreases on attachment, viral yield and replication of the clinical isolate after fucosidase treatment of HIEs (Fig. 30). This might indicate that the treatment with these enzymes is detrimental for the attaching/detaching balance for human NoVs *in vitro*. HIEs have been extensively used in the study of human NoV replication [169,224,225] as well as antivirals experiments [226,227]. The original method was designed to use HIE on 2D monolayers, which is labour intensive and time consuming. However, a promising protocol in which NoV infections are performed on 3D HIEs showed equally efficient results and was the one selected to perform the experiments with the fucosidase inhibitor in the present thesis. The use of 3D HIEs allows for reduced experimental times, reproducibility, and simpler procedures [225]. The differences detected on RV replication between 2D and 3D infections (Fig. 21f, g) could be attributable to the different line employed, being J2 for 2D infections and InEpC for 3D infections.

The role of fucosidases was also studied *in vivo* in a mice model previously described by our research group [170,171]. The AfcA enzyme was selected because its activity had demonstrated to produce an increase in viral replication *in vitro* in the two RV filtrates. Furthermore, mice possess and express the FUT2 in the gut [228]. Although it has been stated and demonstrated along the thesis that cell culture-adapted strains like Wa do not behave the same than clinical isolates, as RV7 and RV39, Wa still keeps lectin activity [53]. This is a viral strain that is available in many laboratories and this fact will facilitate the reproducibility of the experiments for other research groups. Also, no information is available about mice infection with non-cell culture-adapted RVs, so initial experiments were decided to employ Wa. For NoVs, since there are not yet cultured strains, a new viral filtrate was prepared from a clinical sample belonging to the GII.4 Sydney 2012 genotype. Fortunately, an increase in RV shedding was observed in mice treated with AfcA, with statistically significant differences at 1 and 2 dpi compared to control mice (Fig. 34a). Furthermore, the duration of the viral shedding was extended by two days, since viral RNA was detected at 5 and 6 dpi compared to the control group that only shed viruses for 4 days. More interestingly, the experiment performed with NoV also showed significative increased viral shedding at 1 and 4 dpi (Fig. 34b). It is important

to notice that the mice infection model has its microbiota depleted with antibiotics and most of the fucosidase activity will be the one provided in the experiment. The differences found *in vitro* and *in vivo* with the RV Wa strain and the NoV stool filtrate might be explained as well by the lectin/fucosidase balance. The gut of the mice has a thicker mucin layer than the culture models, in this scenario it is reasonable to think that the increased fucosidase activity will facilitate the crossing of the viruses through the mucus layer and the glycocalyx. Indeed, it has been previously reported for a bovine coronavirus that crossed the species barrier and infected humans that the only mutation needed for its adaptation to humans was the loss of esterase activity that is thought to be needed to cross the thicker mucus layer of the bovine respiratory airways [229]. This might also explain the reduced replication of RV7 and RV39 filtrates on HT29M6, which possess a mucus layer, as compared to HT29 (Fig. 21). That layer would be more difficult to cross without the addition of fucosidases.

To our knowledge this is the first time that the role of fucosidases have been assayed for RV infections, but previous research has looked into the role of sialidases. It was early established that most non-human RVs were dependent on the presence of sialic acid after the treatment of monolayers with sialidase previous to infection [230], more recently, studies utilizing porcine intestinal enteroids have shown that the sialidase treatment might both decrease RV replication as well as increase it [231,232]. This results also point to the lectin/glycosidase balance theory to explain different outcomes after the treatment of cells with glycosidases prior to RV infection.

Previous researchers had studied the role of fucosidases and fucosidase expressing bacteria utilizing NoV VLPs in different experimental setups. Eshaghi *et al* discovered that treating oyster digestive tissue extract with *B. bifidum* JCM 1254 attracted more GII.4 NoV VLPs compared to controls [119]. Oysters retain NoVs due to the presence of structures similar to human HBGAs on their digestive ducts [233,234], whereas *B. bifidum* JCM 1254 is the bacterial strain that produces the fucosidases AfcA and AfcB [85,91]. Like the *in vivo* study with mice, the addition of fucosidases in this case favours the lectin/glycosidase balance, thus increasing viral attachment. It was also studied the impact of a commercial α1-2 fucosidase treatment on lettuce regarding the attachment of GI.1 and GII.4 NoV VLPs, which binds NoV thanks to the presence of H-like HBGA on the leaves. The results showed binding inhibition of VLPs after fucosidase treatment [235,236]. In this case, the fucosidases seem to cause a disequilibrium that results in a decreased attachment. Other researchers found that treatment of paraffin-embedded human duodenal tissue sections with an α1-2 fucosidase (fucosidase II from *Xanthomonas manihotis*) for 6 h resulted in an increased NoV VLPs attachment,

which favours the lectin/glycosidase balance. However, treatment for 18 h with renewal of enzyme every 6 h resulted in the binding loss [237], and thus, the loss of equilibrium. The mentioned studies did not investigate whether fucosidase treatment led to a complete or partial removal of fucoses present and since VLPs were utilized, viral replication could not be studied.

Since the addition of fucosidases led to an increased replication for both RV and NoV, the effect of a fucosidase inhibitor was also evaluated. The initial hypothesis was that the viral filtrates would carry certain amount of bacterial fucosidases, for instance AfcA and AfcB are extracellular enzymes that would co-purificate with the viruses after filtration and many other extracellular fucosidases have been found in the microbiome of stools [187]. To test this, the viral filtrates were incubated with a fucosidase inhibitor (DFJ) for 1 h previously to infection. The DFJ is an iminosugar, a sugar analogue in which the endocyclic oxygen is replaced by a nitrogen atom [238]. Due to the structure similarity to sugar molecules, the tested compound binds to the active site of fucosidases, inhibiting fucose removal of carbohydrates. Armstrong and colleagues revealed the cryo-EM structure of the inhibitor bound to the active site of the human fucosidase FucA1 [239]. The fucosidase inhibitor has been proven to be active against a wide range of α-L-fucosidases *in vitro* [240–243]. Prior to perform the experiments with the viruses, the inhibitor properties of DFJ were confirmed on four different bacterial fucosidases from different bacterial species (Fig. 24). The compound did not show activity against a different glycosidase, the lacto-N-biosidase LnbB (Fig. 24e), enzyme at the tested concentrations, showing its specificity for fucosidases.

The *in vitro* experiments showed that infection of dCaco-2 cells with fucosidase inhibitor-treated RVs resulted in a decrease in viral replication as observed by both qPCR and impedance measurements. By qPCR, it was observed that the maximum inhibition was obtained at DFJ 800 nM, with different levels of inhibition depending on the virus utilized (Fig. 25). Interestingly, the Wa strain was also inhibited despite its cell culture origin, this implies that the cellular fucosidase FucA1, present in the endosomes of the host cells [244,245], may also play a role in RV infections *in vitro*. In impedance experiments, the cell index is measured in real-time and indicates monolayer integrity. The higher the cell index, the better the monolayer integrity. When RVs infect cells, monolayer integrity is compromised, with the lowest cell index measured when cells were infected with untreated RV7 or Wa (Fig. 27). On the other hand, treatment of the virus with the fucosidase inhibitor leads to a decrease in the cell index but not as much as the untreated virus, which implies less cellular damage and, indirectly, less viral replication. Results from the time course experiment (Fig. 17)

showed that the highest replication was achieved at 72 - 96 hpi. However, it was observed that the cell index decreased up to 20 hpi, point from which it remained steady. These data suggest that monolayer integrity damage occurs during the first 24 hpi, and even though RVs continue to replicate, no additional monolayer damage occurs. Although RV did not cause cell detachment as observed under the microscope during infections, it might have caused the loss of tight junctions, which is detected by the equipment. The measure of the electrical resistance to study how viruses affect monolayer integrity has been previously used. It is also well established that RV infection causes a decrease in the transepithelial electrical resistance in polarized cells [246,247]. Other investigation detected that SA11 infection of dCaco-2, another cell culture-adapted RV strain, caused occludin reduction, the major component of tight junctions. They also observed that electrical resistance reduction was significantly prevented by *L. rhamnosus* GG [248], a bacterium that reduces viral faecal shedding and diarrhea duration [249,250].

The effect of the fucosidase inhibitor on NoVs filtrates replication was studied on HIEs. The viral filtrate employed replicated efficiently in 3D HIEs and the replication decreased significantly when 2 µM of the fucosidase inhibitor was used. (Fig. 29, Fig. 30).

Finally, the effect of the fucosidase inhibitor was tested on mice, which were infected with Wa or GII.4 Sydney 2012 stool filtrate NoV along with 20 mM of DFJ. When compared to control groups, the same pattern was found for both viruses. There was a slight reduction in viral shedding that was not significative during the three first days of infection. More interestingly, the mice showed a significative reduction in viral shedding at 4 dpi in both viruses (Fig. 35). For RV there was a 2.87-fold decrease in viral shedding at 4 dpi while in human NoV, the mice only shed viruses for 3 days in the treated group. To our knowledge, this is the first time that this iminosugar has been used *in vivo* so the bioavailability of the compound is unknown, which might be interfering with the results. Iminosugars have been investigated as antivirals for influenza [251–253], human immunodeficiency [254,255], hepatitis C [256] and dengue viruses [257,258], among others, which paves the way to the investigation of fucosidase inhibitors as RV and NoV inhibitors. In the case of influenza, one of the commercially available treatments consist of a neuraminidase inhibitor, that is, a sialidase inhibitor. Oseltamivir, commercially known as Tamiflu, is the most used option, and it is administered twice a day for five days. Multiple research studies have demonstrated the efficacy of the inhibitor in reducing complications related to influenza and mortality, particularly when administered within 2 days of the appearance of clinical symptoms [259,260], with no severe secondary effects [261,262].

These data indicate that the administration of occasional GH inhibitor for viral treatment does not involve health risks. Owing to the thousands of hundreds of cases and deaths that RV and NoV cause yearly worldwide, mainly on low-income countries, the introduction of an antiviral that decreases even slightly those numbers would have a great impact on human health.

In the present work we focused on the effect of HBGA modifications on RV and NoV infection, that is, their receptors and/or co-receptors. Specifically, on the role of fucosidases. To this end, fucosidases with α1-2 and α1-3/4 activities were employed on dCaco-2, HIEs and mice prior to RV or NoV infection. It was detected an increased replication of RV clinical isolates, the cell culture-adapted RV strain Wa and NoV clinical isolates in the different models when there was present a lectin/fucosidase balance. Later, a fucosidase inhibitor was evaluated. Our results confirmed that the fucosidase activity is relevant for the biology of both viruses. The fact that most respiratory viruses with hemagglutinin activity carry their own glycosidases to balance the attachment/detachment process while both RV and NoV do not carry such glycosidase activity could be explained by a role of the gut microbiota fucosidases as well as to the human endosomal FucA1 fucosidase. The results presented here show for the first time a novel therapeutic target for two viruses that need fucose for their infection process.

6. CONCLUSIONS

6. Conclusions

1. Gut microbiota express a wide range of GHs, as determined by the metagenome study. Among others, it was detected the presence of β-galactosidases, β-N-acetylhexosaminidases, α-sialidases, and α-L-fucosidases that might be used by microbiota members to feed from host glycans present on the surface of gastrointestinal tract.
2. Western blot and Dionex are sensitive and suitable techniques to characterize enzymes. However, the complexity of the glycans use in Western blot makes this technique more appropriate for the detection of fucosidases with complete activity on complex substrates.
3. The α-L-fucosidases AfcA and AfcB demonstrated complete α1-2 and α1-3/4 fucosidase activity, respectively, on neoglycoproteins, which led to their selection for further experiments.
4. The RV screening on dCaco-2 revealed the low percentage of positive samples able to replicate, which can be attributed to co-infection with other viruses or bacteria, presence of viral replication inhibitors or long storage times.
5. VP4 and VP7 sequences are conserved among P[8] circulating RVs, but they differ from Wa probably due to the adaptation steps performed on MA104.
6. The appropriate infection time for RV on dCaco-2 is 72 hpi, and on HIEs is 48 hpi in the suspension format.
7. Clinical isolates RV7 and RV39 replicated more efficiently on those cellular types with HBGA expression, mainly on dCaco-2 and 3D HIEs. In contrast, the cell culture-adapted Wa showed a higher replication on MA104, which lacks HBGAs expression, thus reinforcing its preference for cell lines without HBGAs.
8. Infection of RV clinical isolates of dCaco-2 cells treated with the α1-3/4 fucosidase resulted in an increased viral attachment. Cellular treatment with the α1-2 fucosidase enhanced viral replication. Treatment with both fucosidases resulted in a synergic effect where the maximum viral yield was obtained.
9. Wa infection of dCaco-2 showed significant results after treatment with the α1-3/4 fucosidase AfcB, that provoked an increased attachment and thereby higher yield.
10. The role of fucosidases on the infection of the clinical NoV isolate on 3D HIEs showed a decrease in viral attachment (AfcB) and replication (AfcA and/or AfcB) after treatment with bacterial fucosidases.

11. The fucosidase inhibitor DFJ was active against the tested α-L-fucosidases, where more than a 94% of activity reduction was detected. Its specificity was confirmed after the incubation with a lacto-N-fucosidase, when only a 10% activity reduction was obtained.
12. The incubation of RVs with DFJ resulted in a decreased viral replication in dCaco-2 for both clinical and cell culture-adapted RVs, detected by qPCR and impedance experiments.
13. DFJ decreases NoV replication, as observed after infection of DFJ-treated NoV in 3D HIEs.
14. Lyophilization and liposome formation processes performed with AfcA did not affect its fucosidase activity, as detected after incubation with the substrate LNFP I, thus confirming its correct function for mice experiments.
15. The microbiota-depleted mice is a suitable model for the study of RV and NoV replication *in vivo*. Mice infected with RV and NoV shed viruses for 4 days.
16. Fucosidase treatment on mice that were posteriorly infected with RV showed higher viral shedding at 1 and 2 dpi as well as longer shedding period than control mice. In AfcA-treated mice RNA was detected until 6 dpi, while only 4 dpi in the control group.
17. Fucosidase treatment caused higher viral shedding on mice infected with NoV, with significant differences detected at 1 and 4 dpi.
18. The fucosidase inhibitor on mice infected with RV and NoV caused a significant decrease on viral shedding at 4 dpi for both viruses, not even detected for NoV.
19. The antiviral properties of DFJ demonstrated with RV and NoV in the different cellular and animal models makes it suitable for its investigation as an antiviral against viruses that infect through fucoses.

7. BIBLIOGRAPHY

7. Bibliography

1. World Health Organization The Top 10 Causes of Death Available online: https://www.who.int/news-room/fact-sheets/detail/the-top-10-causes-of-death (accessed on 9 June 2023).

2. Monedero, V.; Rodríguez-Díaz, J. Intestinal Microbiota and Susceptibility to Viral Infections. In *Probiotics, Prebiotics, and Synbiotics*; Elsevier, 2016; pp. 813–826.

3. Rodríguez-Díaz, J.; Monedero, V. Probiotics against Digestive Tract Viral Infections. In *Bioactive Food as Dietary Interventions for Liver and Gastrointestinal Disease*; Elsevier, 2013; pp. 271–284.

4. Matthijnssens, J.; Attoui, H.; Bányai, K.; Brussaard, C.P.D.; Danthi, P.; del Vas, M.; Dermody, T.S.; Duncan, R.; Fāng (方勤), Q.; Johne, R.; et al. ICTV Virus Taxonomy Profile: Sedoreoviridae 2022. *J. Gen. Virol.* **2022**, *103*, doi:10.1099/jgv.0.001782.

5. Buesa, J.; Rodriguez-Díaz, J. The Molecular Virology of Enteric Viruses. In *Viruses in Foods*; Springer International Publishing: Cham, 2016; pp. 59–130.

6. Salgado, E.N.; Garcia Rodriguez, B.; Narayanaswamy, N.; Krishnan, Y.; Harrison, S.C. Visualization of Calcium Ion Loss from Rotavirus during Cell Entry. *J. Virol.* **2018**, *92*, doi:10.1128/JVI.01327-18.

7. Aoki, S.T.; Settembre, E.C.; Trask, S.D.; Greenberg, H.B.; Harrison, S.C.; Dormitzer, P.R. Structure of Rotavirus Outer-Layer Protein VP7 Bound with a Neutralizing Fab. *Science (80-.).* **2009**, *324*, 1444–1447, doi:10.1126/science.1170481.

8. Dormitzer, P.R.; Greenberg, H.B.; Harrison, S.C. Purified Recombinant Rotavirus VP7 Forms Soluble, Calcium-Dependent Trimers. *Virology* **2000**, *277*, 420–428, doi:10.1006/viro.2000.0625.

9. Wolf, M.; Vo, P.T.; Greenberg, H.B. Rhesus Rotavirus Entry into a Polarized Epithelium Is Endocytosis Dependent and Involves Sequential VP4 Conformational Changes. *J. Virol.* **2011**, *85*, 2492–2503, doi:10.1128/JVI.02082-10.

10. Crawford, S.E.; Ramani, S.; Tate, J.E.; Parashar, U.D.; Svensson, L.; Hagbom, M.; Franco, M.A.; Greenberg, H.B.; O'Ryan, M.; Kang, G.; et al. Rotavirus Infection. *Nat. Rev. Dis. Prim.* **2017**, *3*, 17083, doi:10.1038/nrdp.2017.83.

11. Rotavirus classification working group Classification of Rotavirus Available online: https://rega.kuleuven.be/cev/viralmetagenomics/virus-classification/rcwg (accessed on 16 July 2023).

12. IVAC Current Vaccine Intro Status Available online: https://view-hub.org/vaccine/rota (accessed on 9 June 2023).

13. Cárcamo-Calvo, R.; Muñoz, C.; Buesa, J.; Rodríguez-Díaz, J.; Gozalbo-Rovira, R. The Rotavirus Vaccine Landscape, an Update. *Pathogens* **2021**, *10*, 520, doi:10.3390/pathogens10050520.

14. International Vaccine Access Center (IVAC), J.H.B.S. of P.H. VIEW-Hub Report: Global Vaccine Introduction and Implementation. *VIEW-hub by IVAC* **2020**, 1–36.

15. Tate, J.E.; Burton, A.H.; Boschi-Pinto, C.; Parashar, U.D.; Agocs, M.; Serhan, F.; De Oliveira, L.; Mwenda, J.M.; Mihigo, R.; Ranjan Wijesinghe, P.; et al. Global, Regional, and National Estimates of Rotavirus Mortality in Children <5 Years of Age, 2000-2013. *Clin. Infect. Dis.* **2016**, *62*, S96–S105, doi:10.1093/cid/civ1013.

16. Wang, H.; Naghavi, M.; Allen, C.; Barber, R.M.; Bhutta, Z.A.; Carter, A.; Casey, D.C.; Charlson, F.J.; Chen, A.Z.; Coates, M.M.; et al. Global, Regional, and National Life Expectancy, All-Cause Mortality, and Cause-Specific Mortality for 249 Causes of Death, 1980–2015: A Systematic Analysis for the Global Burden of Disease Study 2015. *Lancet* **2016**, *388*, 1459–1544, doi:10.1016/S0140-6736(16)31012-1.

17. Troeger, C.; Khalil, I.A.; Rao, P.C.; Cao, S.; Blacker, B.F.; Ahmed, T.; Armah, G.; Bines, J.E.; Brewer, T.G.; Colombara, D. V.; et al. Rotavirus Vaccination and the Global Burden of Rotavirus Diarrhea Among Children Younger Than 5 Years. *JAMA Pediatr.* **2018**, *172*, 958, doi:10.1001/jamapediatrics.2018.1960.

18. Graziano, V.R.; Wei, J.; Wilen, C.B. Norovirus Attachment and Entry. *Viruses* **2019**, *11*, 495, doi:10.3390/v11060495.

19. Campillay-Véliz, C.P.; Carvajal, J.J.; Avellaneda, A.M.; Escobar, D.; Covián, C.; Kalergis, A.M.; Lay, M.K. Human Norovirus Proteins: Implications in the Replicative Cycle, Pathogenesis, and the Host Immune Response. *Front. Immunol.* **2020**, *11*, doi:10.3389/fimmu.2020.00961.

20. Chhabra, P.; de Graaf, M.; Parra, G.I.; Chan, M.C.W.; Green, K.; Martella, V.; Wang, Q.; White, P.A.; Katayama, K.; Vennema, H.; et al. Updated Classification of Norovirus Genogroups and Genotypes. *J. Gen. Virol.* **2019**, *100*, 1393–1406, doi:10.1099/jgv.0.001318.

21. Farahmand, M.; Moghoofei, M.; Dorost, A.; Shoja, Z.; Ghorbani, S.; Kiani, S.J.; Khales, P.; Esteghamati, A.; Sayyahfar, S.; Jafarzadeh, M.; et al. Global Prevalence and Genotype Distribution of Norovirus Infection in Children with Gastroenteritis: A Meta-Analysis on 6 Years of Research from 2015 to 2020. *Rev. Med. Virol.* **2022**, *32*, e2237, doi:10.1002/rmv.2237.

22. Vinjé, J. Advances in Laboratory Methods for Detection and Typing of Norovirus. *J. Clin. Microbiol.* **2015**, *53*, 373–381, doi:10.1128/JCM.01535-14.

23. A. Ford-Siltz, L.; Tohma, K.; I. Parra, G. Understanding the Relationship between Norovirus Diversity and Immunity. *Gut Microbes* **2021**, *13*, 1–13, doi:10.1080/19490976.2021.1900994.

24. Sherwood, J.; Mendelman, P.M.; Lloyd, E.; Liu, M.; Boslego, J.; Borkowski, A.; Jackson, A.; Faix, D. Efficacy of an Intramuscular Bivalent Norovirus GI.1/GII.4 Virus-like Particle Vaccine Candidate in Healthy US Adults. *Vaccine* **2020**, *38*, 6442–6449, doi:10.1016/j.vaccine.2020.07.069.

25. Esposito, S.; Principi, N. Norovirus Vaccine: Priorities for Future Research and Development. *Front. Immunol.* **2020**, *11*, 1–9, doi:10.3389/fimmu.2020.01383.

26. López, P.; López-Medina, E.; Sáez-Llorens, X.; DeAntonio, R.; Masuda, T.; Mendelman, P.M.; Sherwood, J.; Baehner, F.; Borkowski, A. Immunogenicity and Tolerability of a Bivalent Virus-like Particle Norovirus Vaccine Candidate in Children from 6 Months up to 4 Years of Age: A Phase 2 Randomized, Double-Blind Trial. *Hum. Vaccin. Immunother.* **2023**, 2204787, doi:10.1080/21645515.2023.2204787.

27. Baker, M.; Prasad, B.V.V. Rotavirus Cell Entry. In; Johnson, J.E., Ed.; Current Topics in Microbiology and Immunology; Springer Berlin Heidelberg: Berlin, Heidelberg, 2010; Vol. 343,

pp. 121–148.

28. Crawford, S.E.; Mukherjee, S.K.; Estes, M.K.; Lawton, J.A.; Shaw, A.L.; Ramig, R.F.; Prasad, B.V.V. Trypsin Cleavage Stabilizes the Rotavirus VP4 Spike. *J. Virol.* **2001**, *75*, 6052–6061, doi:10.1128/jvi.75.13.6052-6061.2001.

29. Li, Z.; Baker, M.L.; Jiang, W.; Estes, M.K.; Prasad, B.V.V. Rotavirus Architecture at Subnanometer Resolution. *J. Virol.* **2009**, *83*, 1754–1766, doi:10.1128/JVI.01855-08.

30. Zárate, S.; Romero, P.; Espinosa, R.; Arias, C.F.; López, S. VP7 Mediates the Interaction of Rotaviruses with Integrin Alphavbeta3 through a Novel Integrin-Binding Site. *J. Virol.* **2004**, *78*, 10839–10847, doi:10.1128/JVI.78.20.10839-10847.2004.

31. Graham, K.L.; Halasz, P.; Tan, Y.; Hewish, M.J.; Takada, Y.; Mackow, E.R.; Robinson, M.K.; Coulson, B.S. Integrin-Using Rotaviruses Bind A2β1 Integrin A2 I Domain via VP4 DGE Sequence and Recognize AXβ2 and AVβ3 by Using VP7 during Cell Entry. *J. Virol.* **2003**, *77*, 9969–9978, doi:10.1128/JVI.77.18.9969-9978.2003.

32. Haselhorst, T.; Fleming, F.E.; Dyason, J.C.; Hartnell, R.D.; Yu, X.; Holloway, G.; Santegoets, K.; Kiefel, M.J.; Blanchard, H.; Coulson, B.S.; et al. Sialic Acid Dependence in Rotavirus Host Cell Invasion. *Nat. Chem. Biol.* **2009**, *5*, 91–93, doi:10.1038/nchembio.134.

33. Guerrero, C.A.; Bouyssounade, D.; Zárate, S.; Iša, P.; López, T.; Espinosa, R.; Romero, P.; Méndez, E.; López, S.; Arias, C.F. Heat Shock Cognate Protein 70 Is Involved in Rotavirus Cell Entry. *J. Virol.* **2002**, *76*, 4096–4102, doi:10.1128/JVI.76.8.4096-4102.2002.

34. Mayer, M.P.; Bukau, B. Hsp70 Chaperones: Cellular Functions and Molecular Mechanism. *Cell. Mol. Life Sci.* **2005**, *62*, 670–684, doi:10.1007/s00018-004-4464-6.

35. Hu, L.; Sankaran, B.; Laucirica, D.R.; Patil, K.; Salmen, W.; Ferreon, A.C.M.; Tsoi, P.S.; Lasanajak, Y.; Smith, D.F.; Ramani, S.; et al. Glycan Recognition in Globally Dominant Human Rotaviruses. *Nat. Commun.* **2018**, *9*, 2631, doi:10.1038/s41467-018-05098-4.

36. Trask, S.D.; McDonald, S.M.; Patton, J.T. Structural Insights into the Coupling of Virion Assembly and Rotavirus Replication. *Nat. Rev. Microbiol.* **2012**, *10*, 165–177, doi:10.1038/nrmicro2673.

37. Crawford, S.E.; Criglar, J.M.; Liu, Z.; Broughman, J.R.; Estes, M.K. COPII Vesicle Transport Is Required for Rotavirus NSP4 Interaction with the Autophagy Protein LC3 II and Trafficking to Viroplasms. *J. Virol.* **2019**, *94*, doi:10.1128/JVI.01341-19.

38. Hyser, J.M.; Utama, B.; Crawford, S.E.; Broughman, J.R.; Estes, M.K. Activation of the Endoplasmic Reticulum Calcium Sensor STIM1 and Store-Operated Calcium Entry by Rotavirus Requires NSP4 Viroporin Activity. *J. Virol.* **2013**, *87*, 13579–13588, doi:10.1128/JVI.02629-13.

39. Hou, G.; Zeng, Q.; Matthijnssens, J.; Greenberg, H.B.; Ding, S. Rotavirus NSP1 Contributes to Intestinal Viral Replication, Pathogenesis, and Transmission. *MBio* **2021**, *12*, doi:10.1128/mBio.03208-21.

40. Piron, M. Rotavirus RNA-Binding Protein NSP3 Interacts with EIF4GI and Evicts the Poly(A) Binding Protein from EIF4F. *EMBO J.* **1998**, *17*, 5811–5821, doi:10.1093/emboj/17.19.5811.

41. Groft, C.M.; Burley, S.K. Recognition of EIF4G by Rotavirus NSP3 Reveals a Basis for MRNA Circularization. *Mol. Cell* **2002**, *9*, 1273–1283, doi:10.1016/S1097-2765(02)00555-5.

42. Katpally, U.; Smith, T.J. The Caliciviruses. In *Cell Entry by Non-Enveloped Viruses*; Prof. John E. Johnson, Ed.; 2010; pp. 23–41 ISBN 978-3-642-13331-2.

43. Goodfellow, I.; Chaudhry, Y.; Gioldasi, I.; Gerondopoulos, A.; Natoni, A.; Labrie, L.; Laliberté, J.; Roberts, L. Calicivirus Translation Initiation Requires an Interaction between VPg and EIF4E. *EMBO Rep.* **2005**, *6*, 968–972, doi:10.1038/sj.embor.7400510.

44. Belliot, G.; Sosnovtsev, S. V.; Chang, K.-O.; Babu, V.; Uche, U.; Arnold, J.J.; Cameron, C.E.; Green, K.Y. Norovirus Proteinase-Polymerase and Polymerase Are Both Active Forms of RNA-Dependent RNA Polymerase. *J. Virol.* **2005**, *79*, 2393–2403, doi:10.1128/JVI.79.4.2393-2403.2005.

45. de Graaf, M.; van Beek, J.; Koopmans, M.P.G. Human Norovirus Transmission and Evolution in a Changing World. *Nat. Rev. Microbiol.* **2016**, *14*, 421–433, doi:10.1038/nrmicro.2016.48.

46. Marionneau, S.; Cailleau-Thomas, A.; Rocher, J.; Le Moullac-Vaidye, B.; Ruvoën, N.; Clément, M.; Le Pendu, J. ABH and Lewis Histo-Blood Group Antigens, a Model for the Meaning of Oligosaccharide Diversity in the Face of a Changing World. *Biochimie* **2001**, *83*, 565–573,

doi:10.1016/S0300-9084(01)01321-9.

47. Tan, M.; Jiang, X. Histo-Blood Group Antigens: A Common Niche for Norovirus and Rotavirus. *Expert Rev. Mol. Med.* **2014**, *16*, e5, doi:10.1017/erm.2014.2.

48. Peña-Gil, N.; Santiso-Bellón, C.; Gozalbo-Rovira, R.; Buesa, J.; Monedero, V.; Rodríguez-Díaz, J. The Role of Host Glycobiology and Gut Microbiota in Rotavirus and Norovirus Infection, an Update. *Int. J. Mol. Sci.* **2021**, *22*, 13473, doi:10.3390/ijms222413473.

49. Barbé, L.; Le Moullac-Vaidye, B.; Echasserieau, K.; Bernardeau, K.; Carton, T.; Bovin, N.; Nordgren, J.; Svensson, L.; Ruvoën-Clouet, N.; Le Pendu, J. Histo-Blood Group Antigen-Binding Specificities of Human Rotaviruses Are Associated with Gastroenteritis but Not with in Vitro Infection. *Sci. Rep.* **2018**, *8*, 12961, doi:10.1038/s41598-018-31005-4.

50. Marionneau, S.; Ruvoën, N.; Le Moullac–Vaidye, B.; Clement, M.; Cailleau–Thomas, A.; Ruiz–Palacois, G.; Huang, P.; Jiang, X.; Le Pendu, J. Norwalk Virus Binds to Histo-Blood Group Antigens Present on Gastroduodenal Epithelial Cells of Secretor Individuals. *Gastroenterology* **2002**, *122*, 1967–1977, doi:10.1053/gast.2002.33661.

51. Ayouni, S.; Sdiri-Loulizi, K.; de Rougemont, A.; Estienney, M.; Ambert-Balay, K.; Aho, S.; Hamami, S.; Aouni, M.; Neji-Guediche, M.; Pothier, P.; et al. Rotavirus P[8] Infections in Persons with Secretor and Nonsecretor Phenotypes, Tunisia. *Emerg. Infect. Dis.* **2015**, *21*, 2055–2058, doi:10.3201/eid2111.141901.

52. Huang, P.; Xia, M.; Tan, M.; Zhong, W.; Wei, C.; Wang, L.; Morrow, A.; Jiang, X. Spike Protein VP8* of Human Rotavirus Recognizes Histo-Blood Group Antigens in a Type-Specific Manner. *J. Virol.* **2012**, *86*, 4833–4843, doi:10.1128/JVI.05507-11.

53. Gozalbo-Rovira, R.; Ciges-Tomas, J.R.; Vila-Vicent, S.; Buesa, J.; Santiso-Bellón, C.; Monedero, V.; Yebra, M.J.; Marina, A.; Rodríguez-Díaz, J. Unraveling the Role of the Secretor Antigen in Human Rotavirus Attachment to Histo-Blood Group Antigens. *PLOS Pathog.* **2019**, *15*, e1007865, doi:10.1371/journal.ppat.1007865.

54. Li, D.; Wang, M.; Qi, J.; Zhang, Q.; Wang, H.; Pang, L.; Sun, X.; Duan, Z. Human Group A Rotavirus P[25] VP8* Specifically Binds to A-Type Histo-Blood Group Antigen. *Virology* **2021**, *555*, 56–63,

doi:10.1016/j.virol.2020.12.016.

55. Liu, Y.; Huang, P.; Tan, M.; Liu, Y.; Biesiada, J.; Meller, J.; Castello, A.A.; Jiang, B.; Jiang, X. Rotavirus VP8*: Phylogeny, Host Range, and Interaction with Histo-Blood Group Antigens. *J. Virol.* **2012**, *86*, 9899–9910, doi:10.1128/JVI.00979-12.

56. Hu, L.; Crawford, S.E.; Czako, R.; Cortes-Penfield, N.W.; Smith, D.F.; Le Pendu, J.; Estes, M.K.; Prasad, B.V.V. Cell Attachment Protein VP8* of a Human Rotavirus Specifically Interacts with A-Type Histo-Blood Group Antigen. *Nature* **2012**, *485*, 256–259, doi:10.1038/nature10996.

57. Liu, Y.; Huang, P.; Jiang, B.; Tan, M.; Morrow, A.L.; Jiang, X. Poly-LacNAc as an Age-Specific Ligand for Rotavirus P[11] in Neonates and Infants. *PLoS One* **2013**, *8*, e78113, doi:10.1371/journal.pone.0078113.

58. Ramani, S.; Cortes-Penfield, N.W.; Hu, L.; Crawford, S.E.; Czako, R.; Smith, D.F.; Kang, G.; Ramig, R.F.; Le Pendu, J.; Prasad, B.V.V.; et al. The VP8* Domain of Neonatal Rotavirus Strain G10P[11] Binds to Type II Precursor Glycans. *J. Virol.* **2013**, *87*, 7255–7264, doi:10.1128/JVI.03518-12.

59. Liu, Y.; Ramelot, T.A.; Huang, P.; Liu, Y.; Li, Z.; Feizi, T.; Zhong, W.; Wu, F.-T.; Tan, M.; Kennedy, M.A.; et al. Glycan Specificity of P[19] Rotavirus and Comparison with Those of Related P Genotypes. *J. Virol.* **2016**, *90*, 9983–9996, doi:10.1128/JVI.01494-16.

60. Pérez-Ortín, R.; Vila-Vicent, S.; Carmona-Vicente, N.; Santiso-Bellón, C.; Rodríguez-Díaz, J.; Buesa, J. Histo-Blood Group Antigens in Children with Symptomatic Rotavirus Infection. *Viruses* **2019**, *11*, 339, doi:10.3390/v11040339.

61. Imbert-Marcille, B.-M.; Barbé, L.; Dupé, M.; Le Moullac-Vaidye, B.; Besse, B.; Peltier, C.; Ruvoën-Clouet, N.; Le Pendu, J. A FUT2 Gene Common Polymorphism Determines Resistance to Rotavirus A of the P[8] Genotype. *J. Infect. Dis.* **2014**, *209*, 1227–1230, doi:10.1093/infdis/jit655.

62. Payne, D.C.; Currier, R.L.; Staat, M.A.; Sahni, L.C.; Selvarangan, R.; Halasa, N.B.; Englund, J.A.; Weinberg, G.A.; Boom, J.A.; Szilagyi, P.G.; et al. Epidemiologic Association Between FUT2 Secretor Status and Severe Rotavirus Gastroenteritis in Children in the United States. *JAMA Pediatr.* **2015**, *169*, 1040–1045, doi:10.1001/jamapediatrics.2015.2002.

63. Nordgren, J.; Sharma, S.; Bucardo, F.; Nasir, W.; Günaydın, G.; Ouermi, D.; Nitiema, L.W.; Becker-Dreps, S.; Simpore, J.; Hammarström, L.; et al. Both Lewis and Secretor Status Mediate Susceptibility to Rotavirus Infections in a Rotavirus Genotype-Dependent Manner. **2014**, doi:10.1093/cid/ciu633.

64. Zhang, X.-F.; Long, Y.; Tan, M.; Zhang, T.; Huang, Q.; Jiang, X.; Tan, W.-F.; Li, J.-D.; Hu, G.-F.; Tang, S.; et al. P[8] and P[4] Rotavirus Infection Associated with Secretor Phenotypes Among Children in South China. *Sci. Rep.* **2016**, *6*, 34591, doi:10.1038/srep34591.

65. Pollock, L.; Bennett, A.; Jere, K.C.; Dube, Q.; Mandolo, J.; Bar-Zeev, N.; Heyderman, R.S.; Cunliffe, N.A.; Iturriza-Gomara, M. Nonsecretor Histo–Blood Group Antigen Phenotype Is Associated With Reduced Risk of Clinical Rotavirus Vaccine Failure in Malawian Infants. *Clin. Infect. Dis.* **2019**, *69*, 1313–1319, doi:10.1093/cid/ciy1067.

66. Van Trang, N.; Vu, H.T.; Le, N.T.; Huang, P.; Jiang, X.; Anh, D.D. Association between Norovirus and Rotavirus Infection and Histo-Blood Group Antigen Types in Vietnamese Children. *J. Clin. Microbiol.* **2014**, *52*, 1366–1374, doi:10.1128/JCM.02927-13.

67. Lee, B.; Dickson, D.M.; deCamp, A.C.; Ross Colgate, E.; Diehl, S.A.; Uddin, M.I.; Sharmin, S.; Islam, S.; Bhuiyan, T.R.; Alam, M.; et al. Histo–Blood Group Antigen Phenotype Determines Susceptibility to Genotype-Specific Rotavirus Infections and Impacts Measures of Rotavirus Vaccine Efficacy. *J. Infect. Dis.* **2018**, *217*, 1399–1407, doi:10.1093/infdis/jiy054.

68. Nordgren, J.; Sharma, S.; Bucardo, F.; Nasir, W.; Günaydın, G.; Ouermi, D.; Nitiema, L.W.; Becker-Dreps, S.; Simpore, J.; Hammarström, L.; et al. Both Lewis and Secretor Status Mediate Susceptibility to Rotavirus Infections in a Rotavirus Genotype–Dependent Manner. *Clin. Infect. Dis.* **2014**, *59*, 1567–1573, doi:10.1093/cid/ciu633.

69. Henry, S.; Oriol, R.; Samuelsson, B. Lewis Histo-Blood Group System and Associated Secretory Phenotypes. *Vox Sang.* **1995**, *69*, 166–182, doi:10.1111/j.1423-0410.1995.tb02591.x.

70. Sharma, S.; Hagbom, M.; Svensson, L.; Nordgren, J. The Impact of Human Genetic Polymorphisms on Rotavirus Susceptibility, Epidemiology, and Vaccine Take. *Viruses* **2020**, *12*, 324, doi:10.3390/v12030324.

71. Bergman, H.; Henschke, N.; Hungerford, D.; Pitan, F.; Ndwandwe, D.; Cunliffe, N.; Soares-Weiser, K. Vaccines for Preventing Rotavirus Diarrhoea: Vaccines in Use. *Cochrane Database Syst. Rev.* **2021**, *2021*, doi:10.1002/14651858.CD008521.pub6.

72. Huang, P.; Farkas, T.; Zhong, W.; Tan, M.; Thornton, S.; Morrow, A.L.; Jiang, X. Norovirus and Histo-Blood Group Antigens: Demonstration of a Wide Spectrum of Strain Specificities and Classification of Two Major Binding Groups among Multiple Binding Patterns. *J. Virol.* **2005**, *79*, 6714–6722, doi:10.1128/JVI.79.11.6714-6722.2005.

73. Sharma, S.; Hagbom, M.; Carlsson, B.; Nederby Öhd, J.; Insulander, M.; Eriksson, R.; Simonsson, M.; Widerström, M.; Nordgren, J. Secretor Status Is Associated with Susceptibility to Disease in a Large GII.6 Norovirus Foodborne Outbreak. *Food Environ. Virol.* **2020**, *12*, 28–34, doi:10.1007/s12560-019-09410-3.

74. Loureiro Tonini, M.A.; Pires Gonçalves Barreira, D.M.; Bueno de Freitas Santolin, L.; Bondi Volpini, L.P.; Gagliardi Leite, J.P.; Le Moullac-Vaidye, B.; Le Pendu, J.; Cruz Spano, L. FUT2, Secretor Status and FUT3 Polymorphisms of Children with Acute Diarrhea Infected with Rotavirus and Norovirus in Brazil. *Viruses* **2020**, *12*, 1084, doi:10.3390/v12101084.

75. Lopman, B.A.; Trivedi, T.; Vicuña, Y.; Costantini, V.; Collins, N.; Gregoricus, N.; Parashar, U.; Sandoval, C.; Broncano, N.; Vaca, M.; et al. Norovirus Infection and Disease in an Ecuadorian Birth Cohort: Association of Certain Norovirus Genotypes with Host FUT2 Secretor Status. *J. Infect. Dis.* **2015**, *211*, 1813–1821, doi:10.1093/infdis/jiu672.

76. Reyes, Y.; González, F.; Gutiérrez, L.; Blandón, P.; Centeno, E.; Zepeda, O.; Toval-Ruíz, C.; Lindesmith, L.C.; Baric, R.S.; Vielot, N.; et al. Secretor Status Strongly Influences the Incidence of Symptomatic Norovirus Infection in a Genotype-Dependent Manner in a Nicaraguan Birth Cohort. *J. Infect. Dis.* **2022**, *225*, 105–115, doi:10.1093/infdis/jiab316.

77. Menon, V.K.; George, S.; Sarkar, R.; Giri, S.; Samuel, P.; Vivek, R.; Saravanabavan, A.; Liakath, F.B.; Ramani, S.; Iturriza-Gomara, M.; et al. Norovirus Gastroenteritis in a Birth Cohort in Southern India. *PLoS One* **2016**, *11*, e0157007, doi:10.1371/journal.pone.0157007.

78. Nordgren, J.; Kindberg, E.; Lindgren, P.E.; Matussek, A.; Svensson, L. Norovirus Gastroenteritis Outbreak with a Secretor-Independent Susceptibility Pattern, Sweden. *Emerg. Infect. Dis.*

2010, *16*, 81–87, doi:10.3201/eid1601.090633.

79. Rodríguez-Díaz, J.; García-Mantrana, I.; Vila-Vicent, S.; Gozalbo-Rovira, R.; Buesa, J.; Monedero, V.; Collado, M.C. Relevance of Secretor Status Genotype and Microbiota Composition in Susceptibility to Rotavirus and Norovirus Infections in Humans. *Sci. Rep.* **2017**, *7*, 45559, doi:10.1038/srep45559.

80. Treanor, J.J.; Atmar, R.L.; Frey, S.E.; Gormley, R.; Chen, W.H.; Ferreira, J.; Goodwin, R.; Borkowski, A.; Clemens, R.; Mendelman, P.M. A Novel Intramuscular Bivalent Norovirus Virus-Like Particle Vaccine Candidate—Reactogenicity, Safety, and Immunogenicity in a Phase 1 Trial in Healthy Adults. *J. Infect. Dis.* **2014**, *210*, 1763–1771, doi:10.1093/infdis/jiu337.

81. Ravcheev, D.A.; Thiele, I. Comparative Genomic Analysis of the Human Gut Microbiome Reveals a Broad Distribution of Metabolic Pathways for the Degradation of Host-Synthetized Mucin Glycans and Utilization of Mucin-Derived Monosaccharides. *Front. Genet.* **2017**, *8*, doi:10.3389/fgene.2017.00111.

82. Ho, S.B.; Niehans, G.A.; Lyftogt, C.; Yan, P.S.; Cherwitz, D.L.; Gum, E.T.; Dahiya, R.; Kim, Y.S. Heterogeneity of Mucin Gene Expression in Normal and Neoplastic Tissues. *Cancer Res.* **1993**, *53*, 641–651.

83. Audie, J.P.; Janin, A.; Porchet, N.; Copin, M.C.; Gosselin, B.; Aubert, J.P. Expression of Human Mucin Genes in Respiratory, Digestive, and Reproductive Tracts Ascertained by in Situ Hybridization. *J. Histochem. Cytochem.* **1993**, *41*, 1479–1485, doi:10.1177/41.10.8245407.

84. CAZy Carbohydrate-Active Enzymes Database (CAZy) Available online: http://www.cazy.org/Glycoside-Hydrolases.html (accessed on 20 July 2023).

85. Ashida, H.; Miyake, A.; Kiyohara, M.; Wada, J.; Yoshida, E.; Kumagai, H.; Katayama, T.; Yamamoto, K. Two Distinct α-L-Fucosidases from Bifidobacterium Bifidum Are Essential for the Utilization of Fucosylated Milk Oligosaccharides and Glycoconjugates. *Glycobiology* **2009**, *19*, 1010–1017, doi:10.1093/glycob/cwp082.

86. Bunesova, V.; Lacroix, C.; Schwab, C. Fucosyllactose and L-Fucose Utilization of Infant Bifidobacterium Longum and Bifidobacterium Kashiwanohense. *BMC Microbiol.* **2016**, *16*, 248,

doi:10.1186/s12866-016-0867-4.

87. Garrido, D.; Ruiz-Moyano, S.; Kirmiz, N.; Davis, J.C.; Totten, S.M.; Lemay, D.G.; Ugalde, J.A.; German, J.B.; Lebrilla, C.B.; Mills, D.A. A Novel Gene Cluster Allows Preferential Utilization of Fucosylated Milk Oligosaccharides in Bifidobacterium Longum Subsp. Longum SC596. *Sci. Rep.* **2016**, *6*, 35045, doi:10.1038/srep35045.

88. Crost, E.H.; Tailford, L.E.; Le Gall, G.; Fons, M.; Henrissat, B.; Juge, N. Utilisation of Mucin Glycans by the Human Gut Symbiont Ruminococcus Gnavus Is Strain-Dependent. *PLoS One* **2013**, *8*, e76341, doi:10.1371/journal.pone.0076341.

89. Ottman, N.; Davids, M.; Suarez-Diez, M.; Boeren, S.; Schaap, P.J.; Martins dos Santos, V.A.P.; Smidt, H.; Belzer, C.; de Vos, W.M. Genome-Scale Model and Omics Analysis of Metabolic Capacities of Akkermansia Muciniphila Reveal a Preferential Mucin-Degrading Lifestyle. *Appl. Environ. Microbiol.* **2017**, *83*, doi:10.1128/AEM.01014-17.

90. Rodríguez-Díaz, J.; Monedero, V.; Yebra, M.J. Utilization of Natural Fucosylated Oligosaccharides by Three Novel-L-Fucosidases from a Probiotic Lactobacillus Casei Strain Downloaded From. *Appl. Environ. Microbiol.* **2011**, *77*, 703–705, doi:10.1128/AEM.01906-10.

91. Katayama, T.; Sakuma, A.; Kimura, T.; Makimura, Y.; Hiratake, J.; Sakata, K.; Yamanoi, T.; Kumagai, H.; Yamamoto, K. Molecular Cloning and Characterization of Bifidobacterium Bifidum 1,2-α-L-Fucosidase (AfcA), a Novel Inverting Glycosidase (Glycoside Hydrolase Family 95). *J. Bacteriol.* **2004**, *186*, 4885–4893, doi:10.1128/JB.186.15.4885-4893.2004.

92. Navarro, M.A.; Li, J.; McClane, B.A.; Morrell, E.; Beingesser, J.; Uzal, F.A. NanI Sialidase Is an Important Contributor to Clostridium Perfringens Type F Strain F4969 Intestinal Colonization in Mice. *Infect. Immun.* **2018**, *86*, doi:10.1128/IAI.00462-18.

93. Tailford, L.E.; Owen, C.D.; Walshaw, J.; Crost, E.H.; Hardy-Goddard, J.; Le Gall, G.; de Vos, W.M.; Taylor, G.L.; Juge, N. Discovery of Intramolecular Trans-Sialidases in Human Gut Microbiota Suggests Novel Mechanisms of Mucosal Adaptation. *Nat. Commun.* **2015**, *6*, 7624, doi:10.1038/ncomms8624.

94. Huang, K.; Wang, M.M.; Kulinich, A.; Yao, H.L.; Ma, H.Y.; Martínez, J.E.R.; Duan, X.C.; Chen, H.;

Cai, Z.P.; Flitsch, S.L.; et al. Biochemical Characterisation of the Neuraminidase Pool of the Human Gut Symbiont Akkermansia Muciniphila. *Carbohydr. Res.* **2015**, *415*, 60–65, doi:10.1016/j.carres.2015.08.001.

95. Nishiyama, K.; Yamamoto, Y.; Sugiyama, M.; Takaki, T.; Urashima, T.; Fukiya, S.; Yokota, A.; Okada, N.; Mukai, T. Bifidobacterium Bifidum Extracellular Sialidase Enhances Adhesion to the Mucosal Surface and Supports Carbohydrate Assimilation. *MBio* **2017**, *8*, doi:10.1128/mBio.00928-17.

96. Kiyohara, M.; Tanigawa, K.; Chaiwangsri, T.; Katayama, T.; Ashida, H.; Yamamoto, K. An Exo-α-Sialidase from Bifidobacteria Involved in the Degradation of Sialyloligosaccharides in Human Milk and Intestinal Glycoconjugates. *Glycobiology* **2011**, *21*, 437–447, doi:10.1093/glycob/cwq175.

97. Marcobal, A.; Barboza, M.; Sonnenburg, E.D.; Pudlo, N.; Martens, E.C.; Desai, P.; Lebrilla, C.B.; Weimer, B.C.; Mills, D.A.; German, J.B.; et al. Bacteroides in the Infant Gut Consume Milk Oligosaccharides via Mucus-Utilization Pathways. *Cell Host Microbe* **2011**, *10*, 507–514, doi:10.1016/j.chom.2011.10.007.

98. Sebaihia, M.; Wren, B.W.; Mullany, P.; Fairweather, N.F.; Minton, N.; Stabler, R.; Thomson, N.R.; Roberts, A.P.; Cerdeño-Tárraga, A.M.; Wang, H.; et al. The Multidrug-Resistant Human Pathogen Clostridium Difficile Has a Highly Mobile, Mosaic Genome. *Nat. Genet.* **2006**, *38*, 779–786, doi:10.1038/ng1830.

99. Rinninella, E.; Raoul, P.; Cintoni, M.; Franceschi, F.; Miggiano, G.; Gasbarrini, A.; Mele, M. What Is the Healthy Gut Microbiota Composition? A Changing Ecosystem across Age, Environment, Diet, and Diseases. *Microorganisms* **2019**, *7*, 14, doi:10.3390/microorganisms7010014.

100. George, S.; Aguilera, X.; Gallardo, P.; Farfán, M.; Lucero, Y.; Torres, J.P.; Vidal, R.; O'Ryan, M. Bacterial Gut Microbiota and Infections During Early Childhood. *Front. Microbiol.* **2022**, *12*, 1–23, doi:10.3389/fmicb.2021.793050.

101. Yang, M.; Yang, Y.; He, Q.; Zhu, P.; Liu, M.; Xu, J.; Zhao, M. Intestinal Microbiota-A Promising Target for Antiviral Therapy? *Front. Immunol.* **2021**, *12*, 676232, doi:10.3389/fimmu.2021.676232.

102. Shi, Z.; Zou, J.; Zhang, Z.; Zhao, X.; Noriega, J.; Zhang, B.; Zhao, C.; Ingle, H.; Bittinger, K.; Mattei, L.M.; et al. Segmented Filamentous Bacteria Prevent and Cure Rotavirus Infection. *Cell* **2019**, *179*, 644-658.e13, doi:10.1016/j.cell.2019.09.028.

103. Kandasamy, S.; Vlasova, A.N.; Fischer, D.; Kumar, A.; Chattha, K.S.; Rauf, A.; Shao, L.; Langel, S.N.; Rajashekara, G.; Saif, L.J. Differential Effects of Escherichia Coli Nissle and Lactobacillus Rhamnosus Strain GG on Human Rotavirus Binding, Infection, and B Cell Immunity. *J. Immunol.* **2016**, *196*, 1780–1789, doi:10.4049/jimmunol.1501705.

104. Vlasova, A.N.; Shao, L.; Kandasamy, S.; Fischer, D.D.; Rauf, A.; Langel, S.N.; Chattha, K.S.; Kumar, A.; Huang, H.-C.; Rajashekara, G.; et al. Escherichia Coli Nissle 1917 Protects Gnotobiotic Pigs against Human Rotavirus by Modulating PDC and NK-Cell Responses. *Eur. J. Immunol.* **2016**, *46*, 2426–2437, doi:10.1002/eji.201646498.

105. Paim, F.C.; Langel, S.N.; Fischer, D.D.; Kandasamy, S.; Shao, L.; Alhamo, M.A.; Huang, H.-C.; Kumar, A.; Rajashekara, G.; Saif, L.J.; et al. Effects of Escherichia Coli Nissle 1917 and Ciprofloxacin on Small Intestinal Epithelial Cell MRNA Expression in the Neonatal Piglet Model of Human Rotavirus Infection. *Gut Pathog.* **2016**, *8*, 66, doi:10.1186/s13099-016-0148-7.

106. Michael, H.; Paim, F.C.; Langel, S.N.; Miyazaki, A.; Fischer, D.D.; Chepngeno, J.; Amimo, J.; Deblais, L.; Rajashekara, G.; Saif, L.J.; et al. Escherichia Coli Nissle 1917 Enhances Innate and Adaptive Immune Responses in a Ciprofloxacin-Treated Defined-Microbiota Piglet Model of Human Rotavirus Infection. *mSphere* **2021**, *6*, doi:10.1128/mSphere.00074-21.

107. Varyukhina, S.; Freitas, M.; Bardin, S.; Robillard, E.; Tavan, E.; Sapin, C.; Grill, J.-P.; Trugnan, G. Glycan-Modifying Bacteria-Derived Soluble Factors from Bacteroides Thetaiotaomicron and Lactobacillus Casei Inhibit Rotavirus Infection in Human Intestinal Cells. *Microbes Infect.* **2012**, *14*, 273–278, doi:10.1016/j.micinf.2011.10.007.

108. Zhang, B.; Chassaing, B.; Shi, Z.; Uchiyama, R.; Zhang, Z.; Denning, T.L.; Crawford, S.E.; Pruijssers, A.J.; Iskarpatyoti, J.A.; Estes, M.K.; et al. Prevention and Cure of Rotavirus Infection via TLR5/NLRC4-Mediated Production of IL-22 and IL-18. *Science (80-.).* **2014**, *346*, 861–865, doi:10.1126/science.1256999.

109. Gozalbo-Rovira, R.; Rubio-Del-campo, A.; Santiso-Bellón, C.; Vila-Vicent, S.; Buesa, J.; Delgado,

S.; Molinero, N.; Margolles, A.; Yebra, M.J.; Collado, M.C.; et al. Interaction of Intestinal Bacteria with Human Rotavirus during Infection in Children. *Int. J. Mol. Sci.* **2021**, *22*, 1–12, doi:10.3390/IJMS22031010.

110. Li, D.; Breiman, A.; le Pendu, J.; Uyttendaele, M. Anti-Viral Effect of Bifidobacterium Adolescentis against Noroviruses. *Front. Microbiol.* **2016**, *7*, doi:10.3389/fmicb.2016.00864.

111. Rubio-del-Campo, A.; Coll-Marqués, J.M.; Yebra, M.J.; Buesa, J.; Pérez-Martínez, G.; Monedero, V.; Rodríguez-Díaz, J. Noroviral P-Particles as an In Vitro Model to Assess the Interactions of Noroviruses with Probiotics. *PLoS One* **2014**, *9*, e89586, doi:10.1371/journal.pone.0089586.

112. Lei, S.; Ramesh, A.; Twitchell, E.; Wen, K.; Bui, T.; Weiss, M.; Yang, X.; Kocher, J.; Li, G.; Giri-Rachman, E.; et al. High Protective Efficacy of Probiotics and Rice Bran against Human Norovirus Infection and Diarrhea in Gnotobiotic Pigs. *Front. Microbiol.* **2016**, *7*, doi:10.3389/fmicb.2016.01699.

113. Kuss, S.K.; Best, G.T.; Etheredge, C.A.; Pruijssers, A.J.; Frierson, J.M.; Hooper, L. V.; Dermody, T.S.; Pfeiffer, J.K. Intestinal Microbiota Promote Enteric Virus Replication and Systemic Pathogenesis. *Science (80-.).* **2011**, *334*, 249–252, doi:10.1126/science.1211057.

114. Kane, M.; Case, L.K.; Kopaskie, K.; Kozlova, A.; MacDearmid, C.; Chervonsky, A. V; Golovkina, T. V Successful Transmission of a Retrovirus Depends on the Commensal Microbiota. *Science (80-.).* **2011**, *334*, 245–249, doi:10.1126/science.1210718.

115. Wilks, J.; Lien, E.; Jacobson, A.N.; Fischbach, M.A.; Qureshi, N.; Chervonsky, A. V.; Golovkina, T. V. Mammalian Lipopolysaccharide Receptors Incorporated into the Retroviral Envelope Augment Virus Transmission. *Cell Host Microbe* **2015**, *18*, 456–462, doi:10.1016/j.chom.2015.09.005.

116. Jones, M.K.; Watanabe, M.; Zhu, S.; Graves, C.L.; Keyes, L.R.; Grau, K.R.; Gonzalez-Hernandez, M.B.; Iovine, N.M.; Wobus, C.E.; Vinje, J.; et al. Enteric Bacteria Promote Human and Mouse Norovirus Infection of B Cells. *Science (80-.).* **2014**, *346*, 755–759, doi:10.1126/science.1257147.

117. Ruvoën-Clouet, N.; Magalhaes, A.; Marcos-Silva, L.; Breiman, A.; Figueiredo, C.; David, L.; Pendu, J. Le Increase in Genogroup II.4 Norovirus Host Spectrum by CagA-Positive Helicobacter Pylori Infection. *J. Infect. Dis.* **2014**, *210*, 183–191, doi:10.1093/infdis/jiu054.

118. Lei, S.; Twitchell, E.L.; Ramesh, A.K.; Bui, T.; Majette, E.; Tin, C.M.; Avery, R.; Arango-Argoty, G.; Zhang, L.; Becker-Dreps, S.; et al. Enhanced GII.4 Human Norovirus Infection in Gnotobiotic Pigs Transplanted with a Human Gut Microbiota. *J. Gen. Virol.* **2019**, *100*, 1530–1540, doi:10.1099/jgv.0.001336.

119. Eshaghi Gorji, M.; Tan, M.T.H.; Li, D. Influence of Fucosidase-Producing Bifidobacteria on the HBGA Antigenicity of Oyster Digestive Tissue and the Associated Norovirus Binding. *Int. J. Food Microbiol.* **2021**, *340*, 109058, doi:10.1016/j.ijfoodmicro.2021.109058.

120. Su, L.; Ma, L.; Liu, H.; Zhao, F.; Su, Z.; Zhou, D. Presence and Distribution of Histo-Blood Group Antigens in Pacific Oysters and the Effects of Exposure to Noroviruses GI.3 and GII.4 on Their Expression. *J. Food Prot.* **2018**, *81*, 1783–1790, doi:10.4315/0362-028X.JFP-18-074.

121. Mäkivuokko, H.; Lahtinen, S.J.; Wacklin, P.; Tuovinen, E.; Tenkanen, H.; Nikkilä, J.; Björklund, M.; Aranko, K.; Ouwehand, A.C.; Mättö, J. Association between the ABO Blood Group and the Human Intestinal Microbiota Composition. *BMC Microbiol.* **2012**, *12*, 94, doi:10.1186/1471-2180-12-94.

122. Gampa, A.; Engen, P.A.; Shobar, R.; Mutlu, E.A. Relationships between Gastrointestinal Microbiota and Blood Group Antigens. *Physiol. Genomics* **2017**, *49*, 473–483, doi:10.1152/physiolgenomics.00043.2017.

123. Bouskra, D.; Brézillon, C.; Bérard, M.; Werts, C.; Varona, R.; Boneca, I.G.; Eberl, G. Lymphoid Tissue Genesis Induced by Commensals through NOD1 Regulates Intestinal Homeostasis. *Nature* **2008**, *456*, 507–510, doi:10.1038/nature07450.

124. Harris, V.C.; Armah, G.; Fuentes, S.; Korpela, K.E.; Parashar, U.; Victor, J.C.; Tate, J.; de Weerth, C.; Giaquinto, C.; Wiersinga, W.J.; et al. Significant Correlation Between the Infant Gut Microbiome and Rotavirus Vaccine Response in Rural Ghana. *J. Infect. Dis.* **2017**, *215*, 34–41, doi:10.1093/infdis/jiw518.

125. Harris, V.; Ali, A.; Fuentes, S.; Korpela, K.; Kazi, M.; Tate, J.; Parashar, U.; Wiersinga, W.J.; Giaquinto, C.; de Weerth, C.; et al. Rotavirus Vaccine Response Correlates with the Infant Gut Microbiota Composition in Pakistan. *Gut Microbes* **2018**, *9*, 93–101, doi:10.1080/19490976.2017.1376162.

126. Robertson, R.C.; Church, J.A.; Edens, T.J.; Mutasa, K.; Min Geum, H.; Baharmand, I.; Gill, S.K.; Ntozini, R.; Chasekwa, B.; Carr, L.; et al. The Fecal Microbiome and Rotavirus Vaccine Immunogenicity in Rural Zimbabwean Infants. *Vaccine* **2021**, *39*, 5391–5400, doi:10.1016/j.vaccine.2021.07.076.

127. Parker, E.P.K.; Praharaj, I.; Zekavati, A.; Lazarus, R.P.; Giri, S.; Operario, D.J.; Liu, J.; Houpt, E.; Iturriza-Gómara, M.; Kampmann, B.; et al. Influence of the Intestinal Microbiota on the Immunogenicity of Oral Rotavirus Vaccine given to Infants in South India. *Vaccine* **2018**, *36*, 264–272, doi:10.1016/j.vaccine.2017.11.031.

128. Fix, J.; Chandrashekhar, K.; Perez, J.; Bucardo, F.; Hudgens, M.G.; Yuan, L.; Twitchell, E.; Azcarate-Peril, M.A.; Vilchez, S.; Becker-Dreps, S. Association between Gut Microbiome Composition and Rotavirus Vaccine Response among Nicaraguan Infants. *Am. J. Trop. Med. Hyg.* **2020**, *102*, 213–219, doi:10.4269/ajtmh.19-0355.

129. Harris, V.C.; Haak, B.W.; Handley, S.A.; Jiang, B.; Velasquez, D.E.; Hykes, B.L.; Droit, L.; Berbers, G.A.M.; Kemper, E.M.; van Leeuwen, E.M.M.; et al. Effect of Antibiotic-Mediated Microbiome Modulation on Rotavirus Vaccine Immunogenicity: A Human, Randomized-Control Proof-of-Concept Trial. *Cell Host Microbe* **2018**, *24*, 197-207.e4, doi:10.1016/j.chom.2018.07.005.

130. Isaac, S.; Scher, J.U.; Djukovic, A.; Jiménez, N.; Littman, D.R.; Abramson, S.B.; Pamer, E.G.; Ubeda, C. Short- and Long-Term Effects of Oral Vancomycin on the Human Intestinal Microbiota. *J. Antimicrob. Chemother.* **2017**, *72*, 128–136, doi:10.1093/jac/dkw383.

131. St Jean, D.T.; Rogawski McQuade, E.T.; Edwards, J.K.; Thompson, P.; Thomas, J.; Becker-Dreps, S. Effect of Early Life Antibiotic Use on Serologic Responses to Oral Rotavirus Vaccine in the MAL-ED Birth Cohort Study. *Vaccine* **2022**, *40*, 2580–2587, doi:10.1016/j.vaccine.2022.03.023.

132. Anderson, E.J.; Lopman, B.; Yi, J.; Libster, R.; Creech, C.B.; El-Khorazaty, J.; Baqar, S.; Yildirim, I.; Kao, C.; Rouphael, N.; et al. Effect of Concomitant Antibiotic and Vaccine Administration on

Serologic Responses to Rotavirus Vaccine. *J. Pediatric Infect. Dis. Soc.* **2020**, *9*, 479–482, doi:10.1093/jpids/piz044.

133. Shin, D.Y.; Yi, D.Y.; Jo, S.; Lee, Y.M.; Kim, J.-H.; Kim, W.; Park, M. ri; Yoon, S. min; Kim, Y.; Yang, S.; et al. Effect of a New Lactobacillus Plantarum Product, LRCC5310, on Clinical Symptoms and Virus Reduction in Children with Rotaviral Enteritis. *Medicine (Baltimore).* **2020**, *99*, e22192, doi:10.1097/MD.0000000000022192.

134. Park, M.; Kwon, B.; Ku, S.; Ji, G. The Efficacy of Bifidobacterium Longum BORI and Lactobacillus Acidophilus AD031 Probiotic Treatment in Infants with Rotavirus Infection. *Nutrients* **2017**, *9*, 887, doi:10.3390/nu9080887.

135. Das, S.; Gupta, P.K.; Das, R.R. Efficacy and Safety of Saccharomyces Boulardii in Acute Rotavirus Diarrhea: Double Blind Randomized Controlled Trial from a Developing Country. *J. Trop. Pediatr.* **2016**, *62*, fmw032, doi:10.1093/tropej/fmw032.

136. Dubey, A.P.; Rajeshwari, K.; Chakravarty, A.; Famularo, G. Use of VSL♯3 in the Treatment of Rotavirus Diarrhea in Children. *J. Clin. Gastroenterol.* **2008**, *42*, S126–S129, doi:10.1097/MCG.0b013e31816fc2f6.

137. Narayanappa, D. Randomized Double Blinded Controlled Trial to Evaluate the Efficacy and Safety of Bifilac in Patients with Acute Viral Diarrhea. *Indian J. Pediatr.* **2008**, *75*, 709–713, doi:10.1007/s12098-008-0134-2.

138. Freedman, S.B.; Xie, J.; Nettel-Aguirre, A.; Pang, X.-L.; Chui, L.; Williamson-Urquhart, S.; Schnadower, D.; Schuh, S.; Sherman, P.M.; Lee, B.E.; et al. A Randomized Trial Evaluating Virus-Specific Effects of a Combination Probiotic in Children with Acute Gastroenteritis. *Nat. Commun.* **2020**, *11*, 2533, doi:10.1038/s41467-020-16308-3.

139. Freedman, S.B.; Williamson-Urquhart, S.; Farion, K.J.; Gouin, S.; Willan, A.R.; Poonai, N.; Hurley, K.; Sherman, P.M.; Finkelstein, Y.; Lee, B.E.; et al. Multicenter Trial of a Combination Probiotic for Children with Gastroenteritis. *N. Engl. J. Med.* **2018**, *379*, 2015–2026, doi:10.1056/NEJMoa1802597.

140. Hong Chau, T.T.; Minh Chau, N.N.; Hoang Le, N.T.; Chung The, H.; Voong Vinh, P.; Nguyen To,

N.T.; Ngoc, N.M.; Tuan, H.M.; Chau Ngoc, T. Le; Kolader, M.-E.; et al. A Double-Blind, Randomized, Placebo-Controlled Trial of Lactobacillus Acidophilus for the Treatment of Acute Watery Diarrhea in Vietnamese Children. *Pediatr. Infect. Dis. J.* **2018**, *37*, 35–42, doi:10.1097/INF.0000000000001712.

141. Dalgic, N.; Sancar, M.; Bayraktar, B.; Pullu, M.; Hasim, O. Probiotic, Zinc and Lactose-Free Formula in Children with Rotavirus Diarrhea: Are They Effective? *Pediatr. Int.* **2011**, *53*, 677–682, doi:10.1111/j.1442-200X.2011.03325.x.

142. Dutta, P.; Mitra, U.; Dutta, S.; Rajendran, K.; Saha, T.K.; Chatterjee, M.K. Randomised Controlled Clinical Trial of Lactobacillus Sporogenes (Bacillus Coagulans), Used as Probiotic in Clinical Practice, on Acute Watery Diarrhoea in Children. *Trop. Med. Int. Heal.* **2011**, *16*, 555–561, doi:10.1111/j.1365-3156.2011.02745.x.

143. Van Dycke, J.; Arnoldi, F.; Papa, G.; Vandepoele, J.; Burrone, O.R.; Mastrangelo, E.; Tarantino, D.; Heylen, E.; Neyts, J.; Rocha-Pereira, J. A Single Nucleoside Viral Polymerase Inhibitor Against Norovirus, Rotavirus, and Sapovirus-Induced Diarrhea. *J. Infect. Dis.* **2018**, *218*, 1753–1758, doi:10.1093/infdis/jiy398.

144. Chen, S.; Ding, S.; Yin, Y.; Xu, L.; Li, P.; Peppelenbosch, M.P.; Pan, Q.; Wang, W. Suppression of Pyrimidine Biosynthesis by Targeting DHODH Enzyme Robustly Inhibits Rotavirus Replication. *Antiviral Res.* **2019**, *167*, 35–44, doi:10.1016/j.antiviral.2019.04.005.

145. Chen, S.; Wang, Y.; Li, P.; Yin, Y.; Bijvelds, M.J.; de Jonge, H.R.; Peppelenbosch, M.P.; Kainov, D.E.; Pan, Q. Drug Screening Identifies Gemcitabine Inhibiting Rotavirus through Alteration of Pyrimidine Nucleotide Synthesis Pathway. *Antiviral Res.* **2020**, *180*, 104823, doi:10.1016/j.antiviral.2020.104823.

146. Eichwald, C.; De Lorenzo, G.; Schraner, E.M.; Papa, G.; Bollati, M.; Swuec, P.; de Rosa, M.; Milani, M.; Mastrangelo, E.; Ackermann, M.; et al. Identification of a Small Molecule That Compromises the Structural Integrity of Viroplasms and Rotavirus Double-Layered Particles. *J. Virol.* **2018**, *92*, 1–16, doi:10.1128/JVI.01943-17.

147. Yin, Y.; Chen, S.; Hakim, M.S.; Wang, W.; Xu, L.; Dang, W.; Qu, C.; Verhaar, A.P.; Su, J.; Fuhler, G.M.; et al. 6-Thioguanine Inhibits Rotavirus Replication through Suppression of Rac1 GDP/GTP

Cycling. *Antiviral Res.* **2018**, *156*, 92–101, doi:10.1016/j.antiviral.2018.06.011.

148. Tohmé, M.J.; Delgui, L.R. Advances in the Development of Antiviral Compounds for Rotavirus Infections. *MBio* **2021**, *12*, 1–14, doi:10.1128/mBio.00111-21.

149. Netzler, N.E.; Enosi Tuipulotu, D.; White, P.A. Norovirus Antivirals: Where Are We Now? *Med. Res. Rev.* **2019**, *39*, 860–886, doi:10.1002/med.21545.

150. Fox, L.M.; Saravolatz, L.D. Nitazoxanide: A New Thiazolide Antiparasitic Agent. *Clin. Infect. Dis.* **2005**, *40*, 1173–1180, doi:10.1086/428839.

151. Rossignol, J.-F.; El-Gohary, Y.M. Nitazoxanide in the Treatment of Viral Gastroenteritis: A Randomized Double-Blind Placebo-Controlled Clinical Trial. *Aliment. Pharmacol. Ther.* **2006**, *24*, 1423–1430, doi:10.1111/j.1365-2036.2006.03128.x.

152. Mahapatro, S.; Mahilary, N.; Satapathy, A.K.; Das, R.R. Nitazoxanide in Acute Rotavirus Diarrhea: A Randomized Control Trial from a Developing Country. *J. Trop. Med.* **2017**, *2017*, 1–5, doi:10.1155/2017/7942515.

153. Rossignol, J.-F.; Abu-Zekry, M.; Hussein, A.; Santoro, M.G. Effect of Nitazoxanide for Treatment of Severe Rotavirus Diarrhoea: Randomised Double-Blind Placebo-Controlled Trial. *Lancet (London, England)* **2006**, *368*, 124–129, doi:10.1016/S0140-6736(06)68852-1.

154. Teran, C.G.; Teran-Escalera, C.N.; Villarroel, P. Nitazoxanide vs. Probiotics for the Treatment of Acute Rotavirus Diarrhea in Children: A Randomized, Single-Blind, Controlled Trial in Bolivian Children. *Int. J. Infect. Dis.* **2009**, *13*, 518–523, doi:10.1016/j.ijid.2008.09.014.

155. La Frazia, S.; Ciucci, A.; Arnoldi, F.; Coira, M.; Gianferretti, P.; Angelini, M.; Belardo, G.; Burrone, O.R.; Rossignol, J.-F.; Santoro, M.G. Thiazolides, a New Class of Antiviral Agents Effective against Rotavirus Infection, Target Viral Morphogenesis, Inhibiting Viroplasm Formation. *J. Virol.* **2013**, *87*, 11096–11106, doi:10.1128/JVI.01213-13.

156. Siddiq, D.M.; Koo, H.L.; Adachi, J.A.; Viola, G.M. Norovirus Gastroenteritis Successfully Treated with Nitazoxanide. *J. Infect.* **2011**, *63*, 394–397, doi:10.1016/j.jinf.2011.08.002.

157. Haubrich, K.; Gantt, S.; Blydt-Hansen, T. Successful Treatment of Chronic Norovirus

Gastroenteritis with Nitazoxanide in a Pediatric Kidney Transplant Recipient. *Pediatr. Transplant.* **2018**, *22*, e13186, doi:10.1111/petr.13186.

158. Capizzi, T.; Makari-Judson, G.; Steingart, R.; Mertens, W.C. Chronic Diarrhea Associated with Persistent Norovirus Excretion in Patients with Chronic Lymphocytic Leukemia: Report of Two Cases. *BMC Infect. Dis.* **2011**, *11*, 131, doi:10.1186/1471-2334-11-131.

159. Echenique, I.A.; Stosor, V.; Gallon, L.; Kaufman, D.; Qi, C.; Zembower, T.R. Prolonged Norovirus Infection after Pancreas Transplantation: A Case Report and Review of Chronic Norovirus. *Transpl. Infect. Dis.* **2016**, *18*, 98–104, doi:10.1111/tid.12472.

160. Kempf, B.; Edgar, J.D.; Mc Caughey, C.; Devlin, L.A. Nitazoxanide Is an Ineffective Treatment of Chronic Norovirus in Patients With X-Linked Agammaglobulinemia and May Yield False-Negative Polymerase Chain Reaction Findings in Stool Specimens. *J. Infect. Dis.* **2017**, *215*, 486–487, doi:10.1093/infdis/jiw497.

161. Lea, T. Caco-2 Cell Line. In *The Impact of Food Bioactives on Health*; Springer International Publishing: Cham, 2015; pp. 103–111 ISBN 9783319161044.

162. Carmona-Vicente, N.; Allen, D.J.; Rodríguez-Díaz, J.; Iturriza-Gómara, M.; Buesa, J. Antibodies against Lewis Antigens Inhibit the Binding of Human Norovirus GII.4 Virus-like Particles to Saliva but Not to Intestinal Caco-2 Cells. *Virol. J.* **2016**, *13*, 82, doi:10.1186/s12985-016-0538-y.

163. Murakami, K.; Kurihara, C.; Oka, T.; Shimoike, T.; Fujii, Y.; Takai-Todaka, R.; Park, Y.; Wakita, T.; Matsuda, T.; Hokari, R.; et al. Norovirus Binding to Intestinal Epithelial Cells Is Independent of Histo-Blood Group Antigens. *PLoS One* **2013**, *8*, e66534, doi:10.1371/journal.pone.0066534.

164. Martínez-Maqueda, D.; Miralles, B.; Recio, I. HT29 Cell Line. In *The Impact of Food Bioactives on Health*; Springer International Publishing: Cham, 2015; pp. 113–124.

165. Foulke-Abel, J.; In, J.; Kovbasnjuk, O.; Zachos, N.C.; Ettayebi, K.; Blutt, S.E.; Hyser, J.M.; Zeng, X.-L.; Crawford, S.E.; Broughman, J.R.; et al. Human Enteroids as an Ex-Vivo Model of Host–Pathogen Interactions in the Gastrointestinal Tract. *Exp. Biol. Med.* **2014**, *239*, 1124–1134, doi:10.1177/1535370214529398.

166. Sato, T.; Stange, D.E.; Ferrante, M.; Vries, R.G.J.; van Es, J.H.; van den Brink, S.; van Houdt, W.J.; Pronk, A.; van Gorp, J.; Siersema, P.D.; et al. Long-Term Expansion of Epithelial Organoids From Human Colon, Adenoma, Adenocarcinoma, and Barrett's Epithelium. *Gastroenterology* **2011**, *141*, 1762–1772, doi:10.1053/j.gastro.2011.07.050.

167. Saxena, K.; Blutt, S.E.; Ettayebi, K.; Zeng, X.-L.; Broughman, J.R.; Crawford, S.E.; Karandikar, U.C.; Sastri, N.P.; Conner, M.E.; Opekun, A.R.; et al. Human Intestinal Enteroids: A New Model To Study Human Rotavirus Infection, Host Restriction, and Pathophysiology. *J. Virol.* **2016**, *90*, 43–56, doi:10.1128/jvi.01930-15.

168. Zachos, N.C.; Kovbasnjuk, O.; Foulke-Abel, J.; In, J.; Blutt, S.E.; de Jonge, H.R.; Estes, M.K.; Donowitz, M. Human Enteroids/Colonoids and Intestinal Organoids Functionally Recapitulate Normal Intestinal Physiology and Pathophysiology. *J. Biol. Chem.* **2016**, *291*, 3759–3766, doi:10.1074/jbc.R114.635995.

169. Ettayebi, K.; Crawford, S.E.; Murakami, K.; Broughman, J.R.; Karandikar, U.; Tenge, V.R.; Neill, F.H.; Blutt, S.E.; Zeng, X.-L.; Qu, L.; et al. Replication of Human Noroviruses in Stem Cell-Derived Human Enteroids. *Science* **2016**, *353*, 1387–1393, doi:10.1126/science.aaf5211.

170. Gozalbo-Rovira, R.; Santiso-Bellón, C.; Buesa, J.; Rubio-del-Campo, A.; Vila-Vicent, S.; Muñoz, C.; Yebra, M.J.; Monedero, V.; Rodríguez-Díaz, J. Microbiota Depletion Promotes Human Rotavirus Replication in an Adult Mouse Model. *Biomedicines* **2021**, *9*, 846, doi:10.3390/biomedicines9070846.

171. Santiso-Bellón, C.; Gozalbo-Rovira, R.; Buesa, J.; Rubio-del-Campo, A.; Peña-Gil, N.; Navarro-Lleó, N.; Cárcamo-Calvo, R.; Yebra, M.J.; Monedero, V.; Rodríguez-Díaz, J. Replication of Human Norovirus in Mice after Antibiotic-Mediated Intestinal Bacteria Depletion. *Int. J. Mol. Sci.* **2022**, *23*, 10643, doi:10.3390/ijms231810643.

172. Van Dycke, J.; Ny, A.; Conceição-Neto, N.; Maes, J.; Hosmillo, M.; Cuvry, A.; Goodfellow, I.; Nogueira, T.C.; Verbeken, E.; Matthijnssens, J.; et al. A Robust Human Norovirus Replication Model in Zebrafish Larvae. *PLOS Pathog.* **2019**, *15*, e1008009, doi:10.1371/journal.ppat.1008009.

173. Van Dycke, J.; Cuvry, A.; Knickmann, J.; Ny, A.; Rakers, S.; Taube, S.; de Witte, P.; Neyts, J.;

Rocha-Pereira, J. Infection of Zebrafish Larvae with Human Norovirus and Evaluation of the in Vivo Efficacy of Small-Molecule Inhibitors. *Nat. Protoc.* **2021**, *16*, 1830–1849, doi:10.1038/s41596-021-00499-0.

174. Tan, M.; Jiang, X. The P Domain of Norovirus Capsid Protein Forms a Subviral Particle That Binds to Histo-Blood Group Antigen Receptors. *J. Virol.* **2005**, *79*, 14017–14030, doi:10.1128/JVI.79.22.14017-14030.2005.

175. Tan, M.; Fang, P.; Chachiyo, T.; Xia, M.; Huang, P.; Fang, Z.; Jiang, W.; Jiang, X. Noroviral P Particle: Structure, Function and Applications in Virus–Host Interaction. *Virology* **2008**, *382*, 115–123, doi:10.1016/j.virol.2008.08.047.

176. Wobus, C.E.; Karst, S.M.; Thackray, L.B.; Chang, K.-O.; Sosnovtsev, S. V.; Belliot, G.; Krug, A.; Mackenzie, J.M.; Green, K.Y.; Virgin, H.W. Replication of Norovirus in Cell Culture Reveals a Tropism for Dendritic Cells and Macrophages. *PLoS Biol.* **2004**, *2*, e432, doi:10.1371/journal.pbio.0020432.

177. HIRNEISEN, K.A.; KNIEL, K.E. Comparing Human Norovirus Surrogates: Murine Norovirus and Tulane Virus. *J. Food Prot.* **2013**, *76*, 139–143, doi:10.4315/0362-028X.JFP-12-216.

178. Bae, J.; Schwab, K.J. Evaluation of Murine Norovirus, Feline Calicivirus, Poliovirus, and MS2 as Surrogates for Human Norovirus in a Model of Viral Persistence in Surface Water and Groundwater. *Appl. Environ. Microbiol.* **2008**, *74*, 477–484, doi:10.1128/AEM.02095-06.

179. Huang, H.; Liao, D.; Zhou, G.; Zhu, Z.; Cui, Y.; Pu, R. Antiviral Activities of Resveratrol against Rotavirus in Vitro and in Vivo. *Phytomedicine* **2020**, *77*, 153230, doi:10.1016/j.phymed.2020.153230.

180. Wang, X.; Yang, Q.; Zhou, X.; Chen, T.; Dou, L.; Wang, F.; Wang, W. Shenling Baizhu Powder Inhibits RV-SA11-Induced Inflammation and Rotavirus Enteritis via TLR4/MyD88/NF-KB Signaling Pathway. *Front. Pharmacol.* **2021**, *12*, doi:10.3389/fphar.2021.642685.

181. Tohmé, M.J.; Giménez, M.C.; Peralta, A.; Colombo, M.I.; Delgui, L.R. Ursolic Acid: A Novel Antiviral Compound Inhibiting Rotavirus Infection in Vitro. *Int. J. Antimicrob. Agents* **2019**, *54*, 601–609, doi:10.1016/j.ijantimicag.2019.07.015.

182. McNeal, M.M.; Sestak, K.; Choi, A.H.-C.; Basu, M.; Cole, M.J.; Aye, P.P.; Bohm, R.P.; Ward, R.L. Development of a Rotavirus-Shedding Model in Rhesus Macaques, Using a Homologous Wild-Type Rotavirus of a New P Genotype. *J. Virol.* **2005**, *79*, 944–954, doi:10.1128/JVI.79.2.944-954.2005.

183. González-Parra, G.; Dobrovolny, H.M.; Aranda, D.F.; Chen-Charpentier, B.; Guerrero Rojas, R.A. Quantifying Rotavirus Kinetics in the REH Tumor Cell Line Using in Vitro Data. *Virus Res.* **2018**, *244*, 53–63, doi:10.1016/j.virusres.2017.09.023.

184. Shen, Z.; He, H.; Wu, Y.; Li, J. Cyclosporin A Inhibits Rotavirus Replication and Restores Interferon-Beta Signaling Pathway In Vitro and In Vivo. *PLoS One* **2013**, *8*, e71815, doi:10.1371/journal.pone.0071815.

185. Gaymard, A.; Le Briand, N.; Frobert, E.; Lina, B.; Escuret, V. Functional Balance between Neuraminidase and Haemagglutinin in Influenza Viruses. *Clin. Microbiol. Infect.* **2016**, *22*, 975–983, doi:10.1016/j.cmi.2016.07.007.

186. Garrido, D.; Nwosu, C.; Ruiz-Moyano, S.; Aldredge, D.; German, J.B.; Lebrilla, C.B.; Mills, D.A. Endo-β-N-Acetylglucosaminidases from Infant Gut-Associated Bifidobacteria Release Complex N-Glycans from Human Milk Glycoproteins. *Mol. Cell. Proteomics* **2012**, *11*, 775–785, doi:10.1074/mcp.M112.018119.

187. Moya-Gonzálvez, E.M.; Peña-Gil, N.; Rubio-del-Campo, A.; Coll-Marqués, J.M.; Gozalbo-Rovira, R.; Monedero, V.; Rodríguez-Díaz, J.; Yebra, M.J. Infant Gut Microbial Metagenome Mining of α- <scp>l</Scp> -Fucosidases with Activity on Fucosylated Human Milk Oligosaccharides and Glycoconjugates. *Microbiol. Spectr.* **2022**, *10*, doi:10.1128/spectrum.01775-22.

188. Pérez-Ortín, R.; Vila-Vicent, S.; Carmona-Vicente, N.; Santiso-Bellón, C.; Rodríguez-Díaz, J.; Buesa, J. Histo-Blood Group Antigens in Children with Symptomatic Rotavirus Infection. *Viruses* **2019**, *11*, doi:10.3390/v11040339.

189. Imbert-Marcille, B.-M.; Barbé, L.; Dupé, M.; Le Moullac-Vaidye, B.; Besse, B.; Peltier, C.; Ruvoën-Clouet, N.; Le Pendu, J. A FUT2 Gene Common Polymorphism Determines Resistance to Rotavirus A of the P[8] Genotype. *J. Infect. Dis.* **2014**, *209*, 1227–1230, doi:10.1093/infdis/jit655.

190. Chen, S.; Huang, T.; Zhou, Y.; Han, Y.; Xu, M.; Gu, J. AfterQC: Automatic Filtering, Trimming, Error Removing and Quality Control for Fastq Data. *BMC Bioinformatics* **2017**, *18*, 80, doi:10.1186/s12859-017-1469-3.

191. Nurk, S.; Meleshko, D.; Korobeynikov, A.; Pevzner, P.A. MetaSPAdes: A New Versatile Metagenomic Assembler. *Genome Res.* **2017**, *27*, 824–834, doi:10.1101/gr.213959.116.

192. Aziz, R.K.; Bartels, D.; Best, A.A.; DeJongh, M.; Disz, T.; Edwards, R.A.; Formsma, K.; Gerdes, S.; Glass, E.M.; Kubal, M.; et al. The RAST Server: Rapid Annotations Using Subsystems Technology. *BMC Genomics* **2008**, *9*, 75, doi:10.1186/1471-2164-9-75.

193. Keegan, K.P.; Glass, E.M.; Meyer, F. MG-RAST, a Metagenomics Service for Analysis of Microbial Community Structure and Function. In; 2016; pp. 207–233.

194. Galperin, M.Y.; Wolf, Y.I.; Makarova, K.S.; Vera Alvarez, R.; Landsman, D.; Koonin, E. V COG Database Update: Focus on Microbial Diversity, Model Organisms, and Widespread Pathogens. *Nucleic Acids Res.* **2021**, *49*, D274–D281, doi:10.1093/nar/gkaa1018.

195. Zhang, H.; Yohe, T.; Huang, L.; Entwistle, S.; Wu, P.; Yang, Z.; Busk, P.K.; Xu, Y.; Yin, Y. DbCAN2: A Meta Server for Automated Carbohydrate-Active Enzyme Annotation. *Nucleic Acids Res.* **2018**, *46*, W95–W101, doi:10.1093/nar/gky418.

196. Petersen, T.N.; Brunak, S.; von Heijne, G.; Nielsen, H. SignalP 4.0: Discriminating Signal Peptides from Transmembrane Regions. *Nat. Methods* **2011**, *8*, 785–786, doi:10.1038/nmeth.1701.

197. Madeira, F.; Park, Y. mi; Lee, J.; Buso, N.; Gur, T.; Madhusoodanan, N.; Basutkar, P.; Tivey, A.R.N.; Potter, S.C.; Finn, R.D.; et al. The EMBL-EBI Search and Sequence Analysis Tools APIs in 2019. *Nucleic Acids Res.* **2019**, *47*, W636–W641, doi:10.1093/nar/gkz268.

198. Larkin, M.A.; Blackshields, G.; Brown, N.P.; Chenna, R.; McGettigan, P.A.; McWilliam, H.; Valentin, F.; Wallace, I.M.; Wilm, A.; Lopez, R.; et al. Clustal W and Clustal X Version 2.0. *Bioinformatics* **2007**, *23*, 2947–2948, doi:10.1093/bioinformatics/btm404.

199. Ritz, C.; Baty, F.; Streibig, J.C.; Gerhard, D. Dose-Response Analysis Using R. *PLoS One* **2015**, *10*, e0146021, doi:10.1371/journal.pone.0146021.

200. Iturriza-Gómara, M.; Dallman, T.; Bányai, K.; Böttiger, B.; Buesa, J.; Diedrich, S.; Fiore, L.; Johansen, K.; Korsun, N.; Kroneman, A.; et al. Rotavirus Surveillance in Europe, 2005-2008: Web-Enabled Reporting and Real-Time Analysis of Genotyping and Epidemiological Data. *J. Infect. Dis.* **2009**, *200 Suppl*, S215-21, doi:10.1086/605049.

201. Navarro-Lleó, N.; Santiso-Bellón, C.; Vila-Vicent, S.; Carmona-Vicente, N.; Gozalbo-Rovira, R.; Cárcamo-Calvo, R.; Rodríguez-Díaz, J.; Buesa, J. Recombinant Noroviruses Circulating in Spain from 2016 to 2020 and Proposal of Two Novel Genotypes within Genogroup I. *Microbiol. Spectr.* **2022**, *10*, doi:10.1128/spectrum.02505-21.

202. Iturriza-Gómara, M.; Kang, G.; Gray, J. Rotavirus Genotyping: Keeping up with an Evolving Population of Human Rotaviruses. *J. Clin. Virol.* **2004**, *31*, 259–265, doi:10.1016/j.jcv.2004.04.009.

203. SAKURAMA, H.; TSUTSUMI, E.; ASHIDA, H.; KATAYAMA, T.; YAMAMOTO, K.; KUMAGAI, H. Differences in the Substrate Specificities and Active-Site Structures of Two α-L-Fucosidases (Glycoside Hydrolase Family 29) from Bacteroides Thetaiotaomicron. *Biosci. Biotechnol. Biochem.* **2012**, *76*, 1022–1024, doi:10.1271/bbb.111004.

204. Wu, H.; Rebello, O.; Crost, E.H.; Owen, C.D.; Walpole, S.; Bennati-Granier, C.; Ndeh, D.; Monaco, S.; Hicks, T.; Colvile, A.; et al. Fucosidases from the Human Gut Symbiont Ruminococcus Gnavus. *Cell. Mol. Life Sci.* **2021**, *78*, 675–693, doi:10.1007/s00018-020-03514-x.

205. Liu, P.; Zhang, H.; Wang, Y.; Chen, X.; Jin, L.; Xu, L.; Xiao, M. Screening and Characterization of an α-L-Fucosidase from Bacteroides Fragilis NCTC9343 for Synthesis of Fucosyl-N-Acetylglucosamine Disaccharides. *Appl. Microbiol. Biotechnol.* **2020**, *104*, 7827–7840, doi:10.1007/s00253-020-10759-w.

206. Zúñiga, M.; Monedero, V.; Yebra, M.J. Utilization of Host-Derived Glycans by Intestinal Lactobacillus and Bifidobacterium Species. *Front. Microbiol.* **2018**, *9*, 1917, doi:10.3389/fmicb.2018.01917.

207. Bartsch, S.M.; Lopman, B.A.; Ozawa, S.; Hall, A.J.; Lee, B.Y. Global Economic Burden of Norovirus Gastroenteritis. *PLoS One* **2016**, *11*, e0151219, doi:10.1371/journal.pone.0151219.

208. Payne, D.C.; Currier, R.L.; Staat, M.A.; Sahni, L.C.; Selvarangan, R.; Halasa, N.B.; Englund, J.A.; Weinberg, G.A.; Boom, J.A.; Szilagyi, P.G.; et al. Epidemiologic Association Between FUT2 Secretor Status and Severe Rotavirus Gastroenteritis in Children in the United States. *JAMA Pediatr.* **2015**, *169*, 1040, doi:10.1001/jamapediatrics.2015.2002.

209. Kocher, J.; Bui, T.; Giri-Rachman, E.; Wen, K.; Li, G.; Yang, X.; Liu, F.; Tan, M.; Xia, M.; Zhong, W.; et al. Intranasal P Particle Vaccine Provided Partial Cross-Variant Protection against Human GII.4 Norovirus Diarrhea in Gnotobiotic Pigs. *J. Virol.* **2014**, *88*, 9728–9743, doi:10.1128/JVI.01249-14.

210. Verma, V.; Tan, W.; Puth, S.; Cho, K.-O.; Lee, S.E.; Rhee, J.H. Norovirus (NoV) Specific Protective Immune Responses Induced by Recombinant P Dimer Vaccine Are Enhanced by the Mucosal Adjuvant FlaB. *J. Transl. Med.* **2016**, *14*, 135, doi:10.1186/s12967-016-0899-4.

211. Kim, L.; Liebowitz, D.; Lin, K.; Kasparek, K.; Pasetti, M.F.; Garg, S.J.; Gottlieb, K.; Trager, G.; Tucker, S.N. Safety and Immunogenicity of an Oral Tablet Norovirus Vaccine, a Phase I Randomized, Placebo-Controlled Trial. *JCI Insight* **2018**, *3*, doi:10.1172/jci.insight.121077.

212. Turroni, F.; Peano, C.; Pass, D.A.; Foroni, E.; Severgnini, M.; Claesson, M.J.; Kerr, C.; Hourihane, J.; Murray, D.; Fuligni, F.; et al. Diversity of Bifidobacteria within the Infant Gut Microbiota. *PLoS One* **2012**, *7*, e36957, doi:10.1371/journal.pone.0036957.

213. Tannock, G.W.; Lawley, B.; Munro, K.; Gowri Pathmanathan, S.; Zhou, S.J.; Makrides, M.; Gibson, R.A.; Sullivan, T.; Prosser, C.G.; Lowry, D.; et al. Comparison of the Compositions of the Stool Microbiotas of Infants Fed Goat Milk Formula, Cow Milk-Based Formula, or Breast Milk. *Appl. Environ. Microbiol.* **2013**, *79*, 3040–3048, doi:10.1128/AEM.03910-12.

214. Lawson, M.A.E.; O'Neill, I.J.; Kujawska, M.; Gowrinadh Javvadi, S.; Wijeyesekera, A.; Flegg, Z.; Chalklen, L.; Hall, L.J. Breast Milk-Derived Human Milk Oligosaccharides Promote Bifidobacterium Interactions within a Single Ecosystem. *ISME J.* **2020**, *14*, 635–648, doi:10.1038/s41396-019-0553-2.

215. Sakanaka, M.; Hansen, M.E.; Gotoh, A.; Katoh, T.; Yoshida, K.; Odamaki, T.; Yachi, H.; Sugiyama, Y.; Kurihara, S.; Hirose, J.; et al. Evolutionary Adaptation in Fucosyllactose Uptake Systems Supports Bifidobacteria-Infant Symbiosis. *Sci. Adv.* **2019**, *5*, doi:10.1126/sciadv.aaw7696.

216. Nordgren, J.; Sharma, S.; Bucardo, F.; Nasir, W.; Günaydın, G.; Ouermi, D.; Nitiema, L.W.; Becker-Dreps, S.; Simpore, J.; Hammarström, L.; et al. Both Lewis and Secretor Status Mediate Susceptibility to Rotavirus Infections in a Rotavirus Genotype–Dependent Manner. *Clin. Infect. Dis.* **2014**, *59*, 1567–1573, doi:10.1093/cid/ciu633.

217. Pohl, C.; Szczepankiewicz, G.; Liebert, U.G. Analysis and Optimization of a Caco-2 Cell Culture Model for Infection with Human Norovirus. *Arch. Virol.* **2022**, *167*, 1421–1431, doi:10.1007/s00705-022-05437-3.

218. Chantret, I.; Chevalier, G.; Dussaulx, E.; Zweibaum, A. A and H Blood Group Antigens as Markers of Sucrase-Isomaltase from the Enterocyte-like Differentiated Human Colon Carcinoma Cell Lines HT-29 and Caco-2. *Cancer Res.* **1987**, *47*, 1426–1433.

219. Sakuma, K.; Aoki, M.; Kannagi, R. Transcription Factors C-Myc and CDX2 Mediate E-Selectin Ligand Expression in Colon Cancer Cells Undergoing EGF/BFGF-Induced Epithelial–Mesenchymal Transition. *Proc. Natl. Acad. Sci.* **2012**, *109*, 7776–7781, doi:10.1073/pnas.1111135109.

220. Haga, K.; Ettayebi, K.; Tenge, V.R.; Karandikar, U.C.; Lewis, M.A.; Lin, S.-C.; Neill, F.H.; Ayyar, B.V.; Zeng, X.-L.; Larson, G.; et al. Genetic Manipulation of Human Intestinal Enteroids Demonstrates the Necessity of a Functional Fucosyltransferase 2 Gene for Secretor-Dependent Human Norovirus Infection. *MBio* **2020**, *11*, doi:10.1128/mBio.00251-20.

221. Rimkute, I.; Thorsteinsson, K.; Henricsson, M.; Tenge, V.R.; Yu, X.; Lin, S.C.; Haga, K.; Atmar, R.L.; Lycke, N.; Nilsson, J.; et al. Histo-Blood Group Antigens of Glycosphingolipids Predict Susceptibility of Human Intestinal Enteroids to Norovirus Infection. *J. Biol. Chem.* **2020**, *295*, 15974–15987, doi:10.1074/jbc.RA120.014855.

222. Amano, J.; Kobayashi, K.; Oshima, M. Comparative Study of Glycosyltransferase Activities in Caco-2 Cells before and after Enterocytic Differentiation Using Lectin-Affinity High-Performance Liquid Chromatography. *Arch. Biochem. Biophys.* **2001**, *395*, 191–198, doi:10.1006/abbi.2001.2572.

223. de Vries, E.; Du, W.; Guo, H.; de Haan, C.A.M. Influenza A Virus Hemagglutinin–Neuraminidase–Receptor Balance: Preserving Virus Motility. *Trends Microbiol.* **2020**, *28*, 57–

67, doi:10.1016/j.tim.2019.08.010.

224. Ettayebi, K.; Tenge, V.R.; Cortes-Penfield, N.W.; Crawford, S.E.; Neill, F.H.; Zeng, X.-L.; Yu, X.; Ayyar, B.V.; Burrin, D.; Ramani, S.; et al. New Insights and Enhanced Human Norovirus Cultivation in Human Intestinal Enteroids. *mSphere* **2021**, *6*, doi:10.1128/mSphere.01136-20.

225. Mirabelli, C.; Santos-Ferreira, N.; Gillilland, M.G.; Cieza, R.J.; Colacino, J.A.; Sexton, J.Z.; Neyts, J.; Taube, S.; Rocha-Pereira, J.; Wobus, C.E. Human Norovirus Efficiently Replicates in Differentiated 3D-Human Intestinal Enteroids. *J. Virol.* **2022**, *96*, doi:10.1128/jvi.00855-22.

226. Randazzo, W.; Costantini, V.; Morantz, E.K.; Vinjé, J. Human Intestinal Enteroids to Evaluate Human Norovirus GII.4 Inactivation by Aged-Green Tea. *Front. Microbiol.* **2020**, *11*, 1917, doi:10.3389/fmicb.2020.01917.

227. Hayashi, T.; Murakami, K.; Hirano, J.; Fujii, Y.; Yamaoka, Y.; Ohashi, H.; Watashi, K.; Estes, M.K.; Muramatsu, M. Dasabuvir Inhibits Human Norovirus Infection in Human Intestinal Enteroids. *mSphere* **2021**, *6*, doi:10.1128/mSphere.00623-21.

228. Otaki, M.; Hirane, N.; Natsume-Kitatani, Y.; Nogami Itoh, M.; Shindo, M.; Kurebayashi, Y.; Nishimura, S.-I. Mouse Tissue Glycome Atlas 2022 Highlights Inter-Organ Variation in Major N-Glycan Profiles. *Sci. Rep.* **2022**, *12*, 17804, doi:10.1038/s41598-022-21758-4.

229. Lang, Y.; Li, W.; Li, Z.; Koerhuis, D.; van den Burg, A.C.S.; Rozemuller, E.; Bosch, B.-J.; van Kuppeveld, F.J.M.; Boons, G.-J.; Huizinga, E.G.; et al. Coronavirus Hemagglutinin-Esterase and Spike Proteins Coevolve for Functional Balance and Optimal Virion Avidity. *Proc. Natl. Acad. Sci.* **2020**, *117*, 25759–25770, doi:10.1073/pnas.2006299117.

230. Fukudome, K.; Yoshie, O.; Konno, T. Comparison of Human, Simian, and Bovine Rotaviruses for Requirement of Sialic Acid in Hemagglutination and Cell Adsorption. *Virology* **1989**, *172*, 196–205, doi:10.1016/0042-6822(89)90121-9.

231. Guo, Y.; Raev, S.; Kick, M.K.; Raque, M.; Saif, L.J.; Vlasova, A.N. Rotavirus C Replication in Porcine Intestinal Enteroids Reveals Roles for Cellular Cholesterol and Sialic Acids. *Viruses* **2022**, *14*, 1825, doi:10.3390/v14081825.

232. Guo, Y.; Candelero-Rueda, R.A.; Saif, L.J.; Vlasova, A.N. Infection of Porcine Small Intestinal

Enteroids with Human and Pig Rotavirus A Strains Reveals Contrasting Roles for Histo-Blood Group Antigens and Terminal Sialic Acids. *PLOS Pathog.* **2021**, *17*, e1009237, doi:10.1371/journal.ppat.1009237.

233. TIAN, P.; ENGELBREKTSON, A.L.; MANDRELL, R.E. Seasonal Tracking of Histo-Blood Group Antigen Expression and Norovirus Binding in Oyster Gastrointestinal Cells. *J. Food Prot.* **2008**, *71*, 1696–1700, doi:10.4315/0362-028X-71.8.1696.

234. Tian, P.; Engelbrektson, A.L.; Jiang, X.; Zhong, W.; Mandrell, R.E. Norovirus Recognizes Histo-Blood Group Antigens on Gastrointestinal Cells of Clams, Mussels, and Oysters: A Possible Mechanism of Bioaccumulation. *J. Food Prot.* **2007**, *70*, 2140–2147, doi:10.4315/0362-028X-70.9.2140.

235. Gao, X.; Esseili, M.A.; Lu, Z.; Saif, L.J.; Wang, Q. Recognition of Histo-Blood Group Antigen-Like Carbohydrates in Lettuce by Human GII.4 Norovirus. *Appl. Environ. Microbiol.* **2016**, *82*, 2966–2974, doi:10.1128/AEM.04096-15.

236. Esseili, M.A.; Gao, X.; Boley, P.; Hou, Y.; Saif, L.J.; Brewer-Jensen, P.; Lindesmith, L.C.; Baric, R.S.; Atmar, R.L.; Wang, Q. Human Norovirus Histo-Blood Group Antigen (HBGA) Binding Sites Mediate the Virus Specific Interactions with Lettuce Carbohydrates. *Viruses* **2019**, *11*, 833, doi:10.3390/v11090833.

237. Marionneau, S.; Airaud, F.; Bovin, N. V.; Pendu, J. Le; Ruvoën-Clouet, N. Influence of the Combined ABO, FUT2, and FUT3 Polymorphism on Susceptibility to Norwalk Virus Attachment. *J. Infect. Dis.* **2005**, *192*, 1071–1077, doi:10.1086/432546.

238. Paulsen, H. Carbohydrates Containing Nitrogen or Sulfur in the“Hemiacetal” Ring. *Angew. Chemie Int. Ed. English* **1966**, *5*, 495–510, doi:10.1002/anie.196604951.

239. Armstrong, Z.; Meek, R.W.; Wu, L.; Blaza, J.N.; Davies, G.J. Cryo-EM Structures of Human Fucosidase FucA1 Reveal Insight into Substrate Recognition and Catalysis. *Structure* **2022**, *30*, 1443-1451.e5, doi:10.1016/j.str.2022.07.001.

240. Winchester, B.; Barker, C.; Baines, S.; Jacob, G.S.; Namgoong, S.K.; Fleet, G. Inhibition of α - l - Fucosidase by Derivatives of Deoxyfuconojirimycin and Deoxymannojirimycin. *Biochem. J.*

1990, *265*, 277–282, doi:10.1042/bj2650277.

241. Perrella, N.N.; Fuzita, F.J.; Moreti, R.; Verhaert, P.D.E.M.; Lopes, A.R. First Characterization of Fucosidases in Spiders. *Arch. Insect Biochem. Physiol.* **2018**, *98*, e21462, doi:10.1002/arch.21462.

242. Perrella, N.N.; Cantinha, R.S.; Nakano, E.; Lopes, A.R. Characterization of α-L-Fucosidase and Other Digestive Hydrolases from Biomphalaria Glabrata. *Acta Trop.* **2015**, *141*, 118–127, doi:10.1016/j.actatropica.2014.08.022.

243. Megson, Z.A.; Koerdt, A.; Schuster, H.; Ludwig, R.; Janesch, B.; Frey, A.; Naylor, K.; Wilson, I.B.H.; Stafford, G.P.; Messner, P.; et al. Characterization of an α-l-Fucosidase from the Periodontal Pathogen Tannerella Forsythia. *Virulence* **2015**, *6*, 282–292, doi:10.1080/21505594.2015.1010982.

244. Merino-Trigo, A.; Rodríguez-Berrocal, F.J.; de Miguel, E.; Páez de la Cadena, M. Activity and Properties of α-l-Fucosidase Are Dependent on the State of Enterocytic Differentiation of HT-29 Colon Cancer Cells. *Int. J. Biochem. Cell Biol.* **2002**, *34*, 1291–1303, doi:10.1016/S1357-2725(02)00067-5.

245. Cordero, O.J.; Merino, A.; de la Cadena, M.P.; Bugía, B.; Nogueira, M.; Viñuela, J.E.; Martínez-Zorzano, V.S.; de Carlos, A.; Rodríguez-Berrocal, F.J. Cell Surface Human α-L-Fucosidase. *Eur. J. Biochem.* **2001**, *268*, 3321–3331, doi:10.1046/j.1432-1327.2001.02237.x.

246. Nava, P.; López, S.; Arias, C.F.; Islas, S.; González-Mariscal, L. The Rotavirus Surface Protein VP8 Modulates the Gate and Fence Function of Tight Junctions in Epithelial Cells. *J. Cell Sci.* **2004**, *117*, 5509–5519, doi:10.1242/jcs.01425.

247. Tafazoli, F.; Zeng, C.Q.; Estes, M.K.; Magnusson, K.-E.; Svensson, L. NSP4 Enterotoxin of Rotavirus Induces Paracellular Leakage in Polarized Epithelial Cells. *J. Virol.* **2001**, *75*, 1540–1546, doi:10.1128/JVI.75.3.1540-1546.2001.

248. Buccigrossi, V.; Poeta, M.; Cioffi, V.; Terranova, S.; Nunziata, F.; Lo Vecchio, A.; Guarino, A. Lacticaseibacillus Rhamnosus GG Counteracts Rotavirus-Induced Ion Secretion and Enterocyte Damage by Inhibiting Oxidative Stress and Apoptosis Through Specific Effects of Living and

Postbiotic Preparations. *Front. Cell. Infect. Microbiol.* **2022**, *12*, 854989, doi:10.3389/fcimb.2022.854989.

249. Guarino, A.; Canani, R.B.; Spagnuolo, M.I.; Albano, F.; Di Benedetto, L. Oral Bacterial Therapy Reduces the Duration of Symptoms and of Viral Excretion in Children with Mild Diarrhea. *J. Pediatr. Gastroenterol. &amp Nutr.* **1997**, *25*, 516–519, doi:10.1097/00005176-199711000-00005.

250. Aggarwal, S.; Upadhyay, A.; Shah, D.; Teotia, N.; Agarwal, A.; Jaiswal, V. Lactobacillus GG for Treatment of Acute Childhood Diarrhoea: An Open Labelled, Randomized Controlled Trial. *Indian J. Med. Res.* **2014**, *139*, 379–385.

251. Hussain, S.; Miller, J.L.; Harvey, D.J.; Gu, Y.; Rosenthal, P.B.; Zitzmann, N.; McCauley, J.W. Strain-Specific Antiviral Activity of Iminosugars against Human Influenza A Viruses. *J. Antimicrob. Chemother.* **2015**, *70*, 136–152, doi:10.1093/jac/dku349.

252. Warfield, K.; Barnard, D.; Enterlein, S.; Smee, D.; Khaliq, M.; Sampath, A.; Callahan, M.; Ramstedt, U.; Day, C. The Iminosugar UV-4 Is a Broad Inhibitor of Influenza A and B Viruses Ex Vivo and in Mice. *Viruses* **2016**, *8*, 71, doi:10.3390/v8030071.

253. Tyrrell, B.E.; Sayce, A.C.; Warfield, K.L.; Miller, J.L.; Zitzmann, N. Iminosugars: Promising Therapeutics for Influenza Infection. *Crit. Rev. Microbiol.* **2017**, *43*, 521–545, doi:10.1080/1040841X.2016.1242868.

254. Gruters, R.A.; Neefjes, J.J.; Tersmette, M.; de Goede, R.E.Y.; Tulp, A.; Huisman, H.G.; Miedema, F.; Ploegh, H.L. Interference with HIV-Induced Syncytium Formation and Viral Infectivity by Inhibitors of Trimming Glucosidase. *Nature* **1987**, *330*, 74–77, doi:10.1038/330074a0.

255. Fleet, G.W.J.; Karpas, A.; Dwek, R.A.; Fellows, L.E.; Tyms, A.S.; Petursson, S.; Namgoong, S.K.; Ramsden, N.G.; Smith, P.W.; Son, J.C.; et al. Inhibition of HIV Replication by Amino-sugar Derivatives. *FEBS Lett.* **1988**, *237*, 128–132, doi:10.1016/0014-5793(88)80185-6.

256. Steinmann, E.; Whitfield, T.; Kallis, S.; Dwek, R.A.; Zitzmann, N.; Pietschmann, T.; Bartenschlager, R. Antiviral Effects of Amantadine and Iminosugar Derivatives against Hepatitis C Virus. *Hepatology* **2007**, *46*, 330–338, doi:10.1002/hep.21686.

257. Wu, S.-F.; Lee, C.-J.; Liao, C.-L.; Dwek, R.A.; Zitzmann, N.; Lin, Y.-L. Antiviral Effects of an Iminosugar Derivative on Flavivirus Infections. *J. Virol.* **2002**, *76*, 3596–3604, doi:10.1128/JVI.76.8.3596-3604.2002.

258. Courageot, M.-P.; Frenkiel, M.-P.; Duarte Dos Santos, C.; Deubel, V.; Desprès, P. α-Glucosidase Inhibitors Reduce Dengue Virus Production by Affecting the Initial Steps of Virion Morphogenesis in the Endoplasmic Reticulum. *J. Virol.* **2000**, *74*, 564–572, doi:10.1128/JVI.74.1.564-572.2000.

259. Louie, J.K.; Yang, S.; Acosta, M.; Yen, C.; Samuel, M.C.; Schechter, R.; Guevara, H.; Uyeki, T.M. Treatment With Neuraminidase Inhibitors for Critically Ill Patients With Influenza A (H1N1)Pdm09. *Clin. Infect. Dis.* **2012**, *55*, 1198–1204, doi:10.1093/cid/cis636.

260. Fry, A.M.; Goswami, D.; Nahar, K.; Sharmin, A.T.; Rahman, M.; Gubareva, L.; Azim, T.; Bresee, J.; Luby, S.P.; Brooks, W.A. Efficacy of Oseltamivir Treatment Started within 5 Days of Symptom Onset to Reduce Influenza Illness Duration and Virus Shedding in an Urban Setting in Bangladesh: A Randomised Placebo-Controlled Trial. *Lancet Infect. Dis.* **2014**, *14*, 109–118, doi:10.1016/S1473-3099(13)70267-6.

261. Dobson, J.; Whitley, R.J.; Pocock, S.; Monto, A.S. Oseltamivir Treatment for Influenza in Adults: A Meta-Analysis of Randomised Controlled Trials. *Lancet* **2015**, *385*, 1729–1737, doi:10.1016/S0140-6736(14)62449-1.

262. Dutkowski, R.; Thakrar, B.; Froehlich, E.; Suter, P.; Oo, C.; Ward, P. Safety and Pharmacology of Oseltamivir in Clinical Use. *Drug Saf.* **2003**, *26*, 787–801, doi:10.2165/00002018-200326110-00004.